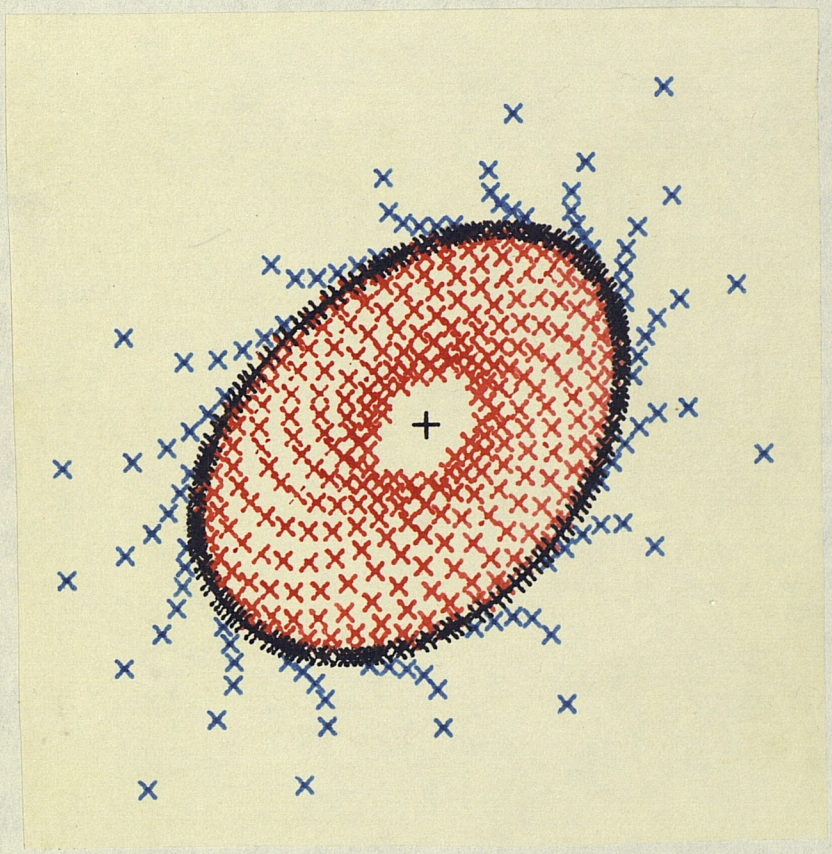

Attracting invariant circle

$(x,y) \rightarrow (y, 0.75y + 1.52x(1-x))$

UNIVERSITY OF SOUTHAMPTON

The Bifurcations and Dynamics of Certain Quadratic Maps of the Plane

by

David Christopher Whitley

Faculty of Mathematical Studies

Thesis submitted for the degree of
Doctor of Philosophy

UNIVERSITY OF SOUTHAMPTON

ABSTRACT

FACULTY OF MATHEMATICAL STUDIES

Doctor of Philosophy

THE BIFURCATIONS AND DYNAMICS OF CERTAIN QUADRATIC MAPS OF THE PLANE

by

David Christopher Whitley

Discrete models of density-dependent population growth provide simple examples of dynamical systems which exhibit complicated dynamics. Single age-class models lead to the study of maps of an interval into itself and we outline the main results which are known in this case.

Here our main concern is with a two age-class model, due to Maynard Smith, which takes the form of a two-parameter family of maps of the plane with a quadratic non-linearity. After a description of the local bifurcations of general two-parameter families in the plane we give a linear stability analysis for the fixed points in our model and analyse their bifurcations. This local theory is extended by finding numerically the boundaries of the regions in the parameter space where the map has a periodic orbit of low period created by resonant Hopf bifurcation. A series of computer-drawn phase portraits is presented for a one-parameter path through the parameter plane, showing the creation of an attracting invariant circle by a Hopf bifurcation followed by a passage to a more complicated attractor.

We examine a three-parameter family connecting our map to the quadratic diffeomorphism studied by Henon and conclude with a discussion of a more realistic model which, however, contains the same complexities associated with resonant Hopf bifurcation found in the simpler model.

ACKNOWLEDGEMENT

The work in this thesis was carried out under the guidance of Professor H.B. Griffiths, to whom I offer my warmest thanks for many hours of helpful conversation. I would also like to thank Dr. D.R.J. Chillingworth and Dr. F. Rhodes for welcome advice and encouragement.

Thanks are also due to Dolores Pendell for typing the manuscript in such an efficient manner.

Financial support was provided by the Science Research Council.

CONTENTS

INTRODUCTION

Discrete models of density-dependent population growth have recently attracted attention as examples of simple dynamical systems which exhibit extremely complicated, and interesting, dynamics. The simplest models describe the growth of a population with nonoverlapping generations by a relationship of the form $x_{n+1} = f(x_n)$, where x_n denotes the size of the population at time n and f is some suitably chosen function. This leads naturally to the study of maps of an interval into itself, and a reasonably complete topological picture of the behaviour of such maps has been developed, and is outlined below. Our main interest however is with a model of a population with two age-classes, which takes account of the time delay involved as members of the first age-class mature into the second. For a time delay of τ units we are led to a discrete system with a $(\tau+1)$-dimensional phase space which extends the one-dimensional maps in two ways. Firstly, when $\tau = 0$ the model reduces to a single age-class model which is identical to those studied previously. Secondly, for $\tau \neq 0$ the model involves two parameters, and for certain parameter values the behaviour of the system is completely determined by knowledge of the one-dimensional case.

The model we shall study was originally proposed by Maynard Smith [29], who derives the following relationship for the growth of a species with egg and adult age-classes:

$$x(n+1) = ax(n) + bx(n-\tau) - cx^2(n-\tau) \qquad (0.1)$$

Here $x(n)$ denotes the size of the adult population at time n, τ is the time taken for an egg to develop into an adult, $a \in (0,1)$ is the probability that an adult at time n survives to time $n+1$, $b > 0$ is the number of eggs laid per adult per unit time which in optimal conditions (i.e. low $x(n)$) survive to become adults, and $c > 0$ represents a density-

dependent constraint on the fecundity of the adults.[5] In fact c is simply a scaling factor which is removed by the change of scale $x \to x/c$ so that

$$x(n+1) = ax(n) + bx(n-\tau) - x^2(n-\tau) \tag{0.2}$$

We introduce new variables $x_1(n) = x(n-\tau)$, $x_2(n) = x(n-\tau+1),\ldots,$ $x_{\tau+1}(n) = x(n)$ to obtain, in the usual way, a map of the phase space which sends $x_i(n)$ to $x_i(n+1)$, $1 \le i \le \tau+1$:

$$F: \mathbb{R}^{\tau+1} \to \mathbb{R}^{\tau+1}, \quad F(x_1,\ldots,x_{\tau+1}) = (x_2,x_3,\ldots,ax_{\tau+1} + bx_1 - x_1^2) \tag{0.3}$$

If $\tau = 0$ this gives a function $F(x) = (a+b)x - x^2$ which is equivalent, by a linear change of coordinates, to either of the quadratic families

$$f_\mu(x) = \mu x(1-x), \qquad \mu \in [0,4] \tag{0.4}$$

$$f_\mu(x) = \mu - x^2, \qquad \mu \in [-\tfrac{1}{4},2] \tag{0.5}$$

The first family (0.4) was considered by May [28] as a simple population model, but it has one slight disadvantage in that it has a 'non-generic' bifurcation at $\mu = 1$, due to the fact that the origin is a fixed point for all values of μ. However a linear coordinate change transforms (0.4) for $\mu \in [1,4]$ into (0.5) for $\mu \in [-\tfrac{1}{4},2]$ and the second family has a 'generic' bifurcation at $\mu = -\tfrac{1}{4}$. The same non-genericity occurs for the map (0.3) and it simplifies matters if we make the coordinate change $x_i \mapsto x_i - \frac{b}{2}$ to obtain

$$F(x_1,\ldots,x_{\tau+1}) = (x_2,\ldots,ax_{\tau+1} + \tilde{b} - x_1^2) \tag{0.6}$$

where $\tilde{b} = \frac{ab}{2} + \frac{b^2}{4} - \frac{b}{2}$.

We will study (0.6) in detail for the case of simplest non-zero time delay: $\tau = 1$. Renaming the coordinates $x_1 = x$, $x_2 = y$ and omitting the

tilde on b we have a two parameter family of maps of the plane:

$$\begin{aligned} F:\ & \mathbb{R}^2 \to \mathbb{R}^2 \\ & (x,y) \mapsto (y, ay+b-x^2) \end{aligned} \tag{0.7}$$

For a certain range of parameters this family is studied in Griffiths and Rand [11], where attention is restricted to those biologically relevant orbits corresponding to positive populations. For the moment we ignore any such restrictions and study (0.7) as a discrete dynamical system in its own right. In Chapter Five we return to the ecological problem and discuss a more realistic model.

The main insights into the behaviour of Maynard Smith's map (0.7) come from bifurcation theory. In Chapter Two we describe the local bifurcations of families of diffeomorphisms, starting with one-parameter familes in $\mathbb{R}$ and working through Hopf bifurcation for one-parameter families in $\mathbb{R}^2$ to the resonant Hopf bifurcations in two-parameter familes in the plane.

This theory is applied to our model in Chapter Three and the local analysis of the bifurcation set is extended, in Chapter Four, with the help of some numerical work. We also present a series of computer-drawn phase portraits for Maynard Smith's map with $a = \frac{1}{2}$, and describe a global bifurcation which destroys an attracting set.

Another family of two-dimensional maps which has received a considerable amount of attention is the Henon map [16]:

$$G(x,y) = (y+1-bx^2, ax)$$

Now if $a \neq 0$ we can change coordinates so that

$$G(x,y) = (y, ax+b-y^2) \tag{0.8}$$

which is clearly similar in form to Maynard Smith's map (0.7). In Chapter Five we examine the three-parameter family

$$H_t(x,y) = tF(x,y) + (1-t)G(x,y) \quad 0 \leq t \leq 1$$

which connects (0.7) and (0.8), and we see that the map $H_{\frac{1}{2}}$ in the middle of this family has (symmetry) properties very similar to those of a map considered by Guckenheimer, Oster and Ipatchki [14].

To begin with, note that when $a = 0$ the behaviour of both the Maynard Smith map (0.7) and the Henon map (0.8) is determined by the one-dimensional family (0.5). Chapter One is devoted to a description of the dynamics of such maps of the interval.

CHAPTER ONE

MAPS OF THE INTERVAL

For a map $f: I \to I$ of an interval $I \subset \mathbb{R}$ and an initial point $x \in I$ we are interested in the orbit of x, $O(x) = \{f^n(x)\}_{n=0}^{\infty}$, and its ω-limit set, $\omega(x) = \bigcap_{N \geq 0} \overline{\bigcup_{n \geq N} f^n(x)}$. A point $x \in I$ and its orbit are periodic, of period m, if $f^m(x) = x$ but $f^n(x) \neq x$ for $0 < n < m$. Of particular relevance are periodic orbits which attract nearby points: a periodic orbit is locally stable or attracting if it has a neighbourhood of points which tend to the orbit under iteration.

Recent interest in maps of the interval stems in part from the work of May [28], who examined several functions found in the biological literature, notably the quadratic family

$$f(x) = rx(1-x) \tag{1.1}$$

and the discrete logistic relation

$$f(x) = x \exp[r(1-x)] \tag{1.2}$$

where the parameter $r > 0$ represents the growth rate of the population. May noted that as r is increased from zero both the families (1.1) and (1.2) have the same bifurcation sequence. For low values of r both maps have an attracting fixed point which becomes unstable as r increases, throwing off a stable orbit of period two. This in turn becomes unstable for higher values of r and gives birth to a stable orbit of period four. As r increases further this period doubling continues: attracting periodic orbits of period 2^n become unstable and create stable orbits of period 2^{n+1}. For sufficiently large values of r ($r > 3.828$ in (1.1), $r > 3.102$ in (1.2)), May showed that these maps have orbits of period three and it follows from the 'Period Three Implies Chaos' of Li and Yorke [25]

that for these parameter values the maps have orbits of all periods.

Of course we do not pass immediately from the sequence of period doubling bifurcations to a point of period three and a "chaotic" regime; the transition is much more complicated. In fact Li and Yorke's result is a special case of the following:

Theorem (Sarkovskii)

Order the natural numbers $\mathbb{N}$ as follows:

$$3\triangle5\triangle7\triangle.....\triangle2.3\triangle2.5\triangle2.7\triangle....\triangle2^2.3\triangle2^2.5\triangle2^2.7\triangle...\triangle2^n\triangle....\triangle2^3\triangle2^2\triangle2\triangle1$$

If $f: \mathbb{R} \to \mathbb{R}$ is a continuous map which has an orbit of period n, then f has an orbit of period m for every $m \in \mathbb{N}$ with $n \triangle m$.

An account of Sarkovskii's proof of this result is contained in Stefan [35]. It is clear from this theorem that periodic points play an important role in determining the structure of maps of the interval, but in general we wish to study points which display a weaker type of recurrence. We say a point $x \in I$ wanders under a map f if there is a neighbourhood U of x with the property that $f^n(U) \cap U = \emptyset$ for each positive integer n. Otherwise x is a non-wandering point and the set of all such points $\Omega(f)$ is called the non-wandering set of f. $\Omega(f)$ is a closed subset of I which contains all periodic points and ω-limit points, and is invariant under f: $f(\Omega(f)) \subset \Omega(f)$.

Many of the basic questions about maps of the interval, including the structure of the non-wandering set, have been answered using the kneading theory of Milnor and Thurston [30]. We will describe these results within the class C of maps of the unit interval $I = [0,1]$ with the following properties:

(1) $f: I \to I$ is C^3 and $f(0) = f(1) = 0$.

(2) f has a single local maximum c. $f''(c) < 0$ and f is strictly increasing on $[0,c]$ and strictly decreasing on $[c,1]$.

(3) The Schwarzian derivative

$$Sf(x) = \frac{f'''(x)}{f'(x)} - \frac{3}{2}\left[\frac{f''(x)}{f'(x)}\right]^2$$

is negative on $I \setminus \{c\}$.

Much of the theory that we outline below applies to larger classes of maps, in particular to functions which are simply continuous with a single local maximum, but the theory is most complete, and the results are simpler to state, with the class C. One of the main reasons for including the condition (3) on the Schwarzian derivative is that it restricts the number of stable periodic orbits a map may have:

Theorem Singer [34]

Let $f: I \to I$ be a C^3 map with a finite number of critical points and $Sf(x) < 0$ for each regular point $x \in I$. If p lies in a stable periodic orbit of f then there is a critical point of f or an endpoint of I whose ω-limit set is the orbit of p.

Thus the number of stable periodic orbits of a map with negative Schwarzian derivative is limited by the number of critical points of the map. For $f \in C$ if we further assume that either $\omega(c) = \{0\}$ or $f'(0) > 1$ then f has at most one stable periodic orbit.

Kneading theory encodes information about the orbit of a point in terms of infinite sequences of symbols and then exploits the natural order of the interval to investigate topological properties of a map. For a map $f \in C$ and a point $x \in I$ let

$$\varepsilon_n(x) = \begin{cases} 0 & \text{if } f^n(x) = c \\ +1 & \text{if } f^n(x) > c \\ -1 & \text{if } f^n(x) < c \end{cases}$$

The sequence $\underline{\varepsilon}(x) = (\varepsilon_n(x))_{n=0}^{\infty}$ is called the itinerary of x. It has the property that $\varepsilon_n(f(x)) = \varepsilon_{n+1}(x)$, i.e. $\underline{\varepsilon}(f(x)) = \sigma\underline{\varepsilon}(x)$ where σ is the shift map

$$\sigma((a_n)_{n=0}^{\infty}) = (b_n)_{n=0}^{\infty}, \quad b_n = a_{n+1}$$

However the mapping $x \mapsto \underline{\varepsilon}(x)$ does not reflect the ordering of the interval, given the lexicographic ordering for sequences. Milnor and Thurston define the invariant coordinate $\underline{\theta}(x)$ to be the sequence $(\theta_n(x))_{n=0}^{\infty}$ where $\theta_n(x) = \prod_{i=0}^{n} \varepsilon_i(x)$, or equivalently

$$\theta_n(x) = \begin{cases} 0 & \text{if } f^m(x) = c \text{ for some } m \text{ with } 0 < m < n \\ +1 & \text{if } f^n \text{ is orientation preserving near } x \\ -1 & \text{if } f^n \text{ is orientation reversing near } x. \end{cases}$$

If the sequences are ordered lexicographically then the map $x \mapsto \underline{\theta}(x)$ is monotone decreasing and the shift invariance for $\underline{\varepsilon}$-sequences is replaced by $\sigma(\underline{\theta}(x)) = \theta_o(x)\ \underline{\theta}(f(x))$.

Jonker [20] recovers Sarkovskii's theorem by considering the relationship between periodic orbits and the periodicity of invariant coordinates.

Besides the structure of the non-wandering set one of the main questions about maps of the interval is to decide when two such maps have the same topological properties. Two maps f, g of I are topologically equivalent or conjugate if there is a homeomorphism $h: I \to I$ so that $hf = gh$. An almost complete invariant of the topological equivalence class of a map $f \in C$ is provided by the itinerary of the critical point c,

which is called the kneading sequence $\underline{\gamma}$ of f. Certainly if h is a conjugacy between two maps f and g in C then it maps the orbit of the critical point of f to the orbit of the critical point of g, and it does so in an order-preserving way. Hence if two maps are topologically equivalent then they have the same kneading sequence.

The converse is not always true. If f and g have the same kneading sequence $\underline{\gamma}$ and do not have stable periodic orbits then it turns out that f and g are conjugate. If they do have stable periodic orbits then $\sigma(\underline{\gamma})$ is periodic, of period n say, and there are three possibilities. $\underline{\gamma}$ is said to be of critical type if $\gamma_n = 0$. If $\gamma_n \neq 0$ then $\underline{\gamma}$ is of positive or negative type as the number of -1's among $\gamma_1,\ldots,\gamma_n$ is even or odd. The precise situation is described by the following result of Guckenheimer [13].

Theorem (Topological Classification)

Let f and g in C have the same kneading sequence $\underline{\gamma}$. Either both f and g have stable periodic orbits or neither does. If f and g do not have stable periodic orbits then they are conjugate. If f and g do have stable periodic orbits then $\sigma(\underline{\gamma})$ is periodic, with period n say, and there are three possibilities. If $\underline{\gamma}$ is of critical type then f is conjugate to g. If $\underline{\gamma}$ is of positive type the stable periodic orbits of f and g have period n and f and g are conjugate if these orbits are both stable from one side or both stable from both sides. If $\underline{\gamma}$ is of negative type then the stable orbits of f and g have period n or $2n$ and f is conjugate to g if and only if these periods are the same.

To illustrate Guckenheimer's theorem we reproduce the following figure from [13]. Figure 1 shows the bifurcation locus for the initial period doubling sequence in a typical quadratic family f_μ and indicates

which orbits have kneading sequences of the three types in the theorem.

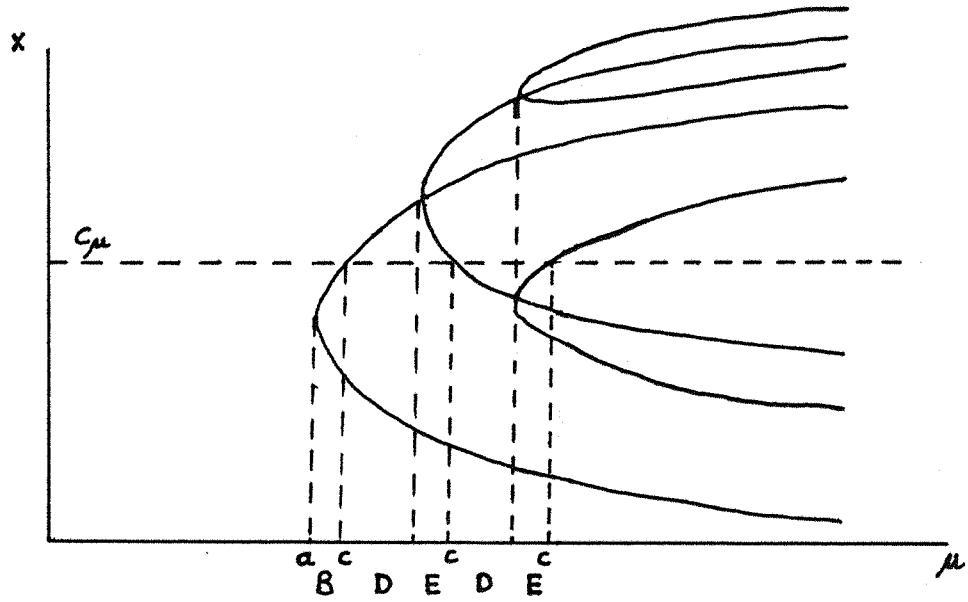

Figure 1.1

Bifurcation locus of a one-parameter family.

a - γ positive type, one sided stable orbit

B - γ positive type, two sided stable orbit

c - γ critical type

D - γ negative type, period γ = period of stable orbit

E - γ negative type, period $\gamma = \frac{1}{2}$ (period of stable orbit)

Intervals D are closed on the right, intervals B and E are open.

To describe the non-wandering set of $f \in C$ we first need some terminology from symbolic dynamics. Let $X = \{1,\ldots,n\}$ with the discrete topology and let $\Sigma_n = X^{\mathbb{N}}$ be the set of infinite sequences $\underline{a} = (a_0,a_1,\ldots)$ of elements of X with the product topology. The (one-sided) shift σ on Σ_n is defined, as above, by $\sigma(\underline{a}) = \underline{b}$ where $b_i = a_{i+1}$. If $A = (A_{ij})$ is an $n\times n$ matrix whose entries are 0's and 1's, define the subset Σ_A of Σ_n by

$$\Sigma_A = \{\underline{a} \in \Sigma_n \mid A_{a_i,a_{i+1}} = 1, \ \forall\, i\}$$

i.e. a sequence $\underline{a}$ is in Σ_A if and only if each of its two-blocks $a_i a_{i+1}$ give a 1 when used as indices for the matrix A. Σ_A is a closed σ-invariant subset of Σ_n and $\sigma|\Sigma_A$ is called a <u>subshift of finite type</u>. If A is a permutation matrix then Σ_A is a single periodic sequence, otherwise Σ_A is homeomorphic to a Cantor set. $\sigma|\Sigma_A$ is <u>transitive</u> if there is a sequence $\underline{a} \in \Sigma_A$ whose orbit $\{\sigma^n(\underline{a})\}_{n=0}^{\infty}$ under the shift is dense in Σ_A.

A closed invariant set $\Lambda \subset \Omega(f)$ for a C^1 function $f: \mathbb{R} \to \mathbb{R}$ is <u>hyperbolic</u> if there are numbers $c > 0$ and $\tau > 1$ so that for $x \in \Lambda$ either

$$|(f^k)'(x)| > c\tau^k \quad \text{or} \quad |(f^k)'(x)| < c(\tfrac{1}{\tau})^k \quad \text{for all } k \in \mathbb{N}.$$

Let $\mathrm{Per}(f)$ denote the set of periodic points of f.

<u>Theorem</u> (<u>Decomposition of $\Omega(f)$</u>)

<u>If $f \in C$ there is a decomposition of the non-wandering set $\Omega(f)$ into a finite or countably infinite number of closed, invariant subsets, Ω_j, $j = 0,1,\ldots$, including a set Ω_∞ if the number of sets is infinite. The decomposition has the following properties</u>:

(1) $\Omega_o = \{0\}$

(2) If the decomposition is finite, $\Omega(f) = \Omega_o \cup \cdots \cup \Omega_p$, then $\Omega_i \cap \Omega_j = \emptyset$, if $i \neq j$, $0 \leq i < p$, and $\Omega_{p-1} \cap \Omega_p$ contains at most a finite number of points.

(3) Ω_j is hyperbolic for $0 \leq j < p$.
$\Omega_j = \mathrm{Per}_j \cup C_j$, $0 < j < p$, where Per_j is a finite subset of $\mathrm{Per}(f)$, C_j is a Cantor set and $f: C_j \to C_j$ is conjugate to a transitive subshift of finite type.

(4) The set of points $\{x|\omega(x) \in \Omega_p\}$ is open and dense in I if p is finite and residual if $p = \infty$.

(5) If f has a stable periodic orbit then $p < \infty$

(6) If $p < \infty$ there are four possibilities for Ω_p:

(a) Ω_p is a finite subset of $Per(f)$ and contains at most one non-hyperbolic orbit. There is an integer $N > 0$ so that Ω_p consists of one unstable orbit of each period $N.2^i$ with $0 < i < n$ for some n, and one stable orbit of period $N.2^n$.

(b) $\Omega_p = Per_p \cup C_p$ where C_p is an invariant Cantor set and $Fr(Per_p) = C_p$. All periodic orbits are hyperbolic but C_p is non-hyperbolic. Per_p consists of unstable periodic orbits, one of period $N.2^i$ for each $i > 1$, for some $N > 0$.

(c) $\Omega_p = Per_p \cup C_p$ where Per_p is hyperbolic and is a finite subset of $Per(f)$. C_p is an invariant Cantor set which contains exactly one non-hyperbolic periodic orbit. $f: C_p \to C_p$ is conjugate to a transitive subshift of finite type.

(d) Ω_p consists of a finite set of unstable periodic points together with a finite union of intervals. $f:\Omega_p \to \Omega_p$ is conjugate to a piecewise linear map.

(7) If the decomposition has infinitely many sets then $\Omega_\infty(f) = \overline{O(x)}$ for some $x \in I$ and $\Omega_\infty(f)$ is a non-hyperbolic Cantor set.

The main parts of this theorem were proved by Jonker and Rand [20] for continuous maps of the interval with a single extremum. The simplifications within the class C follow from Guckenheimer [12] and van Strien [37], who proves the hyperbolicity statements. Jonker and Rand place more emphasis on the connection with piecewise linear maps and include statements concerning the topological entropy of the maps which we omit here.

A further property of maps of the interval is that the iterates of nearby points may not remain close to one another. Guckenheimer uses the following definition of this phenomenon: f has sensitive

dependence on initial conditions if there is a set $X \subset I$ of positive lebesgue measure and an $\varepsilon > 0$ so that for each $x \in X$ and any neighbourhood U of x there is a point $y \in U$ and an integer $n > 0$ with $d(f^n(y), f^n(x)) > \varepsilon$.

To decide whether or not a map $f \in C$ has sensitive dependence on initial conditions it is necessary to consider certain special points. Denote by x' the unique point $x' \neq x$ with $f(x') = f(x)$. A fixed point p of f^n, $n > 1$, is central if $Df^n(p) > 1$ and f^n is a homeomorphism on the interval (p,c). The central point p is restrictive if $f^n(c) \in (p,p')$, i.e. f^n maps (p,p') into itself.

Theorem (Guckenheimer [13])

Suppose $f \in C$ has no stable periodic orbit. Then f has sensitive dependence on initial conditions if and only if there is an $N > 0$ so that $n \geq N$ implies f^n has no restrictive central point.

If $f \in C$ has a stable periodic orbit then f does not have sensitive dependence on initial conditions.

The connection between sensitive dependence and the decomposition of $\Omega(f)$ is that those f with no stable periodic orbit and a decomposition of $\Omega(f)$ into a finite number of sets have sensitive dependence on initial conditions, while if $\Omega(f)$ consists of infinitely many sets then f has neither a stable periodic orbit nor sensitive dependence on initial conditions. Guckenheimer also shows how sensitive dependence is related to topological entropy and piecewise linear maps.

There is one further aspect of the behaviour of maps of the interval which deserves mention and this differs from the properties described above in being quantitative rather than qualitative. Suppose that a differentiable map $f: I \to I$ with a single critical point c has a point

p of period m. If $g = f^m$ then the local stability of the periodic orbit containing p is determined by the linear approximation to g at p. In a new coordinate $y = x-p$ we have

$$g(y) = yg'(p) + O(y^2)$$

and so $g^n(y) \to 0$ as $n \to \infty$ provided $|g'(p)| < 1$. If $r = |g'(p)| < 1$ then $g^n(y)\ \alpha r^n$ and if $r \neq 0$ the convergence is geometric. Now if the orbit of p contains the critical point c then $r = 0$ and convergence is faster than geometric, and such an orbit is called <u>superstable</u>. In the initial period doubling sequence for a one-parameter family such as (1.1) or (1.2) there is a sequence of parameter values $r_0, r_1, r_2, \ldots$ so that f_{r_j} has a superstable orbit of period 2^j and Feigenbaum [10] observed that the limit

$$\lim_{n\to\infty} \frac{r_{n+1}-r_n}{r_{n+2}-r_{n+1}} = \delta$$

exists and is independent of the particular family f_r. δ depends only on the type of the critical value and for a quadratic family $\delta = 4.6692\ldots$. Also, as the period of an attracting periodic orbit doubles with a change of parameter the behaviour of f^n repeats itself for f^{2n} on a smaller scale. In the limit as $n \to \infty$ this rescaling approaches multiplication by α^{-1} where $\alpha = -2.5029\ldots$.

Feigenbaum's observations have been rigourously justified by Collet, Eckmann and Lanford [7] for maps of the form $f(|x|^{1+\varepsilon})$, for ε sufficiently small, and by Campanino and Epstein [6] for C^2 maps.

As we mentioned in the introduction, all these results apply to Maynard Smith's map (0.7) or the Henon map (0.8) when the parameter $a = 0$. Much less is known about maps of the plane, for example if $a \neq 0$ in (0.7) or (0.8). An analogue of Li and Yorke's 'Period Three Implies Chaos'

result [25] is given by Marotto [27]. Suppose $F: \mathbb{R}^n \to \mathbb{R}^n$ is differentiable in $B_r(z)$, the closed ball of radius r with centre $z \in \mathbb{R}^n$, and that F is not one-to-one on $\mathbb{R}^n$. The point $z \in \mathbb{R}^n$ is called an expanding fixed point of F in $B_r(z)$ if $F(z) = z$ and all the eigenvalues of the linearization $dF(x)$ have modulus greater than one for each $x \in B_r(z)$. If z is an expanding fixed point of F in $B_r(z)$ for some $r > 0$, then z is called a <u>snap-back repellor</u> of F if there exists a point $x_o \in B_r(z)$ with $x_o \neq z$, $F^m(x_o) = z$ and $|DF^m(x_o)| \neq 0$ for some positive integer m. The main part of Marotto's result is the following

<u>Theorem</u>

<u>If F has a snap-back repellor then there is a positive integer N so that for each integer $n \geq N$ F has a point of period n.</u>

Rather than search for snap-back repellors in Maynard Smith's family to show that (0.7) has "chaotic" behaviour for certain parameter values we will study (0.7) through the local bifurcation theory described in the next chapter.

Chapter Two

Local Bifurcation Theory

In this chapter we describe the local bifurcations of fixed points in two-parameter families of diffeomorphisms of the plane, and show how these fit together to give an overall picture of the parameter space for a general family of maps.

Let $\mathrm{Diff}^r(\mathbb{R}^n)$ denote the set of C^r-diffeomorphisms of $\mathbb{R}^n$. Two diffeomorphisms $F, G \in \mathrm{Diff}^r(\mathbb{R}^n)$ are conjugate if there is a homeomorphism $h: \mathbb{R}^n \to \mathbb{R}^n$ with $hF = Gh$. If $F: \mathbb{R}^k \times \mathbb{R}^n \to \mathbb{R}^n$, $(\mu,x) \to F_\mu(x)$, is a k-parameter family of elements $F_\mu \in \mathrm{Diff}^r(\mathbb{R}^n)$ we say that $\mu_o \in \mathbb{R}^k$ is a regular point for the family if there is a neighbourhood U of μ_o in $\mathbb{R}^k$ so that for each $\mu \in U$, F_μ is conjugate to F_{μ_o}. If μ_o is not a regular point then it is a bifurcation point and the set of all such points is called the bifurcation set of the family $\{F_\mu\}_{\mu \in \mathbb{R}^k}$.

A fixed point $p \in \mathbb{R}^n$ of $F \in \mathrm{Diff}^r(\mathbb{R}^n)$ is hyperbolic if $dF(p)$ has no eigenvalues of unit modulus. If F_{μ_o} has a hyperbolic fixed point p_o it follows that μ_o is a regular point, so to study the bifurcations of fixed points we must consider those maps F_{μ_o} with a non-hyperbolic fixed point p_o. In such a case we wish to describe the different topological types of phase portrait which occur for F_μ with μ near μ_o. Without loss of generality we may assume $\mu_o = 0$ and $p_o = 0$, and of course the results we give apply to periodic points by considering the relevant iterate of the map.

For a family F_μ of elements of $\mathrm{Diff}^r(\mathbb{R}^2)$ with $F_o(0) = 0$ let us consider the different ways in which 0 may be non-hyperbolic. The first possibility is that a single real eigenvalue of $dF_o(0)$ lies on the unit circle, in which case it is clearly $+1$ or -1. We may then choose coordinates so that $F_\mu(x,y) = (f_\mu(x,y), g_\mu(x,y))$ with $\frac{\partial f_o}{\partial x}(0,0) = \pm 1$

according to whether the critical eigenvalue is $+1$ or -1, and $\frac{\partial g_o}{\partial x}(0,0) \neq 1$. This last condition means that the equation $g_\mu(x,y) = y$ can be solved by the Implicit Function Theorem for a unique C^r function $y(x,\mu)$ near $x = 0$, $\mu = 0$ with $y(0,0) = 0$ and $g_\mu(x,y(x,\mu)) = y(x,\mu)$. The fixed points of F_μ are then found by solving $f_\mu(x,y(x,\mu)) = x$, where f_μ is now a family of maps in a single variable, so the problem is reduced to a one-dimensional one. The bifurcations of one-parameter families of maps in a single real variable are well known and we review the results for this case in §2.1.

If the fixed point should lose stability by a complex conjugate pair of eigenvalues passing out of the unit circle then in general an invariant circle bifurcates from the fixed point through a Hopf bifurcation. In §2.2 we outline a proof, due to Lanford [23], of the Hopf Bifurcation Theorem for one-parameter familes of maps of the plane. The dynamics of the map on the bifurcated circle are rather delicate and, following Arnold [3], are best understood in the context of two-parameter families. In a one-parameter family we would not generally cross the unit circle at points where the eigenvalues $\lambda,\bar{\lambda}$ of $dF_o(0)$ are roots of unity; we only expect these 'resonances' to occur in two-parameter families. In the case of weak resonance, $\lambda^k = 1$, $k \geq 5$, the Hopf Bifurcation Theorem guarantees a bifurcating circle and in §2.3 we extend the analysis of Iooss [19] from the one-parameter to the two-parameter case to describe the behaviour of the map on the circle.

In §2.4 we discuss briefly the strong resonances $\lambda^k = 1$, $k = 1,2,3$ or 4, which involve some unsolved problems. These bifurcations are studied by Arnold [3] and Takens [38], who approximate the map by the time-one map of a vector field invariant under a rotation by $2\pi/k$ and then investigate this vector field. Iooss [19] gives results for one-parameter families of maps in the cases $k = 3$ and 4, and the

latter case is also considered by Wan [40] and Lemaire-Body [24].

We conclude with an indication of how these bifurcations fit together in a family such as the Maynard Smith map (0.7) or the Henon map (0.8). Of course these results can also be applied to maps of $\mathbb{R}^n$, or more generally to maps of a Banach space when a fixed point loses (or gains) stability by one or two eigenvalues crossing the unit circle. The results for maps of $\mathbb{R}^2$ are also of interest for the bifurcation of a limit cycle of a vector field into an invariant torus and the resulting dynamics on the torus. In both instances we refer to Iooss [19] for further details.

§2.1. Bifurcations in One Dimension

For a C^1 map $f: \mathbb{R} \to \mathbb{R}$ recall that a fixed point p is asymptotically stable if $|\frac{df}{dx}(p)| < 1$ and unstable if $|\frac{df}{dx}(p)| > 1$. In a one-parameter family $F: \mathbb{R} \times \mathbb{R} \to \mathbb{R}$, $(x,\mu) \to F_\mu(x)$, with $F(0,0) = 0$ there are two types of bifurcation which can occur, corresponding to the eigenvalue $\lambda(0) = \frac{\partial F}{\partial x}(0,0)$ being $+1$ or -1, and the following propositions, due to Guckenheimer [12], describe the behaviour of the map in each case. We assume that F is C^1 with respect to the parameter.

Proposition 2.1 (Fold Bifurcation)

Let $F: \mathbb{R} \times R \to \mathbb{R}$ be a one-parameter family of C^2 maps satisfying

(1) $F(0,0) = 0$ (2) $\frac{\partial F}{\partial x}(0,0) = 1$ (3) $\frac{\partial^2 F}{\partial x^2}(0,0) > 0$

(4) $\frac{\partial F}{\partial \mu}(0,0) > 0$

Then there are intervals $(\mu_1,0)$ and $(0,\mu_2)$ and $\varepsilon > 0$ so that

(i) If $\mu \in (\mu_1,0)$ then F_μ has two fixed points in $(-\varepsilon,\varepsilon)$. One is stable and the other unstable.

(ii) If $\mu \in (0,\mu_2)$ then F_μ has no fixed points in $(-\varepsilon,\varepsilon)$.

Proof Let $g(x,\mu) = F(x,\mu) - x$, then we have

$$g(0,0) = 0, \quad \frac{\partial g}{\partial x}(0,0) = 0, \quad \frac{\partial^2 g}{\partial x^2}(0,0) > 0 \quad \text{and} \quad \frac{\partial g}{\partial \mu}(0,0) > 0.$$

The first and last of these properties together with the Implicit Function Theorem give a unique C^2 function $\mu(x)$ for x near 0 with $\mu(0) = 0$ and $g(x,\mu(x)) = 0$. Differentiating this equation we find

$$\frac{d\mu}{dx}(0) = 0 \quad \text{and} \quad \frac{d^2\mu}{dx^2}(0) < 0$$

so $\mu(x)$ has a maximum at $x = 0$ and the existence statements follow. For the stability of the fixed points note that (3) implies that $\frac{\partial F}{\partial x}(x,\mu(x))$ is monotone increasing at $x = 0$, so the bottom branch in Figure 2.1 consists of stable fixed points and the top branch of unstable ones.

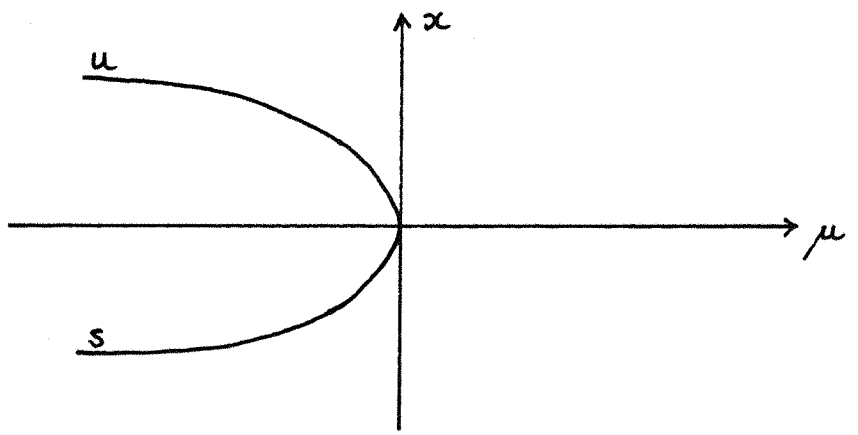

Figure 2.1. Fold Bifurcation

s denotes a branch of stable fixed points, u a branch of unstable ones.

Remark. Reversing one of the inequalities (3) or (4) reverses the roles of the intervals $(\mu_1,0)$ and $(0,\mu_2)$.

Proposition 2.2. (Flip Bifurcation)

Let $F: \mathbb{R} \times \mathbb{R} \to \mathbb{R}$ be a one-parameter family of C^3 maps satisfying

(1) $F(0,0) = 0$ (2) $\frac{\partial F}{\partial x}(0,0) = -1$

Then there is a unique branch of fixed points $x(\mu)$ for μ near 0 with $x(0) = 0$. If the eigenvalue $\lambda(\mu) = \frac{\partial F}{\partial x}(x(\mu),\mu)$ satisfies

$$(3)\quad \frac{d\lambda}{d\mu}(0) > 0$$

and also

$$(4)\quad \frac{\partial^3 F^2}{\partial x^3}(0,0) < 0$$

then there are intervals $(\mu_1,0)$ and $(0,\mu_2)$ and $\varepsilon > 0$ so that

(i) if $\mu \in (\mu_1,0)$ then F_μ has one unstable fixed point and one stable orbit of period two in $(-\varepsilon,\varepsilon)$.

(ii) If $\mu \in (0,\mu_2)$ then F_μ^2 has a single fixed point in $(-\varepsilon,\varepsilon)$ which is a stable fixed point of F_μ.

Proof The existence of the branch of fixed points follows immediately from the Implicit Function Theorem, and the assertions about the stability of the fixed point come from (3). To find the periodic points let $h(x,\mu) = F^2(x,\mu) - x$, then

$$h(0,0) = 0, \quad \frac{\partial h}{\partial x}(0,0) = 0, \quad \frac{\partial^2 h}{\partial x^2}(0,0) = 0 \quad \text{and} \quad \frac{\partial^3 h}{\partial x^3}(0,0) < 0$$

Now factor out the fixed point by defining $g(x,\mu)$ by

$$h(x,\mu) = (x-x(\mu))g(x,\mu),$$

then we have

$$g(0,0) = 0, \quad \frac{\partial g}{\partial x}(0,0) = 0, \quad \frac{\partial^2 g}{\partial x^2}(0,0) < 0 \quad \text{and} \quad \frac{\partial g}{\partial \mu}(0,0) < 0.$$

As in the preceding proof, there is a unique C^2 function $\mu(x)$ for x near 0 with $\mu(0) = 0$ and $g(x,\mu(x)) = 0$. Again, $\frac{d\mu}{dx}(0) = 0$ and $\frac{d^2\mu}{dx^2}(0) < 0$ so $\mu(x)$ has a maximum at $x = 0$ and the statements on the existence of the period two points follow. For the stability of the periodic points note that $\frac{d^2F^2}{dx^2}(0,0) = 0$ and together with (4) this implies

that $\frac{dF^2}{dx}(x,\mu(x))$ has a maximum at $x = 0$.

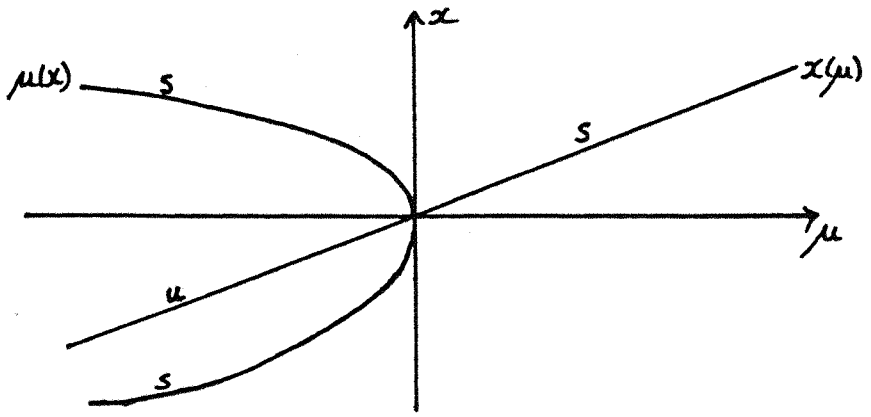

Figure 2.2. Flip Bifurcation.

$\mu(x)$ represents a branch of period two points, $x(\mu)$ a branch of fixed points.

Remarks 1. Changing the inequality (3) reverses the stability of the fixed point, while changing (4) reverses the stability of the period two points. Changing either (3) or (4) reverses the interval in which the period two points lie.

2. In Proposition 2.2 note that

$$\frac{\partial^3 F^2}{\partial x^3}(0,0) = -2\frac{\partial^3 F}{\partial x^3}(0,0) - 3\left(\frac{\partial^2 F}{\partial x^2}(0,0)\right)^2$$

and recall from Chapter One that the Schwarzian derivative of F at x is

$$SF(x) = \frac{F'''(x)}{F'(x)} - \frac{3}{2}\left(\frac{F''(x)}{F'(x)}\right)^2$$

where F' denotes $\frac{\partial F}{\partial x}$. Thus, since $\frac{\partial F}{\partial x}(0,0) = -1$, $\frac{\partial^3 F^2}{\partial x^3}(0,0) = 2SF(0)$

and the sign of the Schwarzian derivative of F_μ restricts the type of flip bifurcation which can occur for F_μ. In particular, for a family of maps with negative Schwarzian derivative a flip bifurcation necessarily involves a stable orbit of period two and the 'subcritical' bifurcation shown in figure 2.3 cannot occur. In this example an

unstable orbit of period two coalesces with a stable fixed point at $\mu = 0$ to leave an unstable fixed point. This remark is the basis for the paper of Allwright [1].

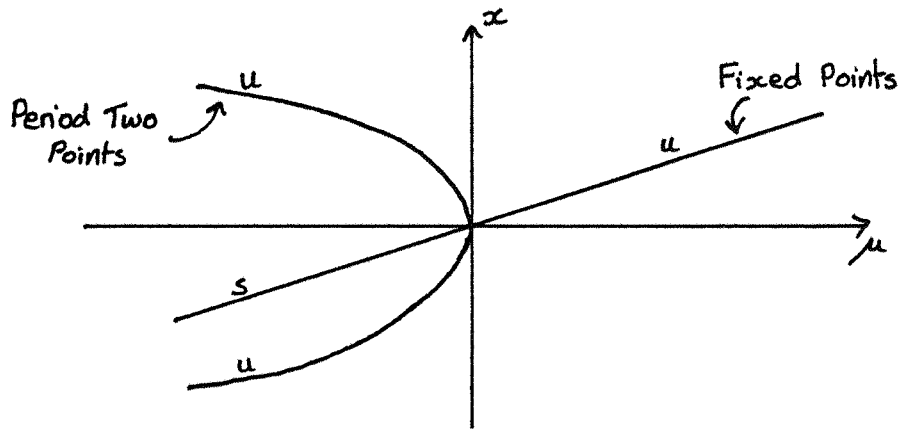

Figure 2.3. Subcritical Flip.

In many applications the class of maps to be considered is likely to be restricted in some way and different bifurcations from those described above may occur. Perhaps the most common restriction is that the origin should be fixed for all values of the parameter and in this case rather than the fold for $\lambda(0) = 1$ we have a transcritical bifurcation as described by the following proposition.

Proposition 2.3.

Let $F: \mathbb{R} \times \mathbb{R} \to \mathbb{R}$ be a one-parameter family of C^2 maps satisfying

(1) $F(0,\mu) = 0$

(2) $\frac{\partial F}{\partial x}(0,\mu) = \lambda(\mu)$, $\lambda(0) = 1$ and $\frac{d\lambda}{d\mu}(0) > 0$

(3) $\frac{\partial^2 F}{\partial x^2}(0,0) > 0$.

Then F has a unique bifurcated branch of fixed points $x(\mu)$ for μ near 0 with $x(0) = 0$ and $x(\mu) \neq 0$ if $\mu \neq 0$. The origin is stable if $\mu < 0$ and unstable if $\mu > 0$ while the fixed points on the bifurcated branch have the opposite stability.

Proof. The Taylor expansion of F_μ at $x = 0$ implies that $F(x,\mu) = \lambda(\mu)x + xh(x,\mu)$ where $h(0,\mu) = 0$ and therefore $\frac{\partial h}{\partial \mu}(0,0) = 0$. Differentiating F we have

$$\frac{\partial F}{\partial x}(x,\mu) = \lambda(\mu) + x\frac{\partial h}{\partial x}(x,\mu) + h(x,\mu)$$

$$\frac{\partial^2 F}{\partial x^2}(x,\mu) = x\frac{\partial^2 h}{\partial x^2}(x,\mu) + 2\frac{\partial h}{\partial x}(x,\mu)$$

and

$$\frac{\partial^2 F}{\partial \mu \partial x}(x,\mu) = \frac{d\lambda}{d\mu}(\mu) + x\frac{\partial^2 h}{\partial \mu \partial x}(x,\mu) + \frac{\partial h}{\partial \mu}(x,\mu)$$

Therefore

$$\frac{\partial h}{\partial x}(0,0) = \frac{1}{2}\frac{\partial^2 F}{\partial x^2}(0,0) > 0$$

and

$$\frac{\partial^2 F}{\partial \mu \partial x}(0,0) = \frac{d\lambda}{d\mu}(0) \neq 0.$$

The non-zero fixed points of F occur at the zeros of $g(x,\mu) = \lambda(\mu) - 1 + h(x,\mu)$. Here we find

$$g(0,0) = 0$$

$$\frac{\partial g}{\partial x}(0,0) = \frac{\partial h}{\partial x}(0,0) > 0$$

and

$$\frac{\partial g}{\partial \mu}(0,0) = \frac{d\lambda}{d\mu}(0) > 0$$

so by the Implicit Function Theorem we may solve $g(x,\mu) = 0$ for either $x(\mu)$ or $\mu(x)$, and these functions are mutual inverses. Thus the branch of bifurcating fixed points exists on both sides of $\mu = 0$ and crosses $x = 0$ transversely. For the stability, differentiating $g(x(\mu),\mu) = 0$ we have

$$\frac{dx}{d\mu}(0) = -\frac{\partial g}{\partial \mu}(0,0) / \frac{\partial g}{\partial x}(0,0)$$

$$= -\frac{d\lambda}{d\mu}(0) / \frac{\partial^2 F}{\partial x^2}(0,0)$$

and so

$$\frac{\partial}{\partial \mu}\left[\frac{\partial F}{\partial x}(x(\mu),\mu)\right]\Big|_{\mu=0} = \frac{\partial^2 F}{\partial x^2}(0,0) \cdot \frac{dx}{d\mu}(0) + \frac{\partial^2 F}{\partial x \partial \mu}(0,0)$$

$$= -\frac{d\lambda}{d\mu}(0)$$

Hence the non-zero fixed point has the opposite stability to the origin for μ near 0.

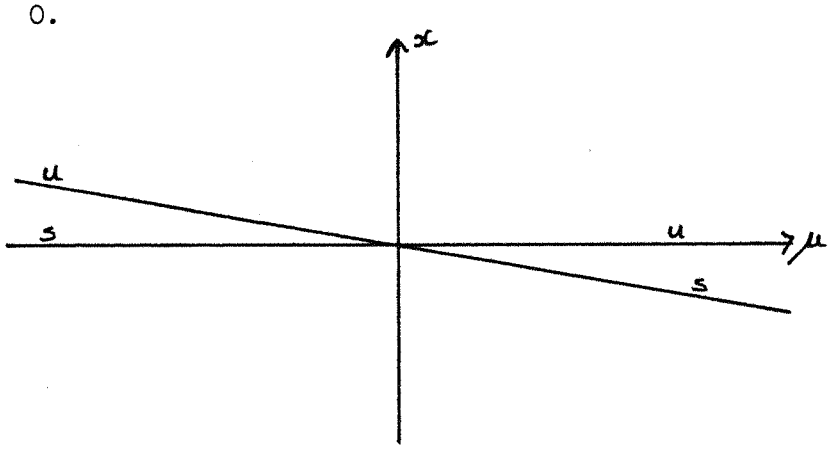

Figure 2.4. Transcritical Bifurcation.

Notice that this is the bifurcation which occurs in the family $f_\mu(x) = \mu x(1-x)$ at $\mu = 1$.

A second possibility is that the map should be restricted by a symmetry such as $F(-x,\mu) = -F(x,\mu)$, i.e. F is an odd function of x. In this case we necessarily have a trivial fixed point, $F(0,\mu) = 0$, but the previous proposition does not apply since we also have $\frac{\partial^2 F}{\partial x^2}(0,0) = 0$. Instead we have a Pitchfork bifurcation as described in the following result.

Proposition 2.4.

Let $F: \mathbb{R} \times \mathbb{R} \to \mathbb{R}$ be a one-parameter family of C^3 maps satisfying

(1) $F(-x,\mu) = -F(x,\mu)$

(2) $\frac{\partial F}{\partial x}(0,\mu) = \lambda(\mu)$, $\lambda(0) = 1$ and $\frac{d\lambda}{d\mu}(0) > 0$

(3) $\frac{\partial^3 F}{\partial x^3}(0,0) < 0$.

Then there are intervals $(\mu_1,0)$ and $(0,\mu_2)$ and $\varepsilon > 0$ so that

(i) if $\mu \in (\mu_1,0)$ then F_μ has a single stable fixed point, at the origin, in $(-\varepsilon,\varepsilon)$.

(ii) If $\mu \in (0,\mu_2)$ then F_μ has three fixed points in $(-\varepsilon,\varepsilon)$. The origin is an unstable fixed point while the other two fixed points are stable.

Proof. As in Proposition 2.3 put $F(x,\mu) = \lambda(\mu)x + xh(x,\mu)$, where $h(0,\mu) = 0$, $\frac{\partial h}{\partial \mu}(0,0) = 0$; but now h is even, i.e. $h(-x,\mu) = h(x,\mu)$ This implies that $\frac{\partial h}{\partial x}(0,0) = 0$ and therefore $\frac{\partial^2 F}{\partial x^2}(0,0) = 2\frac{\partial h}{\partial x}(0,0) = 0$.

The non-zero fixed points of F occur at the zeros of

$$g(x,\mu) = \lambda(\mu)x + xh(x,\mu)$$

and here

$$g(0,0) = 0 \qquad \frac{\partial g}{\partial \mu}(0,0) = \frac{d\lambda}{d\mu}(0) > 0 \quad \text{and} \quad \frac{\partial g}{\partial x}(0,0) = \frac{\partial h}{\partial x}(0) = 0$$

Therefore we may solve $g(x,\mu) = 0$ for a unique $\mu(x)$ for x near 0 with

$$\mu(0) = 0, \qquad \frac{d\mu}{dx}(0) = -\frac{\partial g}{\partial x}(g,0)/\frac{\partial g}{\partial \mu}(0,0) = 0$$

and

$$\frac{d^2\mu}{dx^2}(0) = -\frac{\partial^2 g}{\partial x^2}(0,0)/\frac{\partial g}{\partial \mu}(0,0) = -\frac{1}{3}\frac{\partial^3 F}{\partial x^3}(0,0)/\frac{d\lambda}{d\mu}(0) > 0$$

Here $\mu(x)$ has a minimum at $x = 0$ and the existence statements follow.

For the stability note that $\frac{\partial^2 F}{\partial x^2}(0,0) = 0$ and $\frac{\partial^3 F}{\partial x^3}(0,0) < 0$ imply that $\frac{\partial}{\partial x} F(x,\mu(x))$ has a maximum at $x = 0$.

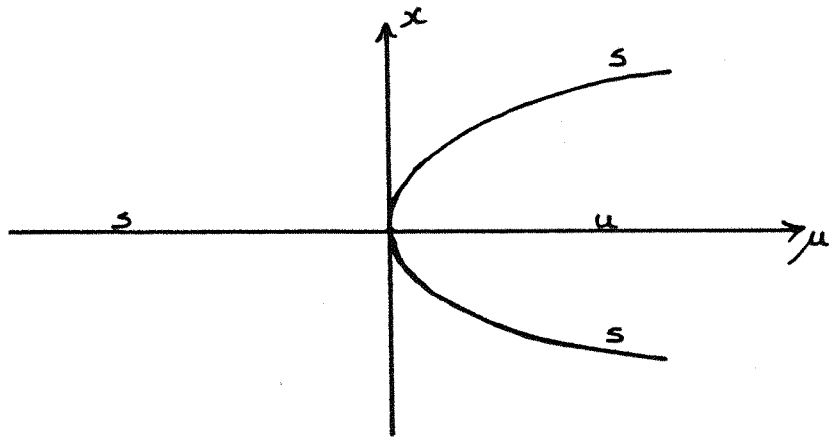

Figure 2.5. Pitchfork Bifurcation.

2.2. Hopf Bifurcation.

We now turn to maps of the plane, $F_\mu : \mathbf{R}^2 \to \mathbf{R}^2$, depending on a single real parameter μ. As usual we say that a hyperbolic fixed point p of F_μ is a sink, saddle or source according to whether $dF_\mu(p)$ has both eigenvalues strictly inside the unit circle in the complex plane, two real eigenvalues λ_1, λ_2, with $|\lambda_1| < 1 < |\lambda_2|$, or both eigenvalues with modulus strictly greater than one. If a single real eigenvalue crosses through ± 1 as the parameter is changed then, as indicated in the introduction to this chapter, we can reduce the problem to a family of maps in $\mathbf{R}$ and apply the results of the previous section. The possibility of most interest here however is that F_o has a fixed point at the origin and $dF_o(0)$ has a complex conjugate pair of eigenvalues on the unit circle. F_μ must then have a fixed point for μ near 0, which we may assume to lie at the origin, and if the eigenvalues pass out of the unit circle as μ passes through 0 then the origin changes from a sink to a source. The following theorem shows that, under certain conditions, an invariant circle bifurcates from the origin. For simplicity of exposition we assume F_μ is smooth (i.e. C^∞) and depends smoothly on the parameter.

Theorem 2.5. (Hopf Bifurcation Theorem)

Let F_μ be a one-parameter family of maps of $\mathbb{R}^2$ satisfying

(a) $F_\mu(0) = 0$ for μ near 0

(b) $dF_\mu(0)$ has two non-real eigenvalues $\lambda(\mu), \overline{\lambda(\mu)}$ for μ near 0 with $|\lambda(0)| = 1$

(c) $\left.\frac{d|\lambda(\mu)|}{d\mu}\right|_{\mu=0} > 0$

and (d) $\lambda = \lambda(0)$ is not an m-th root of unity for $m = 1,2,3$ or 4.

Then there is a smooth μ-dependent change of coordinates bringing F_μ into the form

$$F_\mu(X) = G_\mu(X) + O(|X|^5) \qquad X \in \mathbb{R}^2$$

and there are smooth functions a, b and θ so that in polar coordinates

$$G_\mu(r,\phi) = (|\lambda(\mu)|r - a(\mu)r^3,\ \phi + \theta(\mu) + b(\mu)r^2).$$

Moreoever, for all sufficiently small positive (negative) μ, F_μ has an attracting (repelling) invariant circle if $a(0) > 0$ ($a(0) < 0$); and $a(0)$ is given by the following formula:-

In complex notation we can write

$$F_o(z) = \lambda z + \sum_{\ell=2,3} \sum_{p+q=\ell} \xi_{pq} z^p \bar{z}^q + O(|z|^4)$$

and then

$$a(0) = \mathrm{Re}\left[\frac{(1-2\lambda)\bar{\lambda}^2}{(1-\lambda)} \xi_{11}\xi_{20}\right] + \frac{1}{2}|\xi_{11}|^2 + |\xi_{02}|^2 - \mathrm{Re}(\bar{\lambda}\xi_{21}) \quad (2.1)$$

The bifurcation is said to be <u>supercritical</u> if the circle exists for $\mu > 0$ and <u>subcritical</u> if it exists for $\mu < 0$. The two possibilities

are illustrated below, where the orbits of the map would be sequences of points lying on the curves shown

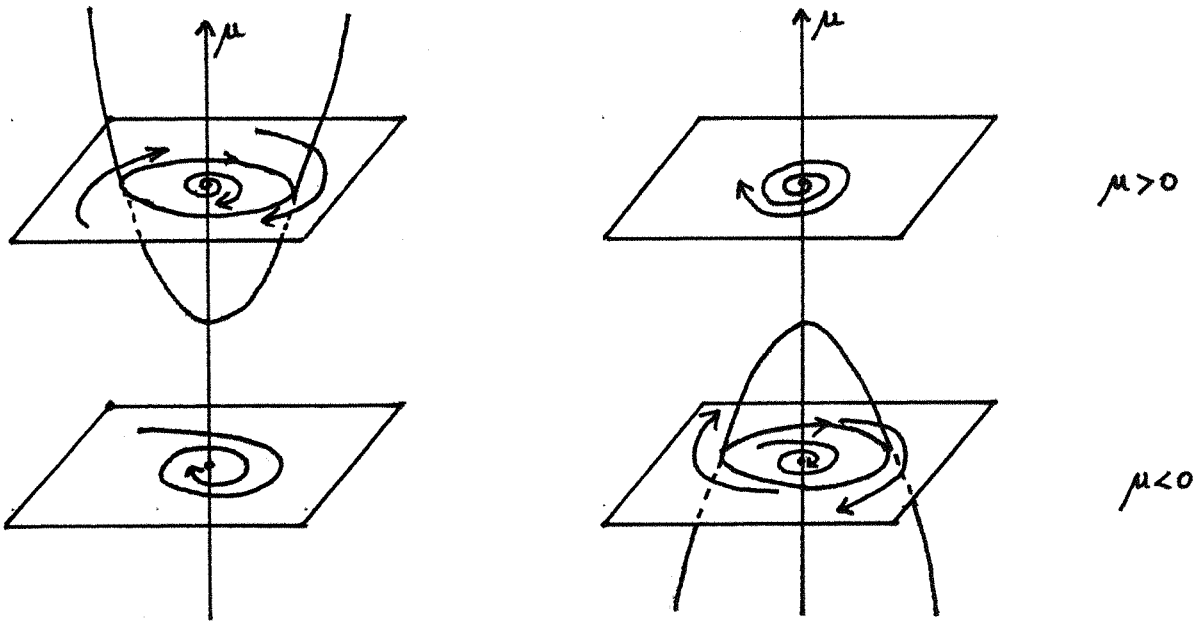

(a) Supercritical (b) Subcritical

Figure 2.6. Hopf Bifurcation

The theorem was originally proved independently by Sacker [33] and by Ruelle and Takens [32]. Below we sketch a proof due to Lanford [23] who also includes the condition $\lambda^5 \neq 1$. A modification to deal with this case may be found in Iooss [19] who gives more precise details of the differentiability conditions required and the regularity of the bifurcating circles. The formula for $a(0)$ is computed by Iooss [19] and by Wan [39].

Sketch of Proof

Since the eigenvalues cross the unit circle with non-zero speed (condition (c)), we may reparameterize so that the eigenvalues of $dF_\mu(0)$ are $(1+\mu)e^{\pm i\theta(\mu)}$ and then we make a smooth μ-dependent coordinate change so that

$$dF_\mu(0) = (1+\mu)\begin{pmatrix} \cos\theta(\mu) & -\sin\theta(\mu) \\ \sin\theta(\mu) & \cos\theta(\mu) \end{pmatrix}$$

In complex notation we then have a map of the form

$$F_\mu(z) = \lambda(\mu)z + R(z,\bar{z},\mu) \qquad z \in \mathbb{C}$$

where R contains the non-linear terms, and we use the following lemma to bring F_μ into the appropriate canonical form.

Lemma 2.6. If $\lambda^n \neq 1$, $n = 1,2,3$ or 4, then there is a smooth μ-dependent change of coordinates bringing F_μ into the form

$$F_\mu(z) = \lambda(\mu)z + \alpha(\mu)z^2\bar{z} + \beta(\mu)\bar{z}^4 + O(|z|^5)$$

Furthermore, if $\lambda^5 \neq 1$ we can make $\beta(\mu) \equiv 0$.

Proof Write $R(z,\bar{z},\mu) = \sum_{\ell=2,3,4} \sum_{p+q=\ell} \xi_{pq}(\mu)z^p\bar{z}^q + O(|z|^5)$ where the ξ_{pq} are smooth for μ near 0. The idea of the proof is to remove as many of the non-linear terms in R as possible, starting with the quadratic terms and dealing successively with terms of higher order. For the quadratic terms, define

$$w = z+\gamma(z) \tag{2.2}$$

where γ is a homogeneous function of degree 2 in z and $\bar{z}$:

$$\gamma(z) = \sum_{p+q=2} \gamma_{pq}(\mu)z^p\bar{z}^q$$

Inverting (2.2) we have

$$z = w - \gamma(w) + O(|w|^3) \tag{2.3}$$

and in the w coordinates the map becomes

$$\tilde{F}(w) = F(z) + \gamma(F(z))$$

where, by (2.3),

$$F(z) = \lambda w - \lambda\gamma(w) + \sum_{p+q=2} \xi_{pq} w^p \bar{w}^q + O(|w|^3)$$

and

$$\gamma(F(z)) = \gamma(\lambda w) + O(|w|^3)$$

Therefore

$$\tilde{F}(w) = \lambda w + (\xi_{20} - \xi_{20} + \lambda^2\gamma_{20})w^2 + (\xi_{11} - \lambda\gamma_{11} + \lambda\bar{\lambda}\gamma_{11})w\bar{w} + (\xi_{02} - \lambda\gamma_{02} + \bar{\lambda}^2\gamma_{02})\bar{w}^2.$$

Since $\lambda \neq 1$ and $\lambda^3 \neq 1$ we can remove all the quadratic terms by choosing

$$\gamma_{20}(\mu) = \frac{\xi_{20}(\mu)}{\lambda(\mu) - \lambda^2(\mu)}, \quad \gamma_{11}(\mu) = \frac{\xi_{11}(\mu)}{\lambda(\mu)(1 - \bar{\lambda}(\mu))}, \quad \gamma_{02}(\mu) = \frac{\xi_{02}(\mu)}{\lambda(\mu) - \bar{\lambda}^2(\mu)}$$

In general, if we make a coordinate change of the form (2.2) with γ homogeneous of degree ℓ in z and $\bar{z}$, and if $\tilde{\xi}_{pq}(\mu)$ is the coefficient of $w^p\bar{w}^q$ in $\tilde{F}(w)$, then

$$\tilde{\xi}_{pq}(\mu) = \xi_{pq}(\mu) - (\lambda(\mu) - \lambda^p(\mu)\,\bar{\lambda}(\mu)^q)\gamma_{pq}$$

Thus we can choose γ_{pq} to make $\tilde{\xi}_{pq}$ vanish except in the cases when

$$\lambda^{p-q-1} = 1, \quad p+q = \ell.$$

Therefore if $\lambda^n \neq 1$ for $n = 1,2,3,4$ or 5 the only term which cannot be removed is that in $z^2\bar{z}$, while if $\lambda^5 = 1$ we cannot remove the term in $\bar{z}^4$. If we carry through all the coordinate changes then a long calculation shows that

$$\alpha(0) = \xi_{11}\xi_{20}\frac{(2\lambda-1)}{\lambda(1-\lambda)} + \frac{|\xi_{11}|^2}{1-\bar{\lambda}} + \frac{2|\xi_{02}|^2}{\lambda^2-\bar{\lambda}} + \xi_{21}. \tag{2.4}$$

Having obtained a suitable normal form the the map the next step is to change to polar coordinates. Let $z = re^{i\phi}$, $F(z) = Re^{i\Phi}$, then

$$\begin{cases} R = (1+\mu)r + a_3(\mu)r^3 + a_4(\mu,\phi)r^4 + O(r^5) \\ \Phi = \phi + \theta(\mu) + b_2(\mu)r^2 + b_3(\mu,\phi)r^3 + O(r^4) \end{cases} \tag{2.5}$$

where

$$a_3(\mu) = \mathrm{Re}[\alpha(\mu)e^{-i\theta(\mu)}] \qquad b_2(\mu) = \mathrm{Im}[\frac{\alpha(\mu)}{\lambda(\mu)}]$$

$$a_4(\mu,\phi) = \mathrm{Re}[\beta(\mu)e^{-i\theta(\mu)-5i\phi}] \quad b_3(\mu,\phi) = \mathrm{Im}[\frac{\beta(\mu)}{\lambda(\mu)}e^{-5i\phi}]$$

Let $a(\mu) = -a_3(\mu)$ and assume $a(0) \neq 0$. Then $a(0) = -\mathrm{Re}[\alpha(0)\bar{\lambda}]$ may be found from (2.4) and has the value given in the statement of the theorem. F_o now takes the form

$$\begin{cases} R = r(1 - a(0)r^2) + O(r^4) \\ \Phi = \phi + \theta(0) + O(r^2) \end{cases}$$

so when $\mu = 0$ the origin is asymptotically stable if $a(0) > 0$ and unstable if $a(0) < 0$.

We illustrate the rest of the proof for the supercritical case $a(0) > 0$. For $a(0) < 0$ the proof proceeds in a similar manner.

First suppose that $\lambda^5 \neq 1$, then by lemma 2.6 we can make the coefficients a_4 and b_3 vanish and the map is

$$\begin{cases} R = (1+\mu)r - a(\mu)r^3 + O(r^5) \\ \Phi = \phi + \theta(\mu) + b_2(\mu)r^2 + O(r^4) \end{cases}$$

Ignoring the terms $O(r^5)$ in the r coordinate and $O(r^4)$ in ϕ gives a truncated map which has an invariant circle of radius $r_o = \sqrt{\frac{\mu}{a(\mu)}}$ for small positive μ. Since the full map is only a small perturbation of the truncated map we look for an invariant circle for the full map close to the circle of radius r_o which is invariant for the truncation. We make the following sequence of coordinate changes:

(1) Rescale so the invariant circle for the truncated map has unit radius:

$$r \mapsto \sqrt{\frac{a(\mu)}{\mu}}\, r$$

(2) Translate the line $r = 1$ in the (r,ϕ)-plane to the ϕ-axis:

$$r \mapsto r-1$$

and (3) Rescale once more:

$$r \mapsto \frac{1}{\sqrt{\mu}}\, r$$

The effect of all this is to introduce a new coordinate

$$x = \frac{1}{\sqrt{\mu}} \left(\sqrt{\frac{a(\mu)}{\mu}}\, r - 1 \right) \tag{2.6}$$

and in the (x,ϕ)-plane the map takes the form

$$\begin{cases} X = (1-2\mu)x + \mu^{3/2} X_1(x,\phi,\mu) \\ \Phi = \phi + \theta_1(\mu) + \mu^{3/2} \Phi_1(x,\phi,\mu) \end{cases} \tag{2.7}$$

where X_1 and Φ_1 are smooth in x,ϕ and μ for $|x| \leq 1$, $\phi \in [0,2\pi]$ and μ small.

For each small, positive μ we look for an invariant manifold of the form $M = \{x = u(\phi)\}$ where

(i) $u(\phi)$ is periodic in ϕ with period 2π,

(ii) $\forall\ \phi$, $|u(\phi)| \leq 1$,

and(iii) $u(\phi)$ is Lipschitz continuous with Lipschitz constant 1

i.e. $|u(\phi_1) - u(\phi_2)| \leq |\phi_1 - \phi_2|$

Let U denote the set of all functions $u: \mathbb{R} \to \mathbb{R}$ satisfying (i) - (iii). Then U is a complete metric space with metric

$$d(u_1,u_2) = \sup_{\phi\in[0,2\pi]} |u_1(\phi)-u_2(\phi)|$$

The main steps in the proof are now to start with a manifold $M = \{x = u(\phi)\}$ with $u \in U$ and to show that the new manifold $F_\mu(M)$ obtained by acting on M by F_μ also has the form $\{x = \hat{u}(\phi)\}$ with $\hat{u} \in U$. The non-linear mapping $f: U \to U$ constructed in this way is then shown to be a contraction for small $\mu > 0$. The Contracting Mapping Principle now guarantees a unique fixed point u^* of f and $\{x = u^*(\phi)\}$ is the required invariant circle. We also have that the circle is attracting, in the sense that if $|x| \leq 1$ and (x_n,ϕ_n) denotes $F^n(x,\phi)$ then

$$\lim_{n\to\infty} (x_n - u^*(\phi_n)) = 0.$$

In the case when $\lambda^5 = 1$, defining x by (2.6) transforms (2.5) to

$$\begin{cases} X = (1-2\mu)x + \mu f(\phi) + \mu^{3/2} X_1(x,\phi,\mu) \\ \Phi = \phi + \frac{2\pi}{5} + A\mu + \mu^{3/2}\ \Phi_1(x,\phi,\mu) \end{cases}$$

where $A = \dfrac{b_2(0)}{a_3(0)}$ and $f(\phi) = \dfrac{a_4(0,\phi)}{a_3(0)^{3/2}}$ has period $\dfrac{2\pi}{5}$ in ϕ. We now look for a change of coordinates so the map takes the form (2.7). Let

$\tilde{x} = x+g(\phi)$ with $g(\phi + \frac{2\pi}{5}) = g(\phi)$; then $\tilde{X} = X + g(\phi)$ satisfies

$$\tilde{X} = (1-2\mu)[\tilde{x}-g(\phi)] + \mu f(\phi) + g(\phi + \frac{2\pi}{5} + A\mu + O(|\mu|^{3/2})) + O(|\mu|^{3/2})$$

Thus we have

$$\tilde{X} = (1-2\mu)\tilde{x} + O(|\mu|^{3/2})$$

provided

$$A \frac{dg}{d\phi}(\phi) + 2g(\phi) + f(\phi) = 0.$$

So we choose a smooth $g(\phi)$ of period $\frac{2\pi}{5}$ which solves this linear differential equation and continue from (2.7) as before.

Remarks 1. The region $|x| \leq 1$ corresponds to an annulus of width $O(\mu)$ about the circle of radius r_o for the truncated map. It is not difficult to show that the basin of attraction of the invariant circle is larger than this annulus and in particular it contains all points inside the circle, except the fixed point. See Iooss [19] for the details.

2. The proof sketched above uses the fact that F_μ is C^k, $k \geq 5$, and asserts that the invariant circle is Lipschitz continuous. By assuming more differentiability of F we can obtain a smoother circle. For details see Iooss [19] or Lanford [23].

3. The essential point in the proof is that when the full map is considered as a perturbation of its truncation then the perturbation must tend to zero faster than μ as $\mu \to 0$. i.e. in the $\mu^{3/2}X_1(x,\phi,\mu)$ term which appears in the x-coordinate, and in the similar term in ϕ, the crucial fact is that the power of μ which appears is larger than one.

Dynamics on the Invariant Circle

Having obtained a (locally) attracting invariant circle the next task is to understand the behaviour of the map restricted to the circle. There are essentially only two possibilities for the non-wandering set $\Omega(F)$, and to distinguish between the two we need the concept of the rotation number ρ of F, an idea which dates back to Poincaré. We describe briefly the definition and properties of ρ; a detailed account may be found in Nitecki [31].

A homeomorphism $F: S^1 \to S^1$ lifts to a map $\tilde{F}: \mathbb{R} \to \mathbb{R}$ via the projection $\exp: \mathbb{R} \to S^1$, $t \to e^{2\pi i t}$. The limit $\rho(F) = \lim_{n\to\infty} \frac{\tilde{F}^n(t)-t}{n}$ exists, is independent of the choice of $\tilde{F}$ and t, and is called the Rotation Number of F. $\rho(F)$ is a continuous function of F in the C^0-topology and has the following basic properties:

(a) If $\rho(F) \in \mathbb{Q}$, $\rho(F) = p/q$ say, then F has a periodic orbit of period q.

(b) If $\rho(F) \in \mathbb{R}\backslash\mathbb{Q}$ then F has no periodic orbit.

If we assume that F is C^1 and its derivative dF has bounded variation then a result of Denjoy states that if $\rho(F) \in \mathbb{R}\backslash\mathbb{Q}$ then F is topologically conjugate to rotation by $\rho(F)$. i.e. there is a homeomorphism $h: S^1 \to S^1$ with $F = h^{-1}R_\rho h$, where $R_\rho: \theta \to \theta+\rho \pmod 1$. For further results on conjugating F with an irrational rotation see Herman [18].

So assuming F is sufficiently smooth, the two possibilities are either

(i) $\rho(F)$ is irrational, in which case F is conjugate to an irrational rotation and $\Omega(F) = S^1$ with the orbit of each point dense in the circle,

or

(ii) $\rho(F)$ is rational, and $\Omega(F)$ contains a periodic orbit.

From the generic point of view the following theorem shows that it is this latter case which occurs.

Theorem (Peixoto)

An open, dense subset of $\mathrm{Diff}^r(S^1)$, $r \geq 1$, consists of diffeomorphisms with the following properties

(i) The non-wandering set $\Omega(F)$ is finite,

(ii) All periodic points of F are hyperbolic.

Any diffeomorphism satisfying (i) and (ii) is structurally stable.

For the proof see Nitecki [31].

Thus the structurally stable diffeomorphisms of the circle are those with rational rotation number and $\Omega(F)$ consists of a finite number of periodic orbits, all of the same period, with sinks and sources alternating around the circle. However, in our application above we have a one-parameter family of diffeomorphisms F_μ and Herman [17] has shown that in such a family with $\mu \in [a,b]$ say, then provided $\rho(F_a) \neq \rho(F_b)$ the set of parameter values μ with F_μ conjugate to an irrational rotation has positive Lebesgue measure. So if we pick a value of μ at random and examine the dynamics of F_μ on the bifurcating circle then generically we expect to see periodic orbits on the circle, but from a measure theoretic point of view we may easily have chosen a μ with F_μ conjugate to an irrational rotation and see an orbit of F_μ which is dense in the circle. Clearly this makes it very difficult indeed to predict which type of behaviour will occur--regardless of any problems we may have in identifying periodic orbits with very large periods. A clearer picture of what happens after the Hopf bifurcation emerges when we study the behaviour of two-parameter families in the next section.

§2.3. Weak Resonance

To understand the dynamics of a family of maps after the Hopf bifurcation requires a closer study of those cases where the eigenvalues cross the unit circle at roots of unity: $\lambda = e^{2\pi ip/q}$, with p/q in lowest terms. These cases fall into two types. The pair (p,q) is said to be a strong resonance if $q = 1,2,3$ or 4, otherwise it is a weak resonance. We deal here with the latter case; the strong resonances involve some unsolved problems and are discussed in the next section.

Now for a one-parameter family $F_\varepsilon:(\mathbb{R}^2,0) \to (\mathbb{R}^2,0)$ whose linearization at the origin $dF_\varepsilon(0)$ has a complex-conjugate pair of eigenvalues $\lambda(\varepsilon),\overline{\lambda(\varepsilon)}$ crossing the unit circle transversely when $\varepsilon = 0$, an orbit of period q can bifurcate from 0 only if $\lambda(0)$ is a q-th root of unity. But Brunovsky [5] has shown that, generically, the eigenvalues of a one-parameter family do not cross the unit circle at roots of unity. So from the generic point of view periodic points never bifurcate from a fixed point of a one-parameter family of maps of $\mathbb{R}^2$ through Hopf bifurcation. However, this is rather misleading since, as we shall see below, in general an infinite number of periodic orbits are created and destroyed on the invariant circle soon after the Hopf bifurcation.

Consider a smooth two-parameter family $F_{(\mu,\nu)}:(\mathbb{R}^2,0) \to (\mathbb{R}^2,0)$ where the eigenvalues of $dF_{(\mu,\nu)}(0)$ are $\lambda(\mu,\nu),\overline{\lambda(\mu,\nu)}$ and $\lambda(0,0)$ is a q-th root of unity. Both Arnold [3] and Takens [38] approximate the map by

$$F_{(\mu,\nu)}(z) = g_{(\mu,\nu)}(z) + O(|z|^N)$$

where N is arbitrarily large and $g_{(\mu,\nu)}$ is the time-one map of a vector field invariant under rotations by $2\pi/q$. For the case of weak resonance, $q \geq 5$, the bifurcation diagram for this vector field is shown in Figure 2.7, and since each corresponding phase portrait for the time-one map $g_{(\mu,\nu)}$

is structurally stable these phase portraits will persist for the map $F_{(\mu,\nu)}$.

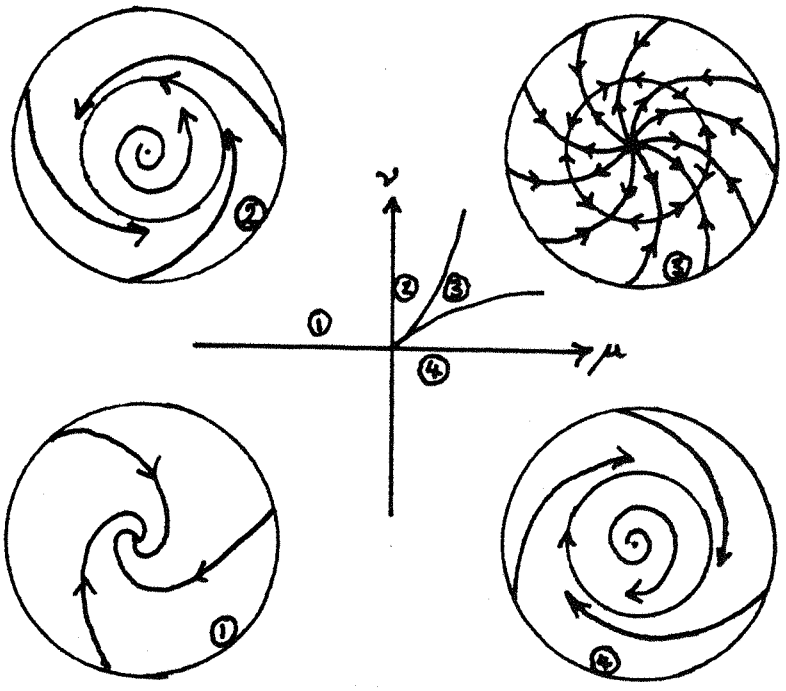

Figure 2.7. Weak Resonance.

We will prove that this is the bifurcation diagram for $F_{(\mu,\nu)}$ - up to a change of parameters and with the obvious changes from a continuous flow to a discrete one - by adapting the analysis of Iooss [19] from the one-parameter to the two-parameter case.

Theorem 2.7. (Weak Resonance)

Let $F_{(\mu,\nu)}$ be a smooth, two-parameter family of maps of $\mathbb{R}^2$ such that for all (μ,ν) in some neighbourhood U of 0 in $\mathbb{R}^2$

(a) $F_{(\mu,\nu)}(0) = 0$

(b) $dF_{(\mu,\nu)}(0)$ has a pair of complex conjugate eigenvalues $\lambda(\mu,\nu)$ and $\overline{\lambda}(\mu,\nu)$ with $|\lambda(0,0)| = 1$ and Arg $\lambda(0,0) = \frac{2\pi p}{q}$, with p/q in lowest terms and $q \geq 5$,

and

(c) The map $(\mu,\nu) \mapsto \lambda(\mu,\nu)$ is non-singular at $\mu = \nu = 0$.

Then there is a smooth, parameter-dependent change of coordinates bringing $F_{(\mu,\nu)}$ into the form

$$F_{(\mu,\nu)}(z) = \lambda(\mu,\nu)z + \sum_{m=1}^{[\frac{q-2}{2}]} \alpha_{2m+1} z^{m+1}\bar{z}^{m} \pm \beta(\mu,\nu)\bar{z}^{q-1} + O(|z|^q) \qquad (2.8)$$

or in polar coordinates, $z = re^{i\phi}$, $G_{(\mu,\nu)}(z) = Re^{i\Phi}$,

$$\begin{cases} R = |\lambda(\mu,\nu)|r + \sum_{m=1}^{[\frac{q-2}{2}]} a_{2m+1}(\mu,\nu)r^{2m+1} + \tilde{a}_{q-1}(\mu,\nu,\phi)r^{q-1} + O(r^q) \\ \Phi = \phi + \text{Arg}\,\lambda(\mu,\nu) + \sum_{m=1}^{[\frac{q-2}{2}]} b_{2m}(\mu,\nu)r^{2m} + \tilde{b}_{q-2}(\mu,\nu,\phi)r^{q-2} + O(r^{q-1}) \end{cases} \qquad (2.9)$$

Here $[\frac{q-2}{2}]$ denotes the integer part of $\frac{q-2}{2}$, the a's and b's, α's and β are smooth functions of μ and ν for (μ,ν) near $(0,0)$, and $\tilde{a}_{q-1}$ and $\tilde{b}_{q-2}$ both have the form

$$A(\mu,\nu)\cos(q\phi) + B(\mu,\nu)\sin(q\phi) \qquad (2.10)$$

For all sufficiently small (μ,ν) with $|\lambda(\mu,\nu)| > 1$ ($|\lambda(\mu,\nu)| < 1$) the map $F_{(\mu,\nu)}$ has an attracting (repelling) invariant circle if $a_3(0,0) < 0$ ($a_3(0,0) > 0$).

Moreover, if $\beta = \beta(0,0) \neq 0$ and $b_2 = b_2(0,0) \neq 0$ then the map has two orbits of period q on the circle, one stable and the other unstable, for values of μ,ν lying within a narrow "tongue" in the parameter plane whose boundaries

$$\nu \simeq \frac{b_2}{a_3}\mu \pm \frac{|\beta|^2}{a_3^{\frac{q-2}{2}}}\mu^{\frac{q-2}{2}}$$

have a common tangent at $\mu = \nu = 0$.

Proof The normal form (2.8) follows from the proof of lemma 2.6.

and in polar coordinates this gives (2.9), where

$$a_3(\mu,\nu) = \mathrm{Re}[\alpha_3(\mu,\nu)\, e^{-i\mathrm{Arg}\lambda(\mu,\nu)}], \quad b_2(\mu,\nu) = \mathrm{Im}\,[\frac{\alpha_3(\mu,\nu)}{\lambda(\mu,\nu)}] \tag{2.11}$$

$$\tilde{a}_{q-1}(\mu,\nu,\phi) = \mathrm{Re}[\beta(\mu,\nu)e^{-iq\phi-i\mathrm{Arg}\lambda(\mu,\nu)}], \quad \tilde{b}_{q-2}(\mu,\nu,\phi) = \mathrm{Im}[\frac{\beta(\mu,\nu)}{\lambda(\mu,\nu)} e^{-iq\phi}]$$

We now reparameterize, defining $\tilde{\mu},\tilde{\nu}$ by

$$\tilde{\mu} = |\lambda(\mu,\nu)| - 1, \quad \tilde{\nu} = \mathrm{Arg}\lambda(\mu,\nu) - \frac{2\pi p}{q}$$

The map $(\mu,\nu) \mapsto (\tilde{\mu},\tilde{\nu})$ is a diffeomorphism from a neighbourhood of the origin in the (μ,ν)-plane to a neighbourhood of the origin in the $(\tilde{\mu},\tilde{\nu})$-plane by (c). Omitting the tilde on the new parameters, the full map in polar coordinates becomes

$$\begin{cases} R = (1+\mu)r + \Sigma a_{2m+1}(\mu,\nu)r^{2m+1} + \tilde{a}_{q-1}(\mu,\nu,\phi)r^{q-1} + O(r^q) \\ \Phi = \phi + \frac{2\pi p}{q} + \nu + \Sigma\, b_{2m}(\mu,\nu)r^{2m} + \tilde{b}_{q-2}(\mu,\nu,\phi)r^{q-2} + O(r^{q-1}) \end{cases}$$

where the functions a_{2m+1}, b_{2m}, $\tilde{a}_{q-1}$ and $\tilde{b}_{q-2}$ are of course different to those in (2.9), but their values at $\mu = \nu = 0$ remain unaltered.

We now proceed as in the proof of Theorem 2.5, restricting attention to the supercritical case $a_3(0,0) < 0$. Truncating the map at terms of order $q-1$ in the r coordinate and looking for a fixed point $R = r$ leads to

$$\mu + \Sigma\, a_{2m+1} r^{2m} = 0$$

which has a unique positive solution $r_o(\mu,\nu)$ near $\mu = \nu = 0$ for $\mu > 0$ with

$$r_o^2(\mu,\nu) = \frac{-\mu}{a_3(\mu,\nu)} + O(\mu^2).$$

Returning to the full map, define a new coordinate x by

$$r = r_o(\mu,\nu)(1 + \mu^{\frac{q-4}{2}} x).$$

so the map becomes

$$\begin{cases} X = (1-2\mu)x + \mu f(\mu,\nu,\phi) + O(\mu^{3/2}) \\ \Phi = \phi + \frac{2\pi p}{q} + \nu + \sum_{n=1}^{[\frac{q-2}{2}]} \hat{b}_m(\mu,\nu)\mu^m + \left[\frac{2b_2(\mu,\nu)}{a_3(\mu,\nu)} x + \frac{\tilde{b}_{q-2}(\mu,\nu,\phi)}{a_3(\mu,\nu)^{\frac{q-2}{2}}}\right]\mu^{\frac{q-2}{2}} + O(\mu^{\frac{q-1}{2}}) \end{cases}$$

where

$$f(\mu,\nu,\phi) = \frac{\tilde{a}_{q-1}(\mu,\nu,\phi)}{a_3(\mu,\nu)^{\frac{q-2}{2}}} \quad \text{and} \quad \hat{b}_1 = \frac{b_2(\mu,\nu)}{a_3(\mu,\nu)}.$$

Next we make a coordinate change similar to that for the case $\lambda^5 = 1$ in the proof of Theorem 2.5. Let $x = g(\mu,\nu,\phi) + \mu^\gamma \tilde{x}$, where $0 < \gamma < \frac{1}{2}$ and $g(\mu,\nu,\phi) = O(|\mu|^{1/2})$ has the form (2.9) and satisfies the differential equation

$$2g(\mu,\nu,\phi) + \frac{1}{\mu}(\nu + \Sigma\hat{b}_m(\mu,\nu)\mu^n)\frac{\partial g}{\partial \phi}(\mu,\nu,\phi) = f(\mu,\nu,\phi).$$

Now

$$\begin{cases} \tilde{X} = (1-2\mu)x + O(\mu^{3/2-\gamma}) \\ \Phi = \phi + \frac{2\pi p}{q} + \nu + \Sigma\hat{b}_n\mu^n + \hat{b}(\mu,\nu,\phi)\mu^{\frac{q-2}{2}} + O(\mu^{\frac{q}{2}+\gamma-1}) \end{cases} \tag{2.12}$$

where

$$\hat{b}(\mu,\nu,\phi) = \frac{\tilde{b}_{q-2}(\mu,\nu,\phi)}{a_3(\mu,\nu)^{\frac{q-2}{2}}}$$

has the form (2.10). The proof of Theorem 2.5 now applies since $3/2 - \gamma > 1$, (see remark 3 above), and the statements on the existence of the invariant circle follow immediately.

Now consider the map on the invariant circle given by the second equation in (2.1), which we write as

$$F_{(\mu,\nu)}(\phi) = \phi + \frac{2\pi p}{q} + f_{(\mu,\nu)}(\phi) + \mu^{q/2+\gamma-1}\, g_{(\mu,\nu)}(\phi) \quad (\mathrm{mod}\, 2\pi)$$

For fixed μ and ν, $f_{(\mu,\nu)}(\phi)$ takes the form $A + B\cos q\phi + C\sin q\phi$ and the equation $f_{(\mu,\nu)}(\phi) = 0$ has two solutions ϕ_1^o, ϕ_2^o with $0 \le \phi_1^o < \phi_2^o = \phi_1^o + \frac{\pi}{q} < \frac{2\pi}{q}$ provided

$$|\nu + \Sigma \hat{b}_n \mu^n| < \sup_{\phi \in [0,2\pi]} \hat{b}(\mu,\nu,\phi)\mu^{\frac{q-2}{2}}.$$

This defines the region of the parameter plane whose boundaries are given in the statement of the theorem.

It now follows from the Implicit Function Theorem that the equation

$$F^q_{(\mu,\nu)}(\phi) = \phi \pmod{2\pi} \quad \text{with} \quad 0 \le \phi < \frac{2\pi}{q}$$

has two solutions $\phi_1(\mu,\nu)$ and $\phi_2(\mu,\nu)$ which depend smoothly on μ,ν within the cusped region and also

$$\phi_i(\mu,\nu) = \phi_i^o + O(\mu^\gamma) \quad i = 1,2$$

The two families of periodic points are then $F^n_{(\mu,\nu)}(\phi_i(\mu,\nu))$, $n = 0,1,\ldots,q-1$; $i = 1,2$.

If the original family of maps were only C^5 then the map restricted to the invariant circle is Lipshitz continuous and the existence of the periodic points follows from a suitable version of the Contraction Mapping Theorem, for example, see Dieudonné [9], p. 260.

For the stability of the periodic points note that

$$F'_{(\mu,\nu)}(\phi_i(\mu,\nu)) = 1 + \hat{b}'(\mu,\nu,\phi_i^o) + O(\mu^{q/2+\gamma-1})$$

and since $\hat{b}'(\mu,\nu,\phi_1^o) = -\hat{b}'(\mu,\nu,\phi_2^o)$ the two families of periodic points have opposite stabilities, and the proof is complete.

Returning to the one-parameter family F_ε, we may embed it in a two-parameter family by considering the real and imaginary parts of the eigenvalue $\lambda(\varepsilon)$ as parameters. Now the eigenvalue $\lambda(\varepsilon)$ corresponds to a path in the $(Re\lambda, Im\lambda)$-plane which in general, as noted by Arnol'd, will intersect an infinite number of these resonance tongues close to the unit circle, as shown in figure 2.8. Thus we can expect to see many periodic orbits, most with very large periods, on the invariant circle soon after the Hopf bifurcation, but the result of Herman implies that the set of parameter values not belonging to any of these tongues has positive lebesgue measure.

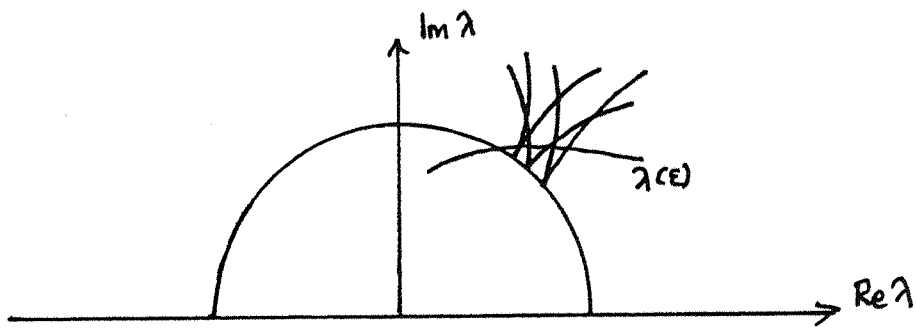

Figure 2.8. (After Arnol'd)

2.4 Strong Resonance

The strong resonances, $\lambda = e^{2\pi ip/q}$, $q = 1, 2, 3$ and 4, which are excluded in the Hopf Bifurcation Theorem 2.5, exhibit rather different behaviour. For $q = 1$ and 2 the bifurcation diagrams for the associated vector fields are again given by Arnol'd [2], [3] and Takens [38]. However these diagrams include a codimension one global bifurcation

involving a saddle loop. That is, along a curve in the parameter plane the vector field has an equilibrium point, a saddle, and the vector field has a trajectory which is asymptotic to the saddle both as $t \to \infty$ and as $t \to -\infty$. The analogue of this situation for a diffeomorphism can be perturbed so that the stable and unstable manifolds of the saddle intersect transversely, giving homoclinic points and horseshoes (Smale [35]), but the details of how this structure arises in the families of interest here are not known.

For $q = 3$ the bifurcation diagram for the vector field is shown in Figure 2.9.

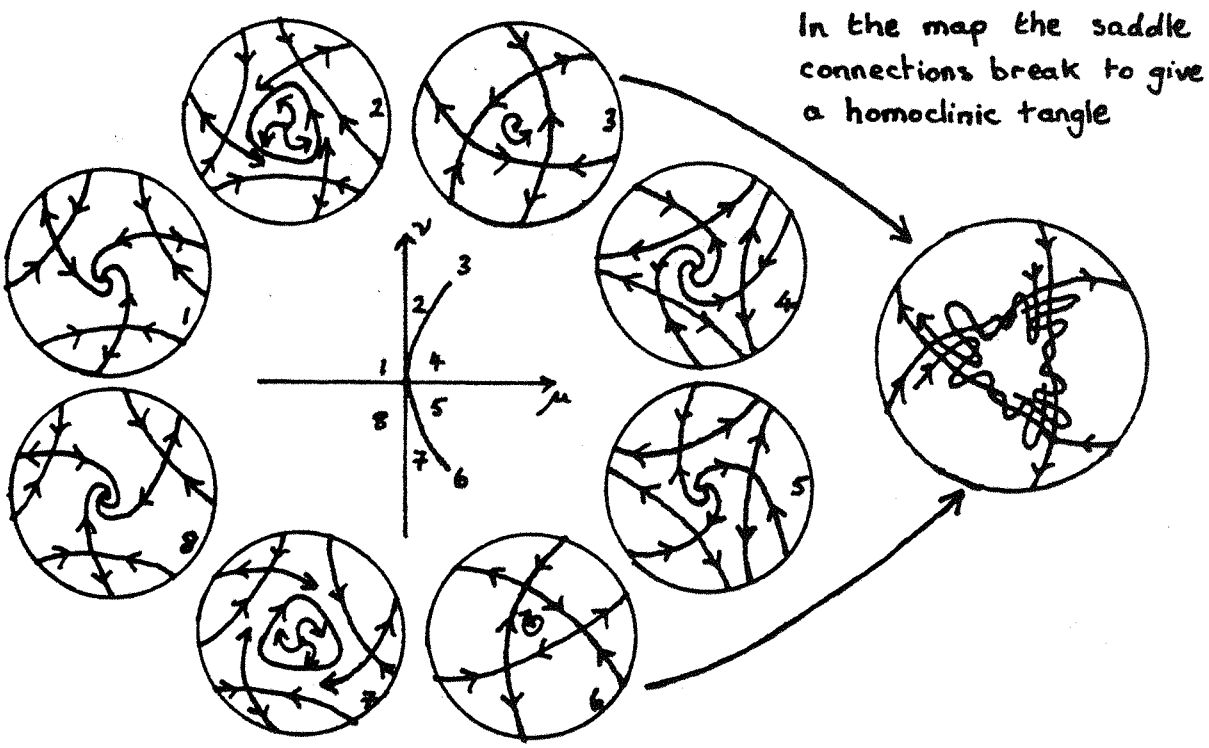

Figure 2.9. Strong Resonance: $q = 3$.

When viewed as the bifurcation diagram for the time-one map the saddle connections which occur can be broken by a small perturbation as shown in the figure, though the saddle points persist as a period three orbit for the map. In fact for a one-parameter family passing through a

strong resonance with $q = 3$ Lemma 2.6 shows that the normal form is

$$F_\mu(z) = \lambda(\mu)z + \alpha(\mu)z^2\bar{z} + \beta(\mu)\bar{z}^2 + O(|z|^4), \quad \lambda(0) = e^{2\pi i/3}$$

and Iooss [19] proves that if $\left.\frac{d|\lambda(\mu)|}{d\mu}\right|_{\mu=0} \neq 0$ and $\beta(0) \neq 0$ then a period three orbit of saddles bifurcates from the origin on both sides of $\mu = 0$.

The results for the case $q = 4$ are even less complete. For a one-parameter family the normal form is

$$F_\mu(z) = \lambda(\mu)z + \alpha(\mu)z^2\bar{z} + \beta(\mu)\bar{z}^3 + O(|z|^5)$$

and if we assume $\left.\frac{d|\lambda(\mu)|}{d\mu}\right|_{\mu=0} > 0$ and let $\lambda_1 = \left.\frac{d\lambda(\mu)}{d\mu}\right|_{\mu=0}$ the following theorem holds.

Theorem 2.8. (1) Suppose that $\left|\operatorname{Im}\frac{\dot{\alpha}(0)}{\lambda_1}\right| > \left|\frac{\beta(0)}{\lambda_1}\right|$. Then no orbit of period four bifurcates from the origin. If $\operatorname{Re}(i\alpha(0)) > 0$ (< 0) then an attracting (repelling) invariant circle bifurcates from the origin for $\mu > 0$ (< 0).

(2) If $\left|\operatorname{Im}\frac{\alpha(0)}{\lambda_1}\right| < \left|\frac{\beta(0)}{\lambda_1}\right|$ then two families of fixed points of F^4 bifurcate from the origin. If $|\alpha(0)| > |\beta(0)|$ the two families bifurcate on the same side of $\mu = 0$ and at least one of the families is unstable, while if $|\alpha(0)| < |\beta(0)|$ the two families bifurcate on opposite sides of $\mu = 0$ and both are unstable.

The statements concerning the periodic points are due to Iooss [19] and the existence of the invariant circle in (1) is proved by Wan [40]. In (2), conditions ensuring the bifurcation of a circle along with the periodic points are unknown.

For a two-parameter family two possibilities for the bifurcation diagram are: (i) the same as in the case of weak resonance, but with

periodic orbits on the circle inside a sector in the parameter plane rather than a cusp, or (ii) the same as figure 2.9, but with an orbit of period four rather than three. A further possibility is given by Arnol'd [3]. We will investigate the first possibility.

Consider the family

$$F_{(\mu,\nu)}(z) = i(1+\mu)e^{i\nu}z + \alpha(\mu,\nu)z^2\bar{z} + \beta(\mu,\nu)\bar{z}^3 + O(|z|^5)$$

obtained from the normal form by reparameterizing. In polar coordinates $z = re^{i\phi}$, $F(z) = Re^{i\Phi}$,

$$\begin{cases} R = (1+\mu)r + \mathrm{Re}Ar^3 + O(r^5) \\ \Phi = \phi + \frac{\pi}{2} + \nu + \mathrm{Im}Ar^2 + O(r^4) \end{cases}$$

where $A = -i\alpha(\mu,\nu)e^{i\nu} - i\beta(\mu,\nu)e^{i\nu}e^{-4i\phi}$

$$= -i[\alpha(0,0) + \beta(0,0)e^{-4i\phi}] + O(|\mu|+|\nu|).$$

Thus if we let $\alpha(0,0) = a+ib$, $\beta(0,0) = c+id$, the map is

$$\begin{cases} R = (1+\mu)r + f(\phi)r^3 + O(r^5 + (|\mu|+|\nu|)r^3) \\ \Phi = \phi + \frac{\pi}{2} + \nu - g(\phi)r^2 + O(r^4 + (|\mu|+|\nu|)r^2) \end{cases}$$

with $f(\phi) = b + d\cos 4\phi - c\sin 4\phi$

$$g(\phi) = a + c\cos 4\phi + d\sin 4\phi.$$

Restricting attention to the supercritical case ($b < 0$) we look for a fixed point in the r-coordinate of the truncated map obtained by dropping the higher order terms. This time, however, the truncation still involves ϕ in the r-coordinate, so we try a solution of the form $r = \sqrt{\mu}r_0(\phi)$

where r_o has period $\frac{\pi}{2}$ in ϕ. This gives

$$r_o(\Phi) = (1+\mu)r_o(\phi) + \mu f(\phi)r_o^3(\phi)$$

and expanding $r_o(\Phi)$ we find

$$r_o(\Phi) = r_o(\phi + \tfrac{\pi}{2} + \nu - g(\phi)r^2 + O(\cdot))$$

$$= r_o(\phi)+[\nu-\mu g(\phi)r_o^2(\phi)] \frac{\partial r_o}{\partial \phi}(\phi) + O(\cdot)$$

where terms of $O(\cdot)$ have already been discarded. Hence the solution of the truncated equation must satisfy the differential equation

$$\mu f(\phi)r_o^3(\phi) + \mu r_o(\phi) - [\nu-\mu g(\phi)r_o^2(\phi)] \frac{\partial r_o}{\partial \phi}(\phi) = 0. \tag{2.14}$$

Let $\rho = \sqrt{\mu} r_o$, then

$$\mu\rho(\phi) + f(\phi)\rho^3(\phi) - [\nu-g(\phi)\rho^2(\phi)] \frac{\partial \rho}{\partial \phi}(\phi) = 0$$

or equivalently,

$$\begin{cases} \dot{\rho} = \mu\rho + f(\phi)\rho^3 \\ \dot{\phi} = \nu-g(\phi)\rho^2 \end{cases}$$

if we assume that the map $\phi \mapsto \nu-g(\phi)\rho^2(\phi)$ is never zero. In complex notation $z = \rho e^{i\phi}$, this becomes

$$\dot{z} = \varepsilon z + \sigma_2 z^2\bar{z} + \sigma_3\bar{z}^3 \tag{2.15}$$

where $\varepsilon = \mu+i\nu$, $\sigma_2 = b-ia$, and $\sigma_3 = d-ic$. Now (2.15) is the vector field invariant under the action $z \mapsto iz$ given by Arnol'd and is also studied by Wan [40]. In fact using Wan's methods we can show that the vector field (2.15) has a periodic orbit when $\mu > 0$ provided

$$(a\mu+b\nu)^2 > (c^2+d^2)(\mu^2+\nu^2) \tag{2.16}$$

The idea is that the vector field has no non-zero equilibria when (2.16) is satisfied, and the function $E = \mathrm{Re}H$ where

$$H = |\sigma_2|^2 \frac{z^2\bar{z}^2}{2} - \frac{\sigma_2\sigma_3}{2} z^4$$

satisfies $E > 0$ on $\mathbb{C}\backslash\{0\}$ and $\frac{dE}{dt} < 0$ on some set $\{z|E(z) \geq e\}$ with $e > 0$. Then, since the origin is a source when $\mu > 0$, the vector field has an invariant annulus which contains no equilibria and by the Poincaré-Bendixson Theorem there is a closed orbit in this annulus.

Given this solution of the truncated equation we change coordinates, putting

$$r = \sqrt{\mu} r_o(\phi)(1 + \sqrt{\mu}x)$$

and in the (x,ϕ)-plane the map takes the form

$$\begin{cases} X = (1+\mu F(\phi))x + O(|\mu|^{3/2} + |\mu|^{1/2}|\nu| + |\nu|^2) \\ \Phi = \phi + \frac{\pi}{2} + \nu \quad -\mu g(\phi) r_o^2(\phi) + O(|\mu|^{3/2} + |\mu||\nu|) \end{cases} \tag{2.17}$$

The coordinate changes given by Lemaire-Body [24] then put the map into a form for which Lanford's proof of Theorem 2.5 works, and the map has an attracting invariant circle for small, positive μ. However, the assumption that the map

$$\phi \mapsto \nu \quad -\mu g(\phi) r_o^2(\phi)$$

is never zero excludes the sector

$$|\nu| \leq \mu \sup_{\phi \in [0, \frac{\pi}{2}]} g(\phi) r_o^2(\phi)$$

which, from the form of (2.17), is precisely where we expect the map on the circle to have periodic orbits.

In the next chapter we apply Theorem 2.8 to the Maynard-Smith family so we need the coefficients $\alpha(0)$ and $\beta(0)$ in the normal form in terms of the coefficients of the original map

$$F(z) = z + \sum_{\ell=2,3} \sum_{p+q=\ell} \xi_{pq} z^p \bar{z}^q + O(|z|^4).$$

Now $\alpha(0)$ is given by (2.1), and carrying through the coordinate changes in Lemma 2.6 gives

$$\beta(0) = \frac{\bar{\lambda}}{(\lambda-1)} \xi_{02}\xi_{11} + \frac{2\bar{\lambda}}{(\lambda-\bar{\lambda}^2)} \bar{\xi}_{20}\xi_{02} + \xi_{03}$$

Thus when $\lambda = i$ we have

$$\alpha(0) = \tfrac{1}{2}(1+3i)\xi_{11}\xi_{20} + \tfrac{1}{2}(1-i)|\xi_{11}|^2 - (1+i)|\xi_{02}|^2 + \xi_{21}$$

$$\beta(0) = \tfrac{1}{2}(1-i)\xi_{11}\xi_{02} - (1+i)\,\bar{\xi}_{20}\xi_{02} + \xi_{03} \qquad (2.18)$$

Note that these do not agree with the formulae given by Wan [40] which are apparently incorrect.

Conclusion.

A useful way to combine the above results for a family of maps F of the plane with a fixed point p is to consider F as a two-parameter family with the determinant, Δ, and trace, σ, of the Jacobian of F at p as the parameters. In the (Δ,σ)-plane the lines $\Delta-\sigma+1 = 0$ and $\Delta+\sigma+1 = 0$ correspond to $dF(p)$ having one eigenvalue equal to $+1$ and -1 respectively, while if $dF(p)$ has complex eigenvalues of modulus one then $\Delta = 1$, $|\sigma| < 2$. The fixed point p is then stable if (Δ,σ) lies within the triangular region

bounded by these three lines which is shown in figure 2.10. Along a one parameter path in the (Δ,σ)-plane generically we expect a fold bifurcation along $\Delta-\sigma+1 = 0$, with no fixed points for the map if $\Delta-\sigma+1 < 0$ and two fixed points if $\Delta-\sigma+1 > 0$, a flip bifurcation along $\Delta+\sigma+1 = 0$ with an orbit of period two existing either above or below this line, and a Hopf bifurcation along $\Delta = 1$, $|\sigma| < 2$. Passing along $\Delta = 1$ from $\sigma = 2$ to $\sigma = -2$ we will encounter all the resonances described above.

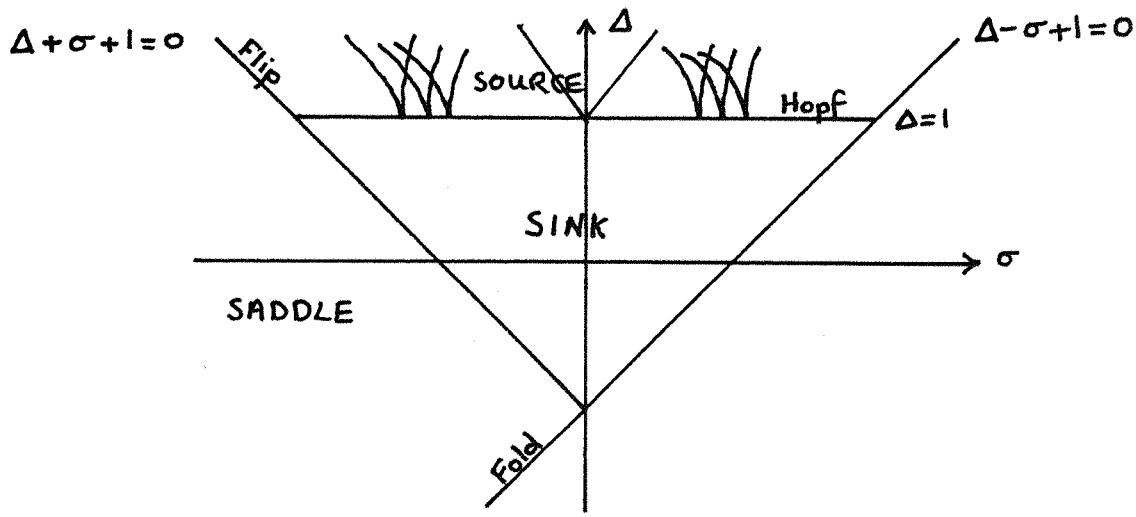

Figure 2.10.

The utility of this figure depends on the properties of the mapping from the parameter space to the (Δ,σ)-plane, and clearly this can only be one-to-one if we have a two-parameter family. For the fixed points of Maynard-Smiths map, which we examine in the next chapter, this mapping is a homeomorphism of the parameter space onto its image in the (Δ,σ)-plane, but in general it will be many-to-one, as it is for the fixed points of iterates of Maynard Smiths map. Note also that for a family of diffeomorphisms we are restricted to either the upper or lower half plane in figure 2.10.

Chapter Three

Maynard Smith's Map: Analysis

We now come to a detailed analysis of Maynard Smith's map

$$F_{(a,b)}(x,y) = (y, ay+b-x^2)$$

which was introduced in chapter one. If $a = 0$ the dynamics of the family $F_b = F_{(a,b)}$ are governed by the one-dimensional family

$$h_b(x) = b-x^2$$

and the results of chapter one immediately yield results for F_b. In §3.1 we describe the initial bifurcation sequence for F_b, showing how the periodic points of h_b are related to those of F_b and pointing out one major difference between the dynamics of h_b and F_b: F_b does not have a unique attractor. For the full two-parameter family a local analysis of the fixed points and their bifurcations is given in §3.2.

Throughout this chapter it will be useful to have in mind the simple geometrical action of the map. We can think of the map as the composition of two simpler ones, namely the quadratic 'fold'

$$f(x,y) = (b-x^2, y)$$

and the linear map

$$g(x,y) = (y, ay+x)$$

Thus $F = g \circ f$ folds the plane about the y-axis and then acts as a linear transformation which takes the fold line $x = 0$ to the line $y = ax+b$, One way to visualize this is to let $z = ay+b-x^2$, then the graph of $H: \mathbb{R}^2 \to \mathbb{R}$ $(x,y) \to z$ is the parabolic tunnel T shown in figure 3.1.

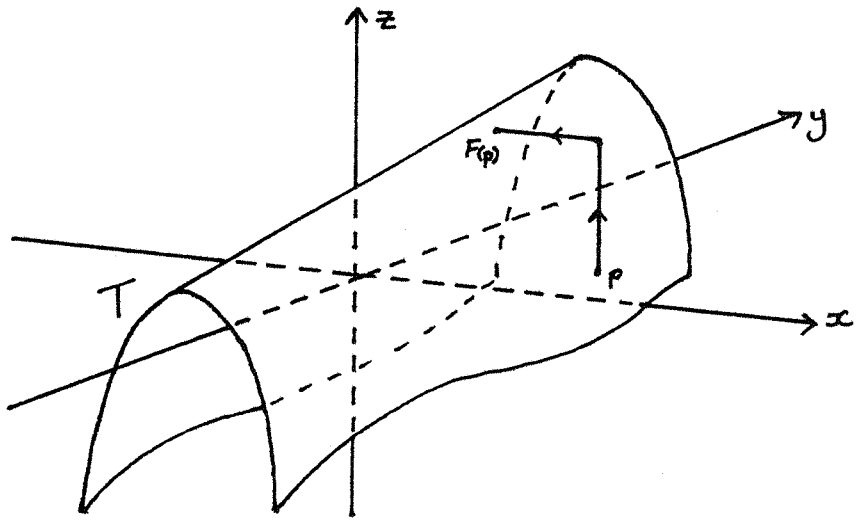

Figure 3.1.

A point P in the (x-y) plane is taken by F to the point on T vertically above P, and then projected onto the (y-z) plane. The (y-z) plane is now identified with the original (x-y) plane to give the image of P under the map. It is not easy to see how successive iterates of F behave from figure 3.1, but it does indicate the way in which the whole plane is mapped below the line $y = ax+b$ in a 2:1 way. The inverse of F is defined only on the half-plane $\{(x,y) | y \leq ax+b\}$. Points in the region $y < ax+b$ have two preimages under F, points on the line $y = ax+b$ have a single preimage, while points in $y > ax+b$ have no preimages.

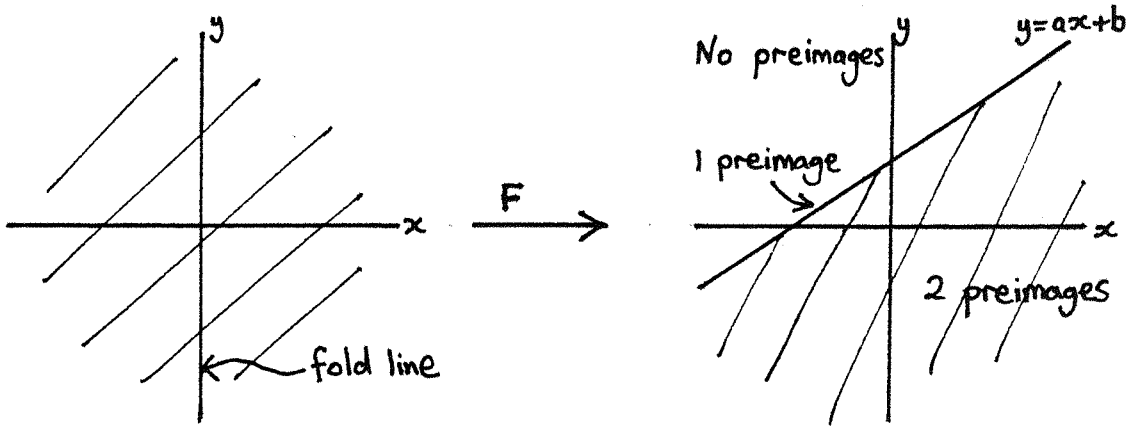

Figure 3.2.

Note that the parameter a governs the 'slope' of T (the images of straight lines x = constant are straight lines with gradient a), while b is the height of the intersection of T with the z-axis in figure 3.1.

3.1 Dynamics of F_b.

When $a = 0$ Maynard Smith's map reduces to

$$F_b(x,y) = (y,h_b(x)),\ h_b(x) = b-x^2$$

so the dynamics of F_b are determined by the dynamics of h_b, which we recall from chapter one. If $b < -\frac{1}{4}$ then for each x, $h(x) < x$ and $h^n(x) \to -\infty$ as $n \to \infty$. When $b = -\frac{1}{4}$ two fixed points, $x_\pm = -\frac{1}{2}\pm\sqrt{b+\frac{1}{4}}$, are created by a fold bifurcation and for $b \in [-\frac{1}{4},2]$ h maps the interval $I = [x_-,-x_-]$ into itself. The fixed point x_- is always unstable (when it exists), while x_+ is stable when $b \in (-1/4,3/4]$. At $b = 3/4$ a stable orbit of period two is created by a flip at x_+, the fixed point itself becoming unstable. The period two orbit remains stable until $b = 5/4$ when it loses stability, creating a stable orbit of period four by a further flip, and this period doubling continues until $b \simeq 1.401\ldots$.

For F_b this means that if $b \in [-\frac{1}{4},2]$ the square $S = I \times I$ is mapped into itself with the boundary ∂S taken into ∂S. F_b folds S about the line $\ell : x = 0$ and takes ℓ to the line $\ell_1 : y = b$. Vertical lines $x = k$ are mapped homeomorphically onto horizontal lines $y = b-k^2$, while horizontal lines $y = k$ are folded onto the vertical line segment $x = k$, $y \leq b$.

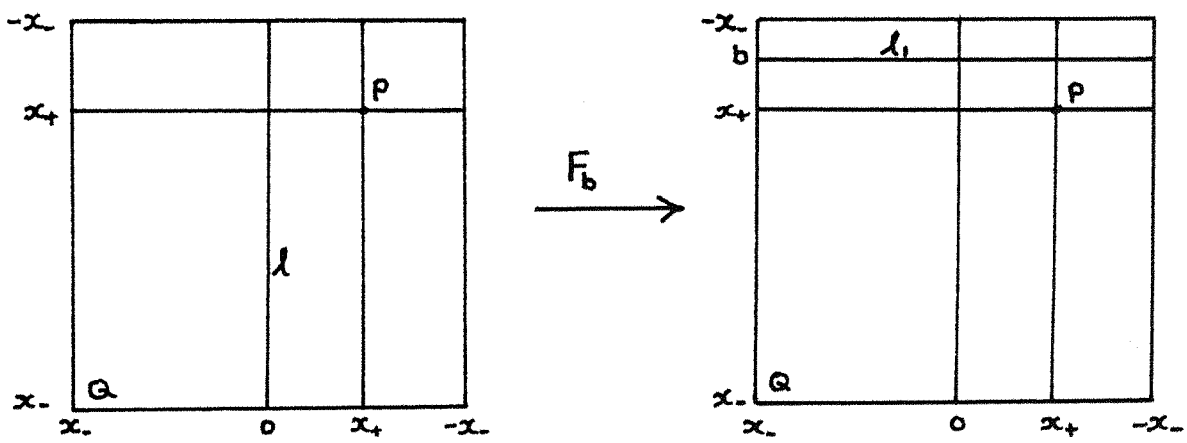

Figure 3.3.

There are two fixed points for F_b, $P = (x_+,x_+)$ and $Q = (x_-,x_-)$, if $b \geq -\frac{1}{4}$. Q is a source for all $b > -1/4$ while P is a sink if $b \in (-1/4,3/4]$. There is also a period two orbit on the boundary of S.

$$(x_+,x_-) \to (x_-,x_+) \to (x_+,x_-)$$

which is a saddle if $b \in (-1/4,3/4]$. At $b = 3/4$ the derivative of F_b at P is $dF_b(P) = \begin{pmatrix} 0 & -1 \\ -1 & 0 \end{pmatrix}$ and this has eigenvalues $\lambda = \pm i$, so that a resonant Hopf bifurcation occurs. This can be analysed as in chapter 2 but we know that for $b \in (3/4,5/4]$ h_b has a stable orbit of period two: $y_+ \to y_- \to y_+$ and this gives a stable orbit of period four for F_b:

$$(y_+,y_+) \to (y_+,y_-) \to (y_-,y_-) \to (y_-,y_+) \to (y_+,y_+)$$

F_b also has two orbits of period four which are saddles, one which bifurcates from the fixed point P:

$$(y_+,x_+) \to (x_+,y_-) \to (y_-,x_+) \to (x_+,y_+) \to (y_+,x_+)$$

and one on the boundary of S:

$$(y_+,x_-) \to (x_-,y_-) \to (y_-,x_-) \to (x_-,y_+) \to (y_+,x_-)$$

which bifurcates from the period two orbit

$$(x_+,x_-) \to (x_-,x_+) \to (x_+,x_-)$$

as it changes from a saddle to a source.

At $b = 5/4$ the stable orbit of period four bifurcates with both eigenvalues of $DF_b^4(y_+,y_+)$ decreasing through -1. Again this is a resonant Hopf bifurcation, although not of one same type which produced the period four orbit, and again it is easy to see what happens by

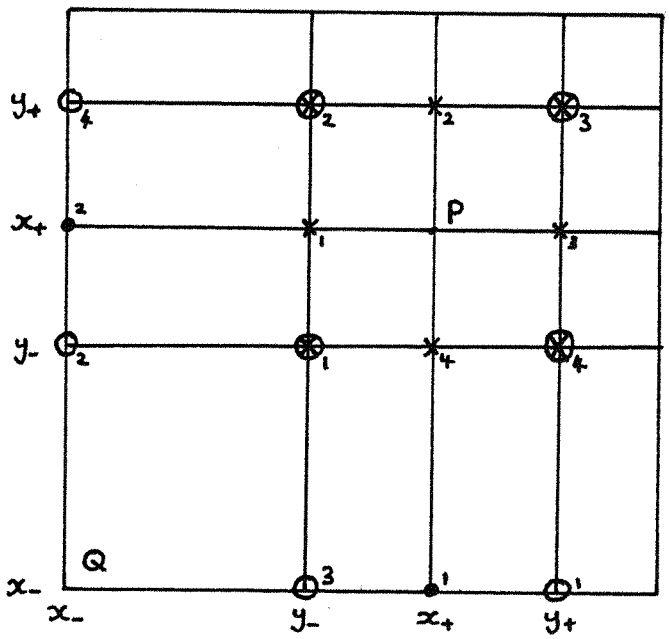

Figure 3.4. Dynamics of F_b, $b \in (3/4, 5/4]$

⊗ denotes a stable orbit of period 4, x and 0 saddles of period 4, . a source of period 2. P and Q are fixed points, both sources.

considering the behaviour of h_b. After this bifurcation there is a total of 50 periodic points: 2 sinks of period 8, 3 saddles of period 8, 2 sources of period 4 and 2 sources. From the data available for h_b, see for example Gumovski and Mira [15], we know that this bifurcation repeats as b increases to $b \simeq 1.401\ldots$ with both eigenvalues of stable orbits of period 2^n passing through -1 and creating stable orbits of period 2^{n+1}.

The following proposition states an easy connection between orbits of h_b and F_b.

Proposition 3.1.

(1) If h has a periodic orbit of even period 2k, then F has k orbits of period 4k.

(2) If h has a periodic orbit of odd period 2k+1,

then F has one orbit of period 2k+1 and k orbits of period 4k+2.

Proof (1) Suppose that x and y lie in the periodic h-orbit. Then

$$F^n(x,y) = (x,y) \iff \begin{cases} h^{n/2}(x) = x,\ h^{n/2}(y) = y & \text{if } n \text{ is even} \\ h^{\frac{n-1}{2}}(y) = x,\ h^{\frac{n+1}{2}}(x) = y & \text{if } n \text{ is odd} \end{cases}$$

If n is even we must then have $n = 4k$ as the least period of (x,y). If n is odd, we have

$$y = h^{\frac{n+1}{2}}(x) = h^{\frac{n+1}{2}}\, h^{\frac{n-1}{2}}(y) = h^n(y)$$

which is impossible since y has even period. Thus all the $(2k)^2$ periodic points of F have period 4k and there are k different orbits.

(2) Suppose $h^{2k+1}(x) = x$ and let $y = h^{k+1}(x)$. Then

$$F^{2k+1}(x,y) = (h^k(y),h^{k+1}(x)) = (h^{2k+1}(x),y) = (x,y)$$

So there is at least one orbit of period 2k+1. If there are two distinct orbits of period 2k+1 then we have

$$F^{2k+1}(x,y) = (x,y), \qquad y = h^{k+1}(x),\ x = h^k(y)$$

and

$$F^{2k+1}(\bar{x},\bar{y}) = (\bar{x},\bar{y}), \qquad \bar{y} = h^{k+1}(\bar{x}),\ \bar{x} = h^k(\bar{y})$$

with $F^n(x,y) \neq (\bar{x},\bar{y})$ for any n. However, $x,y,\bar{x}$ and $\bar{y}$ all belong to the same h-orbit so for some n, $F^n(x,y) = (z,\bar{y})$, say. We will derive a contradiction by showing that $z = \bar{x}$.

If n is even, $n = 2j$, then $F^{2j}(x,y) = (h^j(x),h^j(y))$ and $z = h^j(x)$, $\bar{y} = h^j(y)$. Then $\bar{x} = h^k(\bar{y}) = h^{j+k}(y) = h^j(x) = z$.

If m is odd, $m = 2j+1$, then $z = h^j(y)$, $\bar{y} = h^{j+1}(x)$ and $\bar{x} = h^k(\bar{y}) = h^{j+k+1}(x) = h^j(y) = z$.

Thus there is a single F-orbit of period $2k+1$ and the remaining $2k(2k+1)$ F-periodic points have period $4k+2$.

Clearly F_b will have other periodic points besides those given by the proposition by considering the fixed points P and Q. The important point here is that a single orbit of h_b gives several orbits of F_b, and in particular a single stable orbit of h leads to several stable orbits of F_b. Thus even though h_b is restricted, for each fixed b, to at most one stable periodic orbit by Singer's theorem [34], for many parameter values F_b has a large number of stable periodic orbits.

The proof of Singer's theorem shows that if x belongs to a stable periodic orbit of h_b of period n, then the semi-local stable manifold of x, $s\ell sm(x)$, i.e. the connected component of the stable manifold of x, containing x, must contain a critical point, c, of h^n. By the chain rule c is mapped to 0, the critical point of h, by some iterate h^k with $k < n$ and so the ω-limit set of the critical point $x = 0$ is the periodic orbit containing x. Now suppose that P is a stable periodic point of F. Let ℓ denote the fold line $\{(x,y)|x=0\}$ and put $\ell_{-n} = \{(x,y)|f^n(x,y) \in \ell\}$. The proof of Singer's theorem shows that $s\ell sm(p)$ contains a point $q \in \ell_{-n} \cap \ell_{-m}$ for some $n,m \geq 0$. Now whereas a critical point of h^n must be a preimage of the critical point of h there is no reason why two points $q \in \ell_{-n} \cap \ell_{-m}$ and $q' \in \ell_{-n'} \cap \ell_{-m'}$ should eventually map to the same orbit. For example, consider figure 3.5. This shows the fold line ℓ together with its first, second and third preimages. There are nine points which lie at the intersections of these lines, seven of them, marked x, all map to the origin $(0,0) = \ell \cap \ell_{-1}$ under some iterate. The remaining pair, while being mapped together by F^2, do not necessarily have the same future orbit as the other seven.

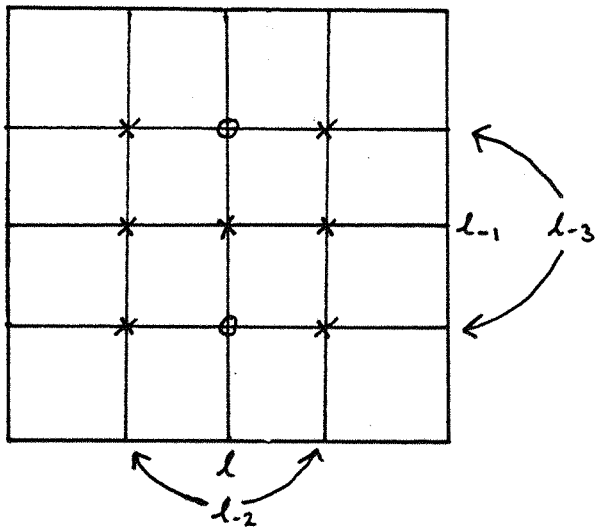

Figure 3.5.

Let $L = \bigcup_{\substack{i,j=0 \\ i \neq j}}^{\infty} (\ell_i \cap \ell_j)$ and define an equivalence relation on L by $x \sim y \iff \exists\, n,m \geq 0$ with $f^n(x) = f^m(y)$. Then Singer's theorem implies that the number of stable periodic orbits of F is at most equal to the number of equivalence classes of $L/\sim$.

It would be interesting to know whether this result extends to a wider class of maps which fold the plane, but for this we need an analogue of the Schwarzian derivative condition for maps in $\mathbb{R}$. If such a class of maps could be found a technique for finding the stable periodic orbits would be to consider the points of intersection of the fold line and its preimages in turn, finding a point in each equivalence class as they appear and iterating this point (on a machine) to find its ω-limit set.

The questions of how far the results for F_b extend to the full two-parameter family when $a \neq 0$ is unresolved. A similar problem occurs in the Henon map $G(x,y) = (y, ax+b-y^2)$, where for $a = 0$ the results on maps of the interval give a reasonably complete picture of the dynamics of G but when $a \neq 0$ very little is known. Some results on extending the singular behaviour at $a = 0$ are given by van Strien [37].

For the Maynard Smith family $F_{(a,b)}$ we can mimic the kneading theory for maps of the interval, associating to the orbit of a point

$p \in \mathbb{R}^2$ its itinerary $\underline{\varepsilon}(p) = \{\varepsilon_n(p)\}_{n=0}^{\infty}$ defined by

$$\varepsilon_n(p) = \begin{cases} +1 & \text{if } F^n(p) \text{ lies in the right half-plane} \\ 0 & \text{if } F^n(p) \text{ lies on the fold line } x = 0. \\ -1 & \text{if } F^n(p) \text{ lies on the left half-plane} \end{cases}$$

However, it is difficult to see how to decide whether a particular sequence corresponds to an orbit of F. In the maps of the interval the key to finding these 'admissible' sequences is to use the invariant coordinate $\underline{\theta}$ to track the orientation preserving or reversing nature of an iterate of the map near a particular point. This can also be done for maps in $\mathbb{R}^2$ but on the interval the orientation is synonymous with the order and this leads to the monotonicity of invariant coordinates and a characterization of the admissible sequences, while in the plane there is no satisfactory ordering.

§3.2 Fixed Points and Bifurcations

Returning to the full two-parameter family (3.1) we now give the local stability analysis for the fixed points and discuss their bifurcations.

Provided $(a-1)^2+4b>0$, $F_{(a,b)}$ has two fixed points: P with coordinates $x = y = \frac{1}{2}(a-1-R)$, where $R = \sqrt{(a-1)^2+4b}$. The local nature of F near the fixed point $\underline{x} = (x,y)$ is determined by the number of eigenvalues of the linearization, $dF_{\underline{x}}$, of F at $\underline{x}$ which lie inside the unit circle in the complex plane. The eigenvalues λ of $dF_{\underline{x}}$ are given by $\det(dF_{\underline{x}} - \lambda I) = 0$, where I is the 2×2 identity matrix and

$$dF_{\underline{x}} = \begin{pmatrix} 0 & 1 \\ -2x & a \end{pmatrix}$$

Thus the eigenvalues satisfy

$$\lambda^2 - a\lambda + 2x = 0 \tag{3.1}$$

and the following result may be applied to determine the stability of the fixed points.

Lemma 3.2. The number of roots of the polynomial $p(\lambda) = a_2\lambda^2+a_1\lambda+a_o$, $a_i \in \mathbb{R}$, which lie inside the unit circle in the complex plane is equal to the number of sign changes in the sequence

$$1,\ |a_o| - a_2,\ (a_o+a_1+a_2)(a_o-a_1+a_2).$$

This is the simplest case of the Schur-Cohn criterion, which in its general form gives conditions on the coefficients of a polynomial $p(\lambda) = a_n\lambda^n+a_{n-1}\lambda^{n-1}+\cdots+a_1\lambda+a_o$ in order for the roots to have modulus less than one. For the case when the coefficients are complex see Marden [26]. When the coefficients are real a simplification due to Jury [22] gives the lemma. For a quadratic polynomial it is also easy to prove directly, being simply a restatement of the information contained in figure 2.10.

We will now apply the lemma to (3.1). Consider first the fixed point P, where the relevant sequence is

$$1,\ |2x|-1,\ (2x+a+1)(2x-a+1) \tag{3.2}$$

with $x = \frac{1}{2}(a-1+R)$. Let $\alpha = |2x|-1$ and $\beta = (2x+a+1)(2x-a+1)$. To determine the sign of α note that if $a < 1$ and $b < 0$ then $x < 0$ and $\alpha = -(2x+1) = -(a+R)$. So when $x < 0$, $\alpha > 0$ if $a+R<0$, i.e. $a < 0$ and $4b<2a-1$, while $\alpha < 0$ if $a+R>0$, i.e. $4b>2a-1$. If $x > 0$ then $a > 1$ or $b > 0$ and $\alpha = 2x-1 = a-2+R$. Therefore $\alpha > 0$ if $R>2-a$, i.e. $a > 2$ or $4b+2a>3$, and $\alpha < 0$ if $R<2-a$, i.e. $a < 2$ and $4b+2a<3$. Figure 3.6a shows the sign of α in the various regions of the parameter plane.

Now $\beta = R(R+2a)$ therefore since $R > 0$, $\beta > 0$ if $R > -2a$, i.e. $a > 0$ or $4b > 3a^2 + 2a-1$, while $\beta < 0$ if $R < -2a$, i.e. $a < 0$ and $4b < 3a^2 + 2a-1$. See figure 3.6(b)

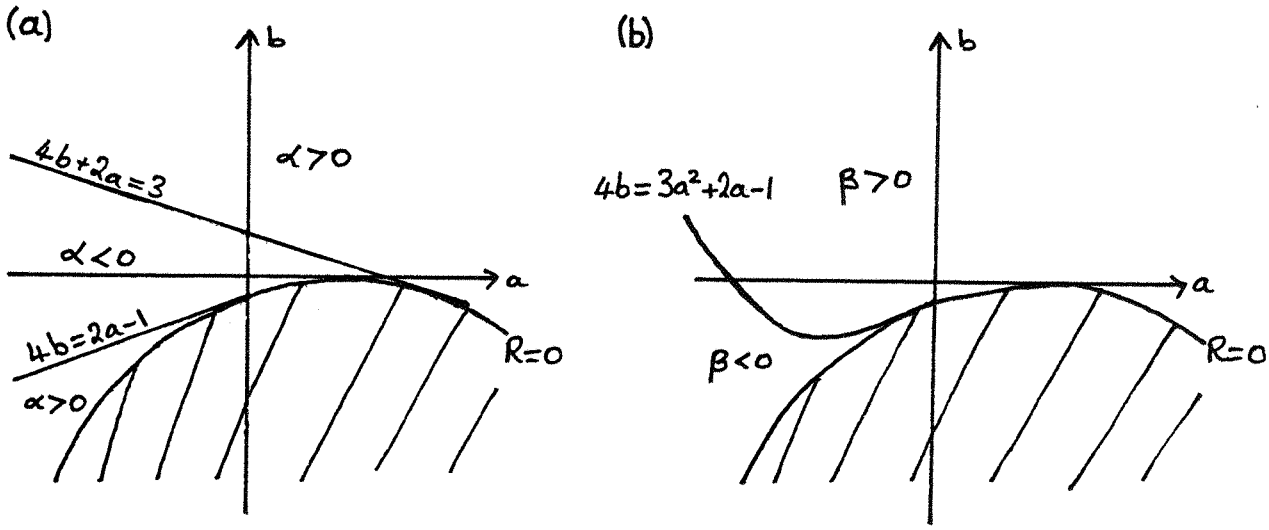

Figure 3.6 (a) Sign of α (b) Sign of β

Combining the information in figures 3.6 (a) and (b) with the lemma we have that P is a sink if $\alpha < 0$ and $\beta > 0$, which is true in the central region of the parameter plane bounded by $(a-1)^2 + 4b = 0$, $4b = 3a^2+2a-1$ and $4b+2a = 3$, P is a source if $\alpha > 0$ and $\beta > 0$, giving the region above these three curves, and P is a saddle if $\beta < 0$, which holds if $a < 0$, $4b$ $3a^2+2a-1$ and $(a-1)^2+4b > 0$. This situation is illustrated in figure 3.7.

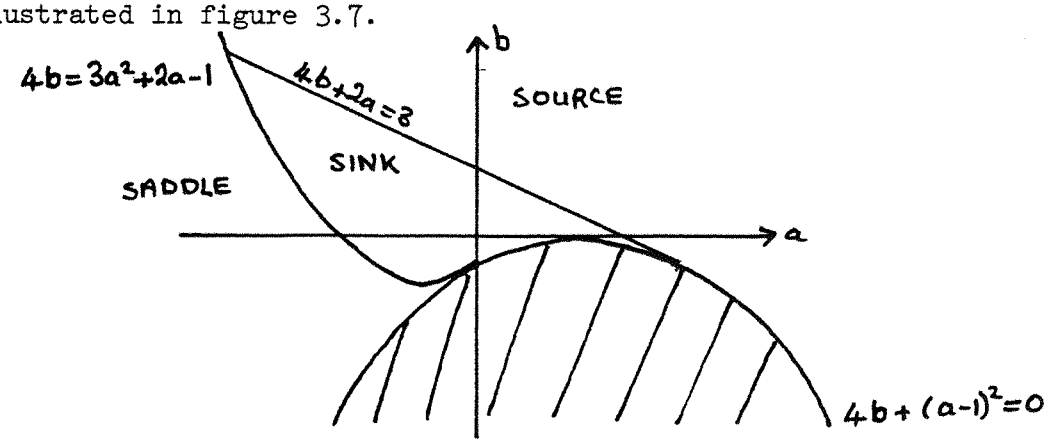

Figure 3.7. Stability of P.

We now apply the same type of analysis to the second fixed point Q. The relevant sequence is (3.2) with $x = \frac{1}{2}(a-1-R)$. Now $x > 0$ only if $a > 1$ and $b > 0$, in which case $\alpha = 2x-1 = a-2-R$. So when $x > 0$, $\alpha > 0$ if $R < a-2$, i.e. $a > 2$ and $4b+3a < 3$, and $\alpha < 0$ if $a < 2$ or $4b+2a > 3$. If $x < 0$ then $a < 1$ or $b < 0$ and $\alpha = -2x-1 = R-a$. Hence $\alpha > 0$ if $R > a$, i.e. if $a < 0$ or $4b > 2a-1$, while $\alpha < 0$ if $R < a$, i.e. $4b < 2a-1$. See figure 3.8a.

$\beta = R(R-2a)$ so $\beta > 0$ if $R > 2a$, i.e. $a < 0$ or $4b > 3a^2+2a-1$, and $\beta < 0$ if $R < 2a$, i.e. $4b < 3a^2+2a-1$ and $a > 0$. See figure 3.8b.

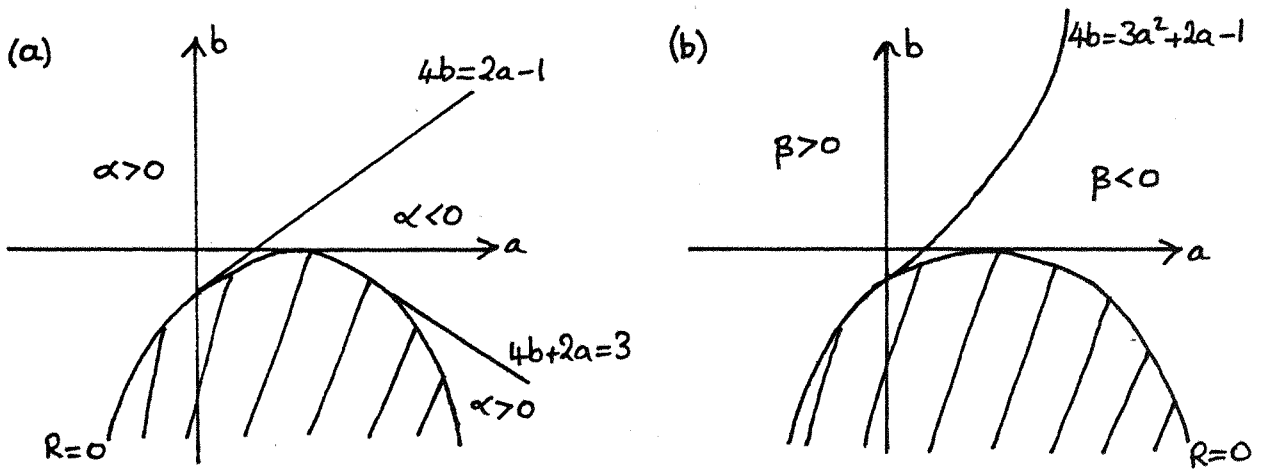

Figure 3.8. (a) Sign of α (b) Sign of β

From the lemma we have that Q is a sink if $\alpha < 0$ and $\beta > 0$, a source of $\alpha > 0$ and $\beta > 0$, and a saddle if $\beta < 0$. It follows that Q is either a saddle or a source depending on whether (a,b) lies to right or life of the curve $4b = 3a^2+2a-1$, $a > 0$, as shown in figure 3.9.

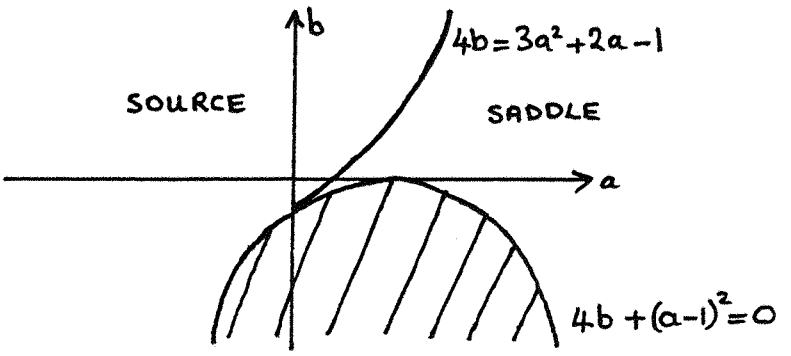

Figure 3.9. Stability of Q.

Given a pair of parameter values (a,b) figures 3.7 and 3.9 indicate the nature of the two fixed points, provided the parameters do not lie on the line

$$H : \quad 2a + 4b = 3, \quad -2 \leq a \leq 2$$

or on either of the parabolae

$$P_1 : \quad (a-1)^2 + 4b = 0$$

or

$$P_2 : \quad 4b = 3a^2 + 2a - 1$$

The next task is therefore to describe the bifurcations which occur as the parameters cross these boundaries.

Firstly, we have already seen that if $(a-1)^2 + 4b > 0$ then F has two fixed points P and Q. If the parameters lie on P_1 the fixed points coincide and if $(a-1)^2 + 4b < 0$ then F has no fixed points. Thus if we follow a path in the parameter space which crosses P_1 two fixed points are created and we may use the theory of the previous chapter and check that the conditions required for a fold bifurcation to occur are in fact satisfied. To do so we must first exclude two points where this approach does not work. At $a = 2$, $b = -\frac{1}{4}$ there is a single fixed point $(\frac{1}{2},\frac{1}{2})$ which has both eigenvalues equal to one. This is one of the strong resonances mentioned in §2.5. At $a = 0$, $b = -\frac{1}{4}$ F has a single fixed point $(-\frac{1}{2},-\frac{1}{2})$ with eigenvalues one and minus one. Here the Implicit Function Theorem may be used to show the existence of an invariant curve $C_{(a,b)}$ in the phase plane, depending on the parameters and with $(-\frac{1}{2},-\frac{1}{2}) \in C_{(0,-\frac{1}{4})}$. We can show that a fold bifurcation occurs for $F|C_{(a,b)}$ if we cross P_1 transversely at $(0,-\frac{1}{4})$, but because the second eigenvalue is minus one we cannot immediately establish the behaviour

of the map transverse to this curve. We will see below that an orbit of period two also appears at this point, but for the moment restrict attention to $\tilde{P}_1 = P_1 \setminus \{(0,-\frac{1}{4}),(2,-\frac{1}{4})\}$.

Let I be a real interval and take a one-parameter path $\rho : I \to \mathbb{R}^2$, $\mu \to \rho(\mu)$, with $\rho(\mu_o) \in \tilde{P}_1$ and with ρ transverse to $\tilde{P}_1$ at μ_o. Now identify μ with $\rho(\mu)$ and consider the one-parameter family $F_\mu \equiv F_\rho(\mu)$. The transversality condition is required in order that condition (4) of Proposition 2.1 will be satisfied, but clearly any transverse path will do and it is convenient to take one-parameter paths parallel to the b-axis. That is, we choose the one-parameter family to be $F_b = F_{(a,b)}$ where a is fixed, $a \neq 0$, $a \neq 2$, and b is considered to be the sole parameter.

Proposition 3.3. For each fixed a, $a \neq 0$ or 2, the one-parameter family F_b has a fold bifurcation at $b = b_o$, where $(a-1)^2 + 4b_o = 0$.

Proof: The bifurcation occurs at the fixed point $x = y = \frac{1}{2}(a-1)$ and to simplify the analysis we first translate this point to the origin. Define new coordintes X, Y by $X = x - \frac{1}{2}(a-1)$, $Y = y - \frac{1}{2}(a-1)$, then the map becomes

$$(X,Y) \to \left(Y, aY-(a-1)X - X^2 + b + \frac{(a-1)^2}{4}\right)$$

Now make a further change of coordinates, reverting to the original notation, defining x, y by

$$\begin{pmatrix} X \\ Y \end{pmatrix} = \begin{pmatrix} 1 & 1 \\ 1 & a-1 \end{pmatrix} \begin{pmatrix} x \\ y \end{pmatrix}$$

so that the map is $(x,y) \to (f_b(x,y), g_b(x,y))$, where

$$f_b(x,y) = \frac{4b+(a-1)^2}{4(2-a)} + x + \frac{(x+y)^2}{a-2} \tag{3.3}$$

and

$$g_b(x,y) = \frac{4b+(a-1)^2}{4(a-2)} + (a-1)y + \frac{(x+y)^2}{2-a}.$$

To find the fixed points of the map we must solve

$$\begin{cases} f_b(x,y) = x \\ g_b(x,y) = y \end{cases} \tag{3.4}$$

If $a \neq 2$ then $\frac{\partial g}{\partial y} \neq 1$ and by the Implicit Function Theorem there is a unique analytic function $y(x,b)$ solving the second equation in (3.4) for (x,b) near $(0,b_o)$ with $y(0,b_o) = 0$ and $\frac{\partial y}{\partial x} = [1 - \frac{\partial g}{\partial y}]^{-1} \frac{\partial g}{\partial x}$. Substituting for $y(x,b)$ in (3.3) gives a family of maps in $\mathbb{R}$:

$$f: \mathbb{R} \times \mathbb{R} \to \mathbb{R}$$
$$(x,b) \to f(x,b) = f_o(x)$$

with $f(0,b_o) = 0$.

Differentiating (3.3) we find

$$\frac{\partial f}{\partial x} = 1 + \frac{2(x+y)}{(a-2)} \left(1 + \frac{\partial y}{\partial x}\right)$$

and

$$\frac{\partial^2 f}{\partial x^2} = \frac{2}{(a-2)} (x+y) \frac{\partial^2 y}{\partial x^2} + \frac{2}{(a-2)} \left(1 + \frac{\partial y}{\partial x}\right)^2$$

The formula given by the Implicit Function Theorem shows that $\frac{\partial y}{\partial x}(a,b_o)$ $= 0$, so

$$\frac{\partial f}{\partial x}(a,b_o) = 1 , \quad \frac{\partial^2 f}{\partial x^2}(0,b_o) = \frac{2}{a-2}$$

and from (3.3) we also have

$$\frac{\partial f}{\partial b}(0,b_o) = \frac{1}{2-a}$$

Thus by Proposition 2.1 f has a fold bifurcation at $b = b_o$, and by the remark following the proposition the bifurcated fixed points exist for $b > b_o$. A consideration of the signs of $\frac{\partial^2 f}{\partial x^2}(0,b_o)$, $\frac{\partial f}{\partial b}(0,b_o)$ and the modulus of the second eigenvalue of F_{b_o}, which, when $a \neq 1$, governs the behaviour of the map transverse to the curve $y = y(x,b)$, shows that the stability of the bifurcated fixed points of F agrees with that given by the local stability analysis above.

The next boundary to consider is the parabola P_2: $4b = 3a^2 + 2a - 1$. Here a flip bifurcation occurs and again we analyse it by taking the one-parameter family F_b with the value of a fixed, after excluding the strong resonances at $a = 0$, $b = -\frac{1}{4}$, where both eigenvalues are $+1$, and at $a = -2$, $b = 7$, where both eigenvalues are -1.

Proposition 3.4. For each fixed a, $a \neq 0$ or -2, the one-parameter family F_b has a flip bifurcation at $b = b_o$ where $4b_o = 3a^2+2a-1$. A saddle-like orbit of period two bifurcates from p if $a < 0$ and from Q if $a > 0$. The period two orbit exists for $b > b_o$.

Proof: There are three cases to consider: $a < -2$, $-2 < a < 0$ and $a > 0$. We give the proof for the first case, the others are similar. Now for $a < 0$ the bifurcation occurs at P: $x = y = \frac{1}{2}(a-1+R(b))$, where $R(b) = \sqrt{(a-1)^2+4b}$, and the eigenvalues $\lambda_\pm(b)$ of $dF_b(P)$ are roots of $\lambda^2 - a\lambda + 2x = 0$, i.e.

$$\lambda_\pm(b) = \tfrac{1}{2}(a \pm s(b)), \quad s(b) = \sqrt{(a-2)^2 - 4R(b)}.$$

Next translate P to the origin, defining new coordinates X,Y by

$$X = x - \tfrac{1}{2}(a-1+R(b)), \quad Y = y-\tfrac{1}{2}(a-1+R(b))$$

so the map is

$$(X,Y) \to (Y, aY-(a-1+R(b))X - X^2)$$

and after a further coordinate change, defining x, y by

$$\begin{pmatrix} X \\ Y \end{pmatrix} = \begin{pmatrix} 1 & 1 \\ \lambda_+(b) & \lambda_-(b) \end{pmatrix} \begin{pmatrix} X \\ Y \end{pmatrix}$$

the map becomes

$$(x,y) \to (f_b(x,y), g_b(x,y))$$

where

$$f_b(x,y) = \lambda_+(b)x + \frac{(x+y)^2}{s(b)} \tag{3.5}$$

and

$$g_b(x,y) = \lambda_-(b)y - \frac{(x+y)^2}{s(b)}$$

The fixed points of F_b are given by

$$\begin{cases} f_b(x,y) = x \\ \\ g_b(x,y) = y \end{cases} \tag{3.6}$$

and when $a < -2$, $s(b_o) = -(a+2)$, therefore $\lambda_+(b_o) = -1$ and $\lambda_-(b_o) = 1+a$, Then since $a \neq 0$ we can solve the second equation in (3.6) for a unique analytic function $y(x,b)$ for (x,b) near $(0,b_o)$ with $y(0,b_o) = 0$ and $\frac{\partial y}{\partial x} = [1 - \frac{\partial g}{\partial y}]^{-1} \frac{\partial g}{\partial x}$. Substituting $y(x,b)$ in (3.5) gives a family of maps in $\mathbb{R}$ with $f(0,b_o) = 0$ and $\frac{\partial f}{\partial x}(0,b_o) = -1$. To ensure that

a flip bifurcation does occur for f_b it remains to check conditions (3) and (4) of Proposition 2.2. For (3), differentiating $\lambda_+(b)$ gives easily

$$\frac{d\lambda_+(b_o)}{db} = \frac{1}{a(a+2)}$$

and for (4), (3.4) shows

$$f^2(x,b) = \lambda_+^2\, b(x) + \frac{\lambda_+(b)}{s(b)}\,(x+y(x,b))^2 + \frac{1}{s(b)}\,(\lambda_+(b)x + \lambda_-(b)y(x,b))$$

from which we find

$$\frac{\partial^3 f^2}{\partial x^2}(x,b) = \frac{2\lambda_+}{s}(x,y)\,\frac{\partial^3 y}{\partial x^3} + \frac{6\lambda_+}{s}\left(1+\frac{\partial y}{x}\right)\frac{\partial^2 y}{\partial x^2} + \frac{2}{s}(\lambda_+ x+\lambda_- y)\lambda_-\,\frac{\partial^2 y}{\partial x^2}$$

$$+ \frac{6\lambda_-}{s}\left(\lambda_+ + \lambda_-\,\frac{\partial y}{\partial x}\right)\frac{\partial^2 y}{\partial x^2}\,.$$

From the Implicit Function Theorem we have

$$\frac{\partial y}{\partial x}(0,b_o) = 0, \quad \frac{\partial^2 y}{\partial x^2}(0,b_o) = \frac{-2}{a^3(a+2)}$$

therefore

$$\frac{\partial^3 f^2}{\partial x^3}(0,b_o) = \frac{-12}{a^3(a+2)}$$

Thus for $a < -2$, $\frac{\partial^3 f^2}{\partial x^2}(0,b_o) < 0$ and $\frac{d\lambda_+}{db}(b_o) < 0$ and by the remark following Proposition 2.2 f_b has a stable fixed point for $b < b_o$ which bifurcates at $b = b_o$ into an unstable fixed point and a stable orbit of period two. The second eigenvalue of $dF_{b_o}(P)$ is $\lambda_-(b_o) = 1+a$ so for $a < -2$ the direction transverse to the curve $y = y(x,b)$ is unstable and F_b has a fixed point which is a saddle for $b < b_o$, a source for $b > b_o$, plus two saddles of period two when $b > b_o$.

In fact the period two points of F may be found explicitly. They are solutions of $F^2(x,y) = (x,y)$, that is

$$(x,y) = (ay+b-x^2,\ a(ay+b-x^2)+b-y^2)$$

and so

$$\begin{cases} x = ay + b - x^2 \\ y = ax + b - y^2 \end{cases} \tag{3.7}$$

Substituting for y from the first of these equations in the second gives the quartic

$$x^4+2x^3+(1+a-2b)x^2 + (a-a^3-2b)x - b(a^2+a-b) = 0 \tag{3.8}$$

Since the fixed points P and Q are also solutions of (3.7), $x^2+(1-a)x-b$ is a factor of (3.8) and the remaining quadratic

$$x^2+(1+a)x + a+a^2+b = 0$$

leads to two solutions

$$x = \tfrac{1}{2}[-(a+1)+\sqrt{4b-3a^2-2a+1}],\ y = \tfrac{1}{2}[-(a+1)-\sqrt{4b-3a^2-2a+1}] \tag{3.9}$$

provided $4b \geq 3a^2+2a-1$. The period two points are then (x,y) and (y,x). If the parameters lie on the parabola P_2: $4b = 3a^2+2a-1$ note that the period two points coincide with the fixed point P if $a < 0$ and with Q if $a > 0$.

From Proposition 3.4 we know that the period two points are saddles if the parameters lie above and close to the parabola P_2. To examine their stability in the rest of the parameter plane we will find the remaining parts of the bifurcation set. If the period two orbit has an

eigenvalue equal to one then, as we saw in the conclusion to the previous chapter, we must have

$$\Delta-\sigma+1 = 0 \tag{3.10}$$

where Δ and σ are the determinant and trace of $dF^2(x,y)$. Here

$$dF^2(x,y) = \begin{pmatrix} -2x & a \\ -2ax & a^2-2y \end{pmatrix}$$

where x,y are given by (3.9) and so

$$\Delta = 4(a^2+a-b),\ \sigma = a^2+2a+2$$

which means that (3.10) corresponds to the parabola P_2 where the periodic points are created. For an eigenvalue equal to minus one (3.10) is replaced by

$$\Delta+\sigma+1 = 0$$

and this gives the parabola $P_3: 4b = 5a^2+ba+3$, while for complex eigenvalues of modulus one we require

$$\Delta = 1,\quad |\sigma| < 2$$

which leads to $4b = 4a^2+4a-1$, $-2 < a < 0$. However, this curve lies entirely below P_2 where there are no period two points, so the map has no period two points with complex eigenvalues on the unit circle. It is then easy to see that the orbit of period two is a saddle between P_2 and P_3, and a source if the parameters lie above P_3. Note that P_3 cuts the b-axis at $b = 3/4$ so this is consistent with what was found for the period two points of $F_{(0,b)}$ in §3.1.

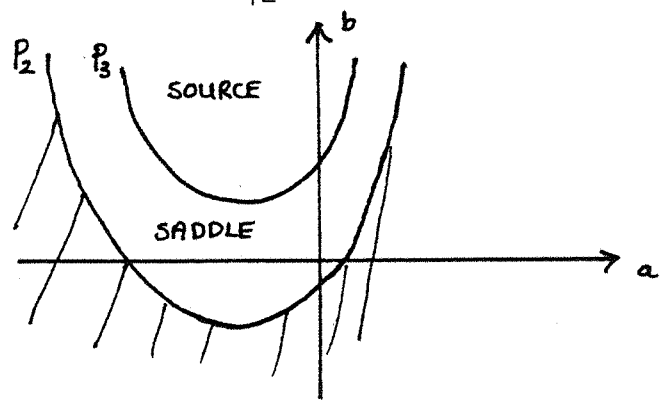

Figure 3.10. Stability of Period Two Points.

Returning to the fixed points of F the third, and most interesting, boundary to consider is the line H: $2a+4b = 3$, $-2 \leq a \leq 2$, which we will refer to as the Hopf line. If the parameters lie on this line with $a \in (-2,2)$ then $dF(P)$ has complex eigenvalues of unit modulus and a Hopf bifurcation occurs as we cross H. The endpoints of the line, $a = -2$, $b = 7$, and $a = 2$, $b = -\frac{1}{4}$, lie on the parabolae P_1 and P_2 respectively and are points of strong resonance, corresponding to both eigenvalues of $dF(p)$ being +1 and both being -1. The Hopf line also contains two more strong resonances. At $a = -1$, $b = 5/4$, $dF(P)$ has eigenvalues which are cube roots of unity and at $a = 0$, $b = 3/4$ the eigenvalues are $\pm i$, fourth roots of unity. Excluding these points Theorem 2.5 yields the following result.

Proposition 3.5. For each fixed $a \in (-2,2)$, $a \neq 0$ or -1, the one-parameter family F_b has a supercritical Hopf bifurcation at $b = b_o$, where $2a+4b_o = 3$.

Proof. We must check that the conditions of Theorem 2.5 hold. First translate P to the origin, then the map is

$$(X,Y) \to (Y, aY-(a-1+R(b))X-X^2)$$

and the derivative at the origin is

$$dF_b(0,0) = \begin{pmatrix} 0 & 1 \\ -(a-1+R(b)) & a \end{pmatrix}$$

The eigenvalues of $dF_b(0,0)$ are

$$\lambda_{\pm}(b) = \tfrac{1}{2}(a \pm \sqrt{(a-2)^2-4R(b)})$$

Thus,

$$\lambda_{\pm}(b_o) = \tfrac{1}{2}(a \pm i\sqrt{4-a^2})$$

and $dF_{b_o}(0,0)$ has non-real eigenvalues of modulus one for $a \in (-2,2)$. Now

$$|\lambda_{\pm}(b)| = \sqrt{R(b)+a-1}$$

and therefore

$$\frac{d|\lambda_{\pm}(b)|}{db}\Big|_{b=b_o} = \frac{1}{2-a}$$

which is positive for $a < 2$, so the eigenvalues pass out of the unit circle as we cross H in the direction of increasing b. Condition (d) of Theorem 2.5 is satisfied since $a \neq \pm 2$, -1 or 0, and it remains to check the sign of the coefficient $a(0)$ of (2.1).

In new coordinates (x,y) defined by

$$\begin{pmatrix} X \\ Y \end{pmatrix} = \begin{pmatrix} 1 & 1 \\ \frac{a+T}{2} & \frac{a-T}{2} \end{pmatrix}\begin{pmatrix} x \\ y \end{pmatrix}$$

we find

$$F_{b_o}(x,y) = \left(\frac{a}{2}x - \frac{T}{2}y - \frac{(x+y)^2}{T}\,,\ \frac{Tx}{2} + \frac{ay}{2} + \frac{(x+y)^2}{T}\right)$$

where $T = \sqrt{4-a^2}$. Now for a map $\Phi : \mathbb{R}^2 \to \mathbb{R}^2$ given by

$$\Phi(x,y) = (\alpha x-\beta y + \sum_{p+q=2} \gamma_{pq}x^p y^q,\ \beta x + \alpha y + \sum_{p+q=2} \tilde{\gamma}_{pq}x^p y^q)$$

if we change to complex notation, putting $z = x+iy$, $\lambda = \alpha+i\beta$, then

$$\Phi(z) = \lambda z + \sum_{p+q=2} \xi_{pq} z^p \bar{z}^q$$

where

$$\xi_{20} = \tfrac{1}{4}[(\gamma_{20}-\gamma_{02} + \tilde{\gamma}_{11}) + i(\tilde{\gamma}_{20} - \tilde{\gamma}_{02} - \gamma_{11})]$$

$$\xi_{11} = \tfrac{1}{2}[(\gamma_{20} + \gamma_{02}) + i(\tilde{\gamma}_{20} + \tilde{\gamma}_{02})]$$

$$\xi_{02} = \tfrac{1}{4}[(\gamma_{20} - \gamma_{02} - \tilde{\gamma}_{11}) + i(\tilde{\gamma}_{20} - \tilde{\gamma}_{02} + \gamma_{11})]$$

Hence in complex notation,

$$F_{b_o}(z) = \lambda z + \frac{1}{2T}(1+i)z^2 - \frac{1}{T}(1-i)z\bar{z} - \frac{1}{2T}(1-i)\bar{z}^2 \qquad (3.11)$$

with $\lambda = \tfrac{1}{2}(a+iT)$. Using the formula (2.1) we find that for $a \in (-2,2)$

$$a(0) = \frac{3-a}{2(2-a)}$$

which is strictly positive and the proposition is proved.

As the parameters move along the Hopf line from $a = 2$ to $a = -2$ the argument of the eigenvalues at P changes from 0 to π and so the family contains all the resonances discussed in chapter two. Provided the relevant coefficients in Theorem 2.7 do not vanish, each point on the Hopf line corresponding to eigenvalues which are q-th roots of unity, $q \geq 5$, is the endpoint of a cusped region which lies above H. For parameter values inside this cusp and sufficiently near H the map has an attracting invariant circle on which there are two orbits of period q, one an orbit of sinks, the other an orbit of saddles.

For the strong resonance at $a = -1$, $b = 5/4$, where the eigenvalues are cube roots of unity, note that the coefficient of $\bar{z}^2$ in (3.11),

$$\xi_{02} = \frac{-1}{2\sqrt{3}}(1+i)$$

is non-zero, so the result of Iooss [19] mentioned in the previous chapter guarantees that a period three orbit of saddles will bifurcate from P on both sides of H as we follow any one-parameter path which crosses H transversely at $a = -1$, $b = 5/4$.

At $a = 0$, $b = 3/4$, the strong resonance with eigenvalues $\pm i$, (3.11) becomes

$$F(z) = iz + \tfrac{1}{4}(1+i)z^2 - \tfrac{1}{2}(1-i)z\bar{z} - \tfrac{1}{4}(1+i)\bar{z}^2$$

and the normal form of Lemma 2.6 is

$$f(z) = iz - \frac{3i}{4}z^2\bar{z} - \frac{i}{4}\bar{z}^3 + O(|z|^5)$$

where the coefficients are calculated from (2.18). To apply Theorem 2.8, take a one-parameter straight line path $a = \varepsilon(b-3/4)$ through the point in question with the slope ε to be determined. Considering this path to be parameterized by b, an easy calculation shows that, in the notation of 2.8,

$$\lambda_1 = \frac{\varepsilon}{2} + i\,\frac{(\varepsilon+2)}{4} \quad .$$

Note the two conditions in 2.8 are separated by the equality

$$\left|\mathrm{Im}\,\frac{\alpha(0)}{\lambda_1}\right| = \left|\frac{\beta(0)}{\lambda_1}\right|$$

which here leads to

$$3\varepsilon^2 - 4\varepsilon - 4 = 0.$$

There is a region in the parameter plane above H whose boundaries have as tangents the lines $a = \varepsilon(b-3/4)$, where ε takes the two values satisfying the equation above. Outside this region Theorem 2.8 (1) applies and there is an attracting invariant circle for the map, while inside this region (2) applies and there are two families of periodic points, of period four, which, since $|\alpha(0)| = 3/4$ is larger than $|\beta(0)| = 1/4$, bifurcate from the origin if we enter this region. We suspect, but cannot prove, that these periodic points lie on an invariant circle. Note that the relevant values of ε are

$$\varepsilon \simeq 0.42 \quad \text{and} \quad \varepsilon \simeq -0.29 \tag{3.12}$$

In the next chapter we describe numerical results which extend the boundaries of the cusped regions corresponding to weak resonances and the sector corresponding to eigenvalues $\pm i$. We also find the region in the parameter plane where the map has an orbit of period three. For such an orbit

$$(x,y) \to (y,z) \to (z,x) \to (x,y)$$

x, y and z satisfy

$$\begin{cases} x = az+b-y^2 \\ y = ax+b-z^2 \\ z = ay+b-x^2 \end{cases}$$

Eliminating y and z from these equations leads to a polynomial of degree eight in x. The fixed points of F satisfy a quadratic equation which is a factor of this polynomial, and cancelling this leaves a polynomial of degree six in x whose coefficients are polynomials in the parameters a and b. Attempts to solve this equation have not been

successful, but from the behaviour of $F_{(0,b)}$ we know that the map does have two orbits of period three when $b > 1.75$. Also, since the equation is of degree six, there are at most two orbits of period three, and the numerical results below show that these exist above a curve in the parameter space, passing through $a = 0$, $b = 1.75$, the two orbits being created by a fold bifurcation along this curve.

CHAPTER FOUR

MAYNARD SMITH'S MAP: NUMERICAL RESULTS

In this chapter we extend the local analysis of Maynard Smith's map in chapter three by finding numerically the boundaries of the tongues associated with resonant Hopf bifurcation at eigenvalues $e^{2\pi ip/q}$ for $q = 3,4,5$ and 6. This gives some insight into the structure and complexity of the bifurcation set and shows how some of the periodic orbits created by resonant Hopf bifurcations are related to those which appear in the one-parameter family F_b of §3.1.

A series of computer-drawn phase portraits is presented in 4.2, showing how the behaviour of the one-parameter family with $a = \frac{1}{2}$ becomes increasingly complex as b increases, with a larger and larger attracting set emerging which abruptly disappears at a certain value of b. We describe the construction of an invariant set in the phase plane which contains all the recurrent behaviour for some parameter values, and we show how a global bifurcation can destroy this set, thereby causing an attractor to disappear as it does in the computer picture.

4.1. The Bifurcation Set.

To find the part of the bifurcation set corresponding to an orbit of period n with one eigenvalue equal to one we must solve

$$\begin{cases} x_n - x_o = 0 \\ x_{n+1} - x_1 = 0 \\ \Delta - \sigma + 1 = 0 \end{cases} \tag{4.1}$$

where the periodic orbit is

$$(x_o,x_1) \to (x_1,x_2) \to \ldots \to (x_n,x_{n+1}) = (x_o,x_1)$$

and Δ and σ are the determinant and trace of $dF^n(x_o,x_1)$. Here x_n, x_{n+1}, Δ and σ depend on the initial point (x_o,x_1) and on the parameters a and b. Solving the first pair of equations in (4.1) gives the fixed points of F^n and substituting these in the third equation leads to an expression involving only the parameters which defines the relevant part of the bifurcation set. For $n \geq 3$ (4.1) is too difficult to solve by hand so instead approximate numerical solutions were found.

Fixing the value of one of the parameters, say a, leads to a map $G: \mathbb{R}^3 \to \mathbb{R}^3$, $G(x_o,x_1,b) = (g_1,g_2,g_3)$, where the components g_i are defined by the left hand side of (4.1), and the problem is to find the zeros of this map. Given a sufficiently good approximation $z_1 = (x_o,x_1,b)$ to a zero of G, Newton's method asserts that the sequence $\{z_i\}_{i=1}^{\infty}$ defined by

$$z_{i+1} = z_i - [dG(z_i)]^{-1}G(z_i)$$

will converge to that zero, and this sequence is easy to compute from the formula for Maynard Smith's map. The first two components of $G(z_i)$ are found from the relation

$$x_{k+2} = ax_{k+1} + b - x_k^2$$

and using the chain rule we find that the entries $\alpha_{ij}(k)$ of $dF^k_{(a,b)}(x_o,x_1)$ satisfy

$$\alpha_{ij}(k) = \alpha_{2j}(k-1)$$

$$\alpha_{2j}(k) = -2x_{k-1}\alpha_{ij}(k-1) + a\alpha_{2j}(k-1) \quad (j = 1,2)$$

from which the determinant Δ and trace σ, and hence $g_3(x_o,x_1,b)$, may be calculated. To obtain the entries in the Jacobian $dG(z_i)$, these relations are differentiated with respect to x_o, x_1 and b in turn

(thinking of x_k as a function of x_0, x_1 and b) to give recurrence relations for the various partial derivatives.

The sequence $\{z_i\}$ is then generated until an approximate solution z_i is found with $|G(z_i)| < \varepsilon$, where ε is suitably small. Having found this approximate solution for a given value of $a = a_1$ it can be used as an initial approximation to a zero of G with $a = a_2$, provided $|a_1 - a_2|$ is sufficiently small. By successively changing the value of a, and computing an approximate zero of G for each one, a series of points on the bifurcation set of F can be found and if there are no large jumps in the values of the approximate zeros then we can assume that the bifurcation set is a continuous curve through these points.

These computations were carried out for orbits of period three, four, five and six using an Algol program on the ICL2970 in the University of Southampton Computing Service, using a routine from the Numerical Algorithms Group library to compute an approximate inverse of the Jacobian $dG(z_i)$. For a given value of a the sequence $\{z_i\}$ was generated until a point was obtained with $|G(z_i)| < 10^{-4}$, and the increment in values of a was in most instances 0.05, though in certain cases this was reduced to improve the rate of convergence. It was also found useful to reverse the roles of the parameters a and b in the above discussion for some parts of the bifurcation set. The third equation in (4.1) was replaced by $\Delta+\sigma+1 = 0$ and $\Delta = 1$ respectively to find the parts of the bifurcation set corresponding to one eigenvalue equal to minus one and complex eigenvalues of modulus one for orbits of period three, four and five. The results are described in the following series of figures. Some of the actual numbers involved are contained in the appendix, where the values of a and b which lie on the relevant part of the bifurcation set are listed, together with the second eigenvalue or the argument of the eigenvalues as appropriate.

The diagrams are labelled as follows. B^n_* denotes the part of the bifurcation set pertaining to an orbit of period n, and $*$ is either +, - or 0, according to whether the critical eigenvalue along this component is +1, -1 or a complex conjugate pair. For periods five and six where there are several different periodic orbits we label the curves $B^n_*(i)$ for the ith periodic orbit.

For period three we find that two orbits appear through a fold bifurcation along a curve B^3_+ which has a single minimum at $a \simeq -0.70$, $b \simeq 0.86$, and one of the orbits is a sink in a narrow region above the lower part of this curve. The precise situation is shown in figure 4.1. Note that on the scale of this figure there are three curves on the right hand side which appear to coalesce, but an inspection of the numerical results show that they do not, and Figure 4.1a, a schematic version of Figure 4.1, shows the relative locations of the curves and the nature of the period three orbits in the various regions of the parameter plane. The point $B^3_+ \cap B^3_o$ where the map has a single orbit of period three with both eigenvalues +1 is $a \simeq 1.2$, $b \simeq 7.3$ so the region where the map has a stable orbit of period three is a long and narrow strip. Also notice that a part of this region lies below the Hopf line where the fixed point P loses stability. Thus for an open set of parameter values the map has a stable fixed point and a stable orbit of period three.

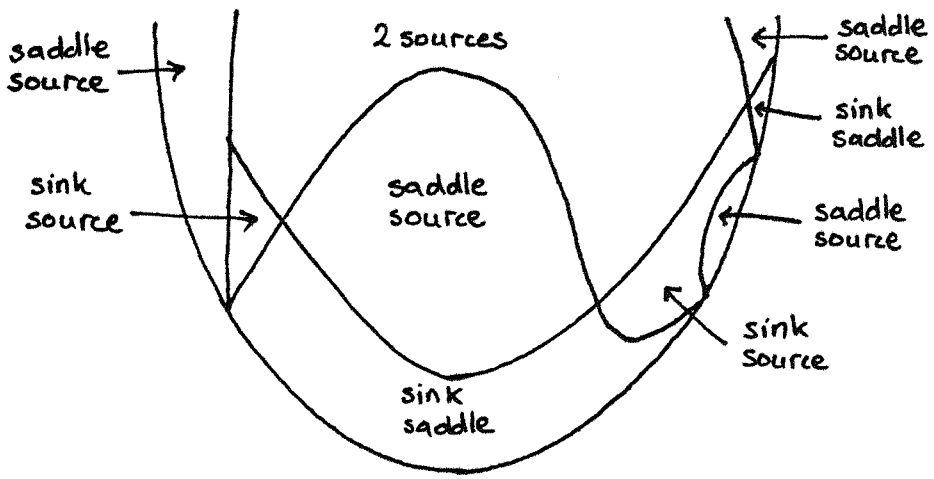

Figure 4.1a.

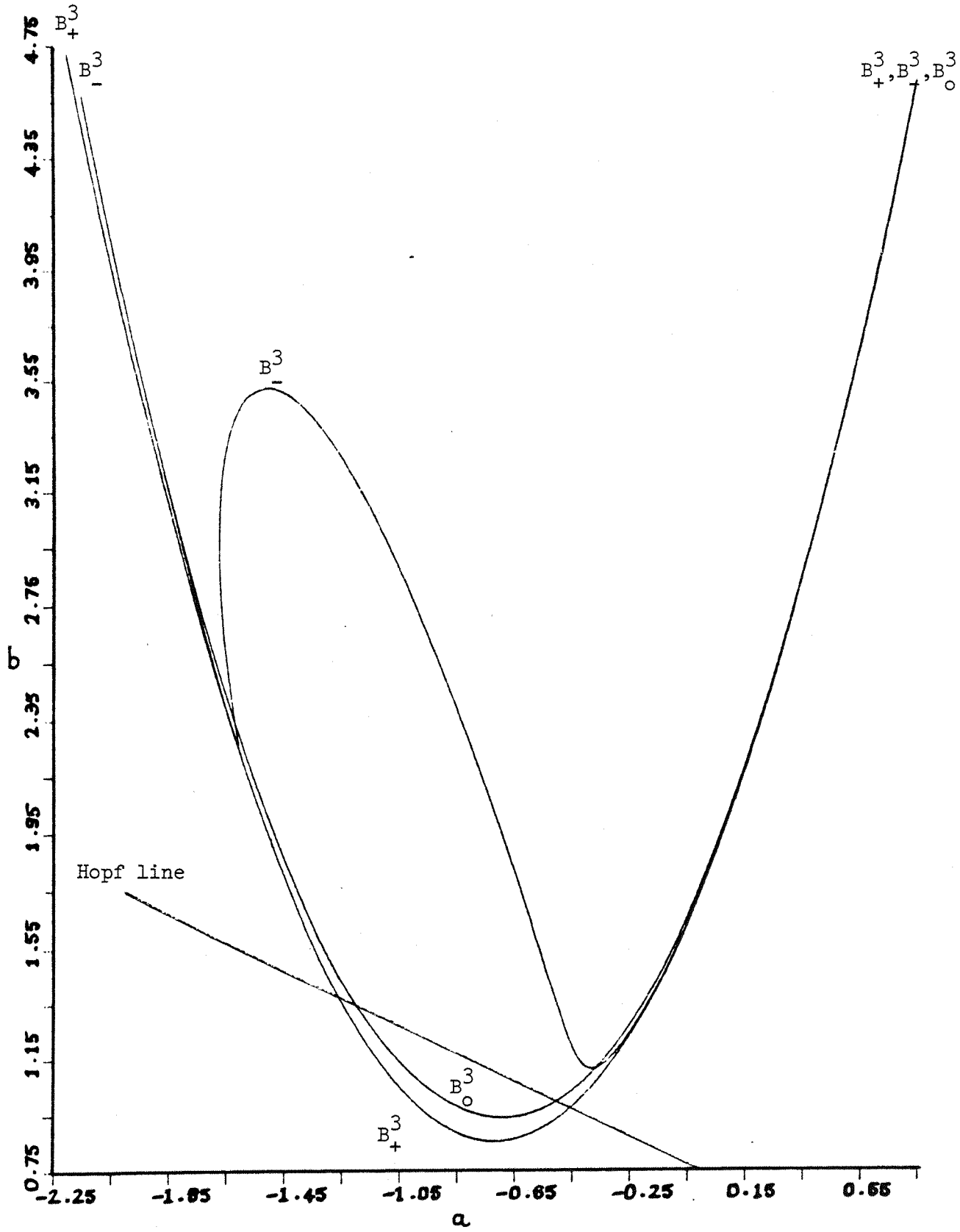

Figure 4.1. Period Three.

The strongly resonant Hopf bifurcation at $a = 0$, $b = 3/4$ leads to the existence of two orbits of period four inside the sector bounded by B^4_+ in figure 4.2. The internal structure of this sector is relatively simple. There are two curves B^4_- which intersect at $a = 0$, $b = 5/4$ and divide the sector into four. In the lower section the period four orbits are a sink and a saddle respectively, two sources in the central upper section, and a saddle and a source in the outer sections. The dashed lines in figure 4.2 show the linear approximation to this sector given by the theory, i.e. they are the lines $a = \varepsilon(b-3/4)$ with ε taking the values in (3.12). These lines are tangent to the boundary of the sector at $a = 0$, $b = 3/4$, but provide a good approximation on the left hand side of the figure well away from this point.

There are two points of weak resonance on the Hopf line corresponding to eigenvalues of $dF(p)$ which are 5th roots of unity: $a = 0.618$, $b = 0.441$ and $a = -1.618$, $b = 1.559$, and we label the components of the bifurcation set containing these points $B^5_+(1)$ and $B^5_+(2)$. $B^5_+(1)$ has a further cusp at $a=-0.162$, $b = 1.656$ which does not lie on the Hopf line. There is also a third pair of orbits of period five created by a fold bifurcation along the curve $B^5_+(3)$ which has a similar shape to B^3_+. In figure 4.3 the second cusp on $B^5_+(1)$ appears to lie on $B^5_+(3)$ but a closer inspection reveals that this is not the case. Of course the points where these curves cross do not represent orbits with both eigenvalues equal to one, rather there are two separate fold bifurcations occuring for F^5 at these parameter values--in different parts of the phase plane.

The internal structure of the five-tongue bounded by $B^5_+(1)$ was also investigated and the results are shown in figures 4.4 and 4.4a. The curve $B^5_o(1)$ has one endpoint on $B^5_+(1)$ slightly above the second cusp and then follows $B^5_+(1)$ down, gradually moving further away until it reaches a minimum above the cusp point on the Hopf line, and then rising

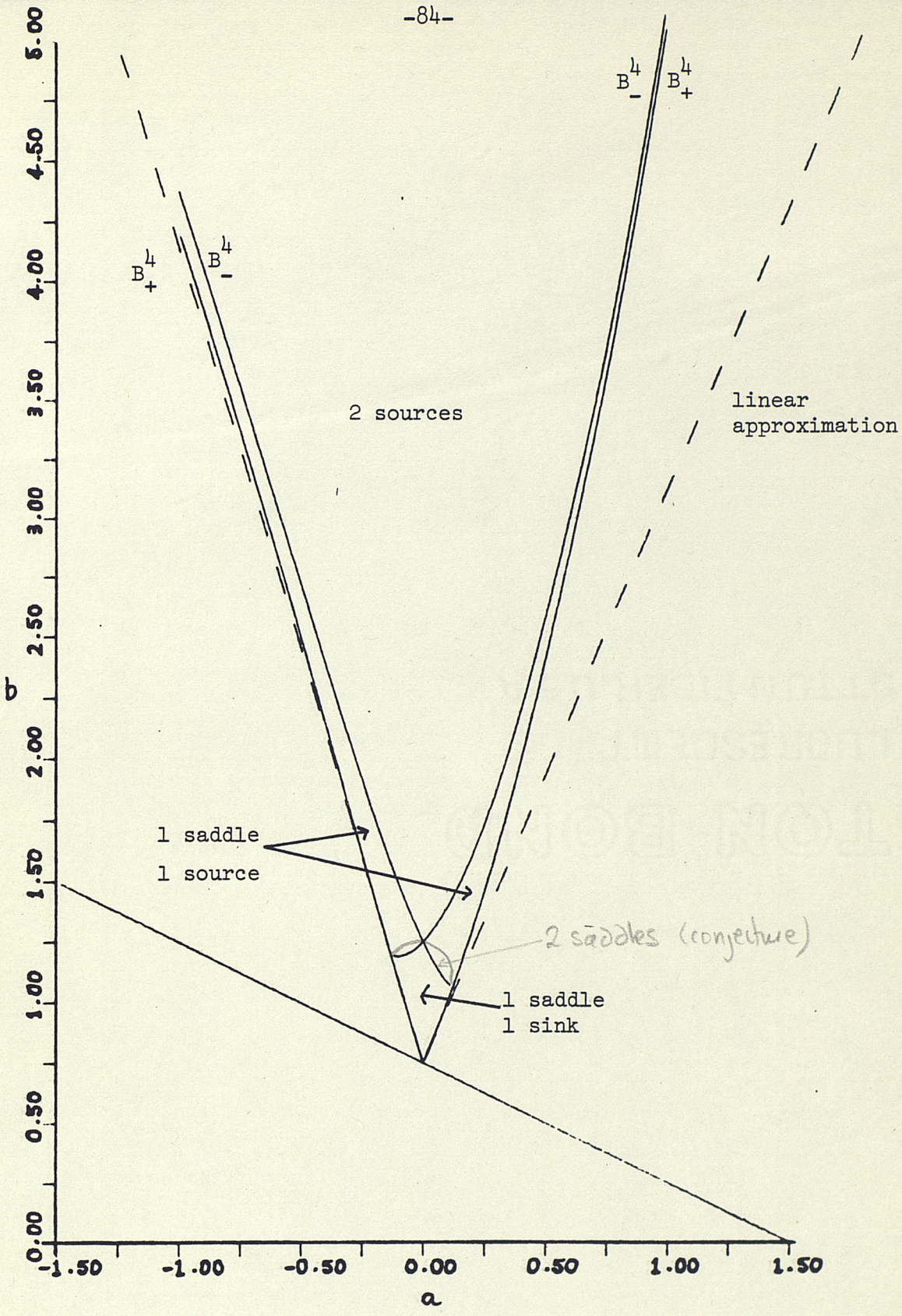

Figure 4.2. Period Four.

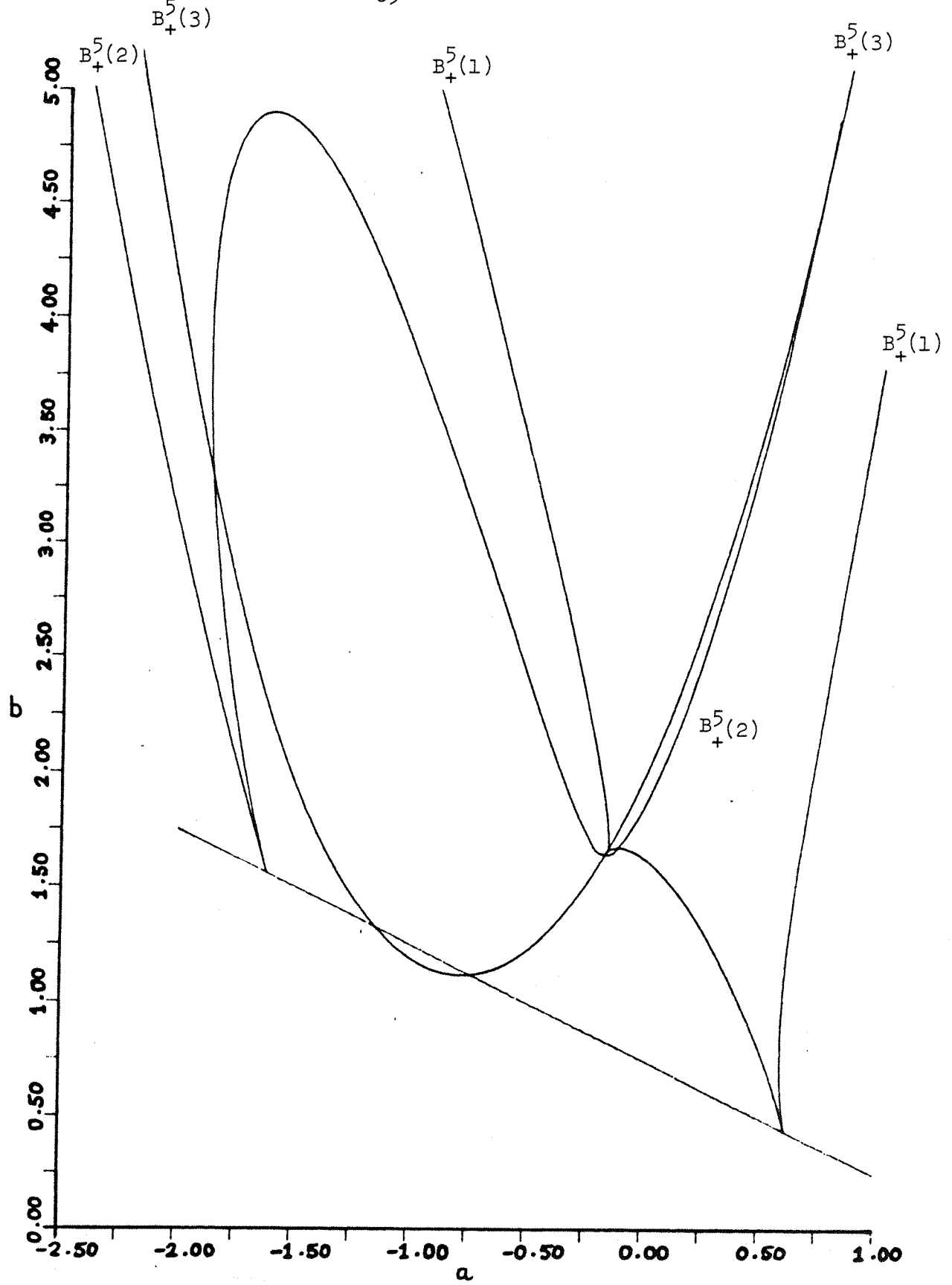

Figure 4.3. Period Five.

to meet $B_{-}^{5}(1)$ at $a \simeq 0.60$, $b \simeq 1.13$. The curve $B_{-}^{5}(1)$, where a five point cycle has an eigenvalue equal to -1, follows $B_{+}^{5}(1)$ down the right hand side of the figure before meeting it at $a \simeq 0.59$, $b \simeq 0.81$, then crossing the cusp to meet $B_{+}^{5}(1)$ again at $a \simeq 0.48$, $b \simeq 0.84$ and following $B_{+}^{5}(1)$ up to $a = 0$, $b = 1.6244$. To obtain a consistent picture of the nature of the two orbits of period five inside $B_{+}^{5}(1)$ we conjecture that there is a further branch of $B_{-}^{5}(1)$, starting at $a = 0$, $b = 1.6244$ and extending up the left hand side of figure 4.4, though this branch has not been found. With this proviso the stability of the two orbits is indicated in figure 4.4a, where the conjectured branch is shown as a dashed line.

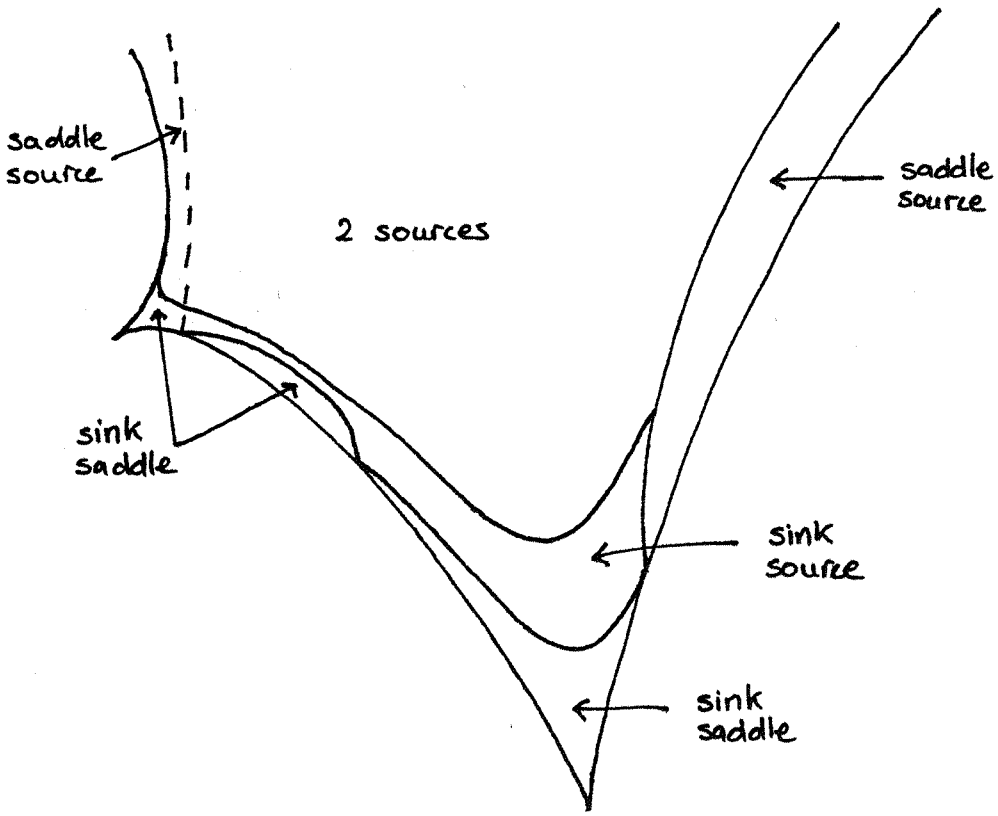

Figure 4.4a. Period Five (1).

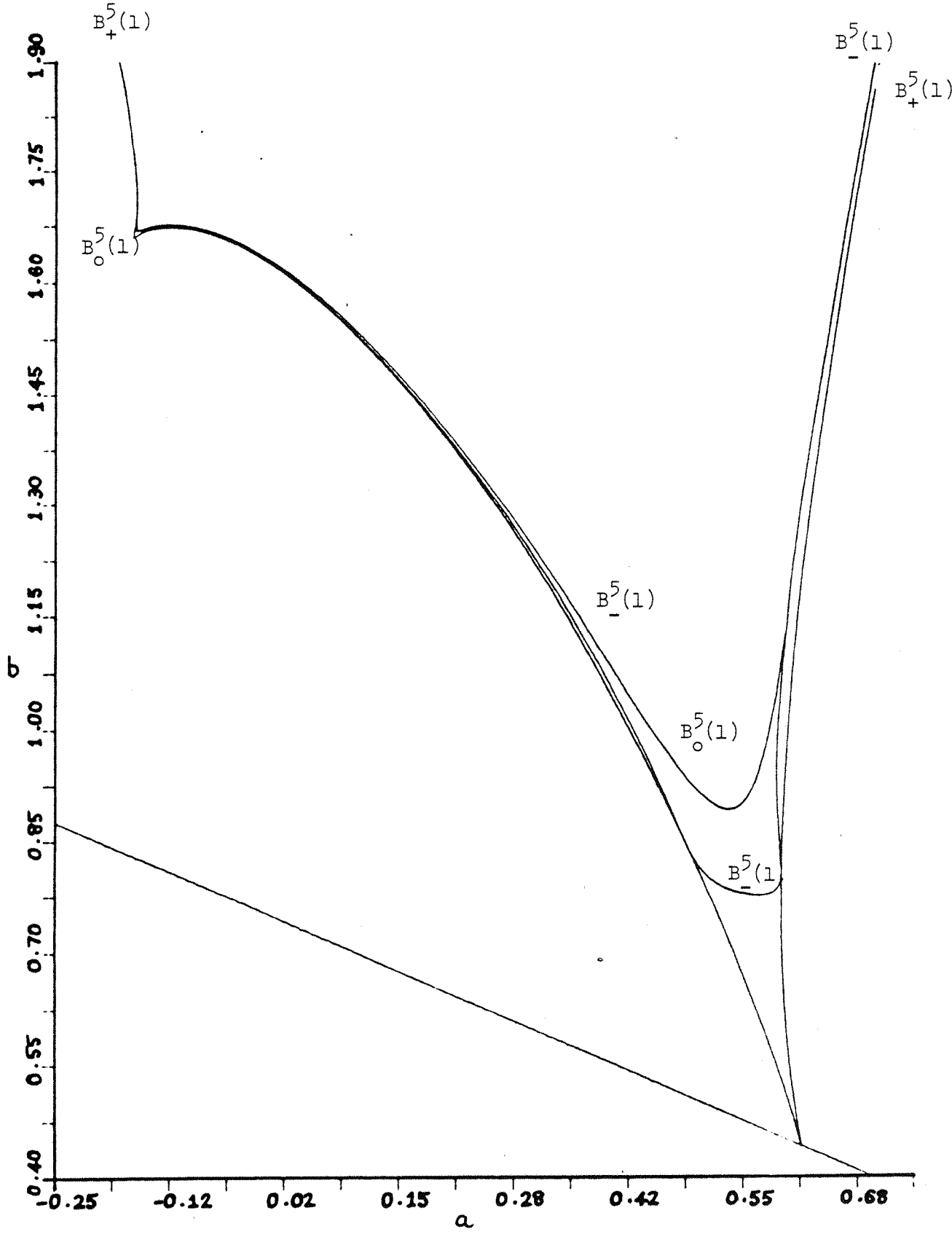

Figure 4.4. Period Five (1).

For the six point cycles there is only one weak resonance on the Hopf line, at $a = 1$, $b = 1/4$, and the left hand side of the cusp at this point crosses the b-axis at $b = 7/4$, intersecting B^3_+, and contains two further cusps, at $a \simeq -0.43$, $b \simeq 1.41$ and $a \simeq -1.95$, $b \simeq 3.49$. Now the point $a = 0$, $b = 7/4$ corresponds to the birth of the orbit of period three in the one-dimensional map h_b and an examination of the dynamics of $F_{(0,7/4)}$ reveals that eight different orbits of period six are created in Maynard-Smith's map at these parameter values. In fact we have the situation shown in the following diagram.

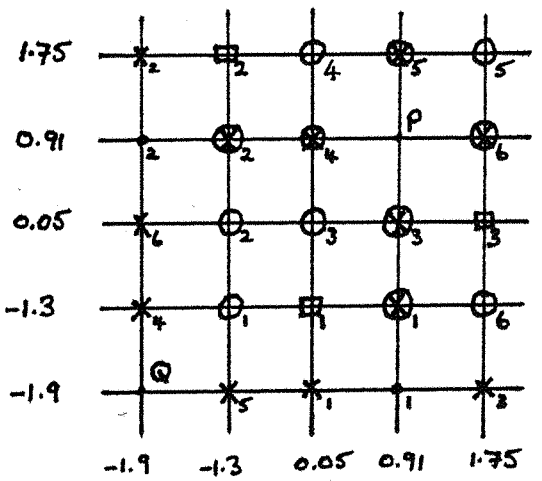

The map $h_{7/4}$ has a non-hyperbolic orbit of period three, which is approximately

$$1.75 \to -1.30 \to 0.05 \to 1.75$$

and together with the fixed points $P \simeq (0.91, 0.91)$ and $Q \simeq (-1.91, -1.91)$ this gives the grid of 25 periodic points for F, connected as one orbit of period two, one of period three, three of period six and the two fixed points. As b increases through $7/4$ the horizontal and vertical lines given by the coordinates of the three point cycle split into two and the period six orbits marked x and ⊗ also split into two, but the orbit O gives four orbits of period six, so eight orbits of period six are

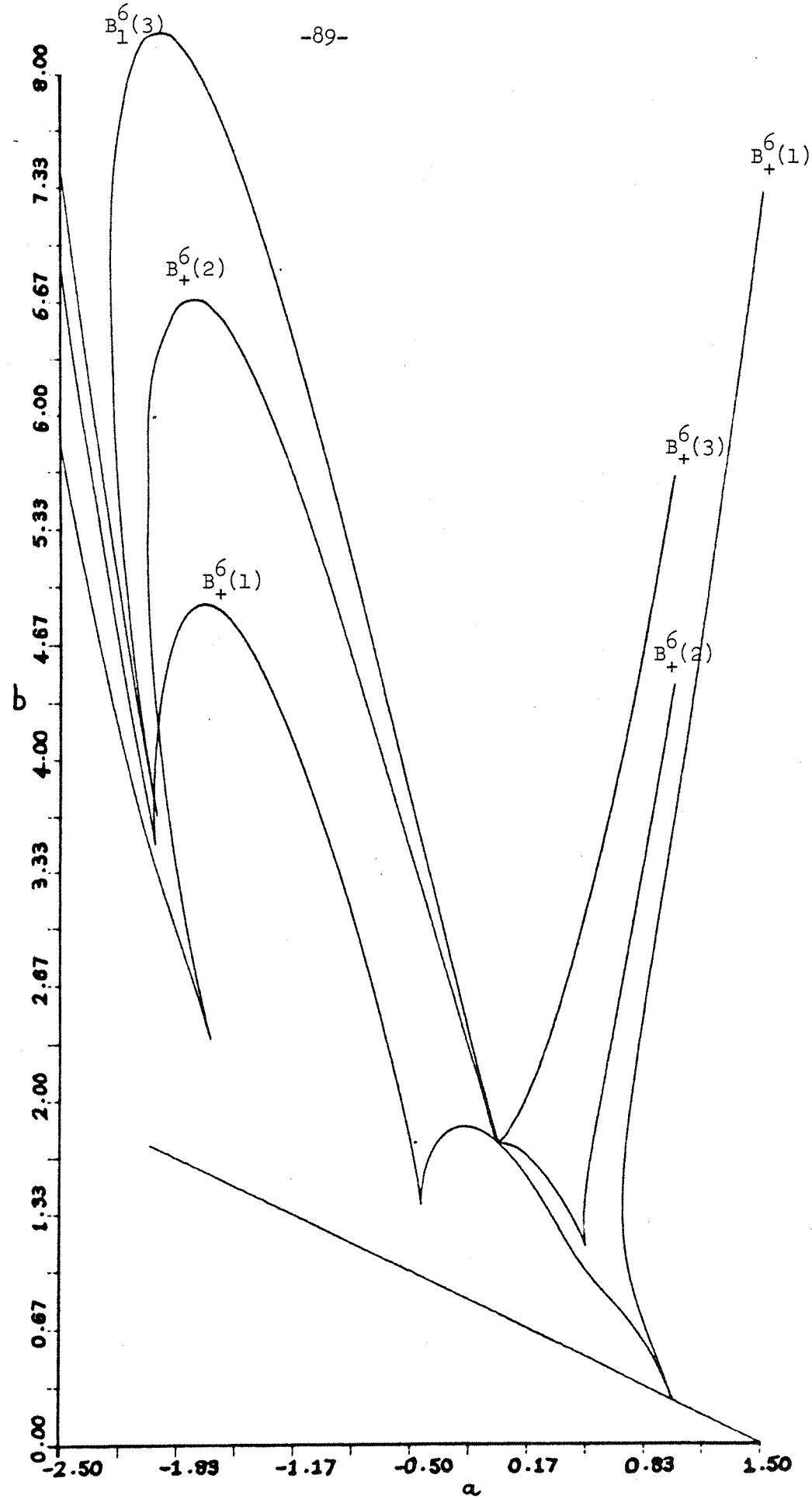

Figure 4.5. Period Six.

born at $a = 0$, $b = 7/4$. The pair which are created on the boundary of the invariant square are associated with a curve of the same shape as B_+^3 and $B_+^5(3)$ with a single minimum, and the orbits created by the bifurcation along this curve are always unstable. The curves where the other orbits are born are shown in figure 4.5. The orbits which bifurcate from the one marked 0 are associated with $B_+^6(2)$ and $B_+^6(3)$, while the orbit marked x corresponds to $B_+^6(1)$.

The internal structure of the tongue bounded by $B_+^6(1)$ contains one intriguing feature. There is a curve B_0^6, see figure 4.6, where the map has an orbit of period six with complex eigenvalues on the unit circle, which joins $B_+^6(1)$ and $B_+^6(2)$. B_0^6 meets $B_+^6(1)$ at $a \simeq 0.46$, $b \simeq 1.24$, has a minimum above the cusp on the Hopf line, then curves close to $B_+^6(1)$ again before moving away and crossing $B_+^6(2)$ on the right hand branch slightly above the cusp, finally joining $B_+^6(2)$ at $a \simeq 0.46$, $b \simeq 1.24$. We have no explanation for this phenomenon and it is difficult to see what the stabilities of the period six points are in figure 3.15, excepting that the numbers in the appendix show the nature of these points as they bifurcate, i.e. close to the boundaries $B_+^6(1)$ and $B_+^6(2)$.

Figure 4.7 shows the boundaries of the 3,4,5 and 6-tongues in the parameter plane together with the parabolae P_1, P_2 and the Hopf line H which bound the various regions of stability for the fixed point P. Note that these are all the orbits of period 3, 4, 5 and 6 associated with Hopf bifurcation at P and from studies of h_b, see for example Gumovski and Mira [15], we know that no other orbits of period 3 or 5 appear as we move up the b-axis, although there is a further pair of orbits of period 4 and several more of period 6. It is not known if any periodic points exist in regions of the parameter plane which do not intersect the b-axis.

Inside each of these tongues the situation shown in Figure 4.7 is repeated. For each family of periodic points there is a (many-to-one) map

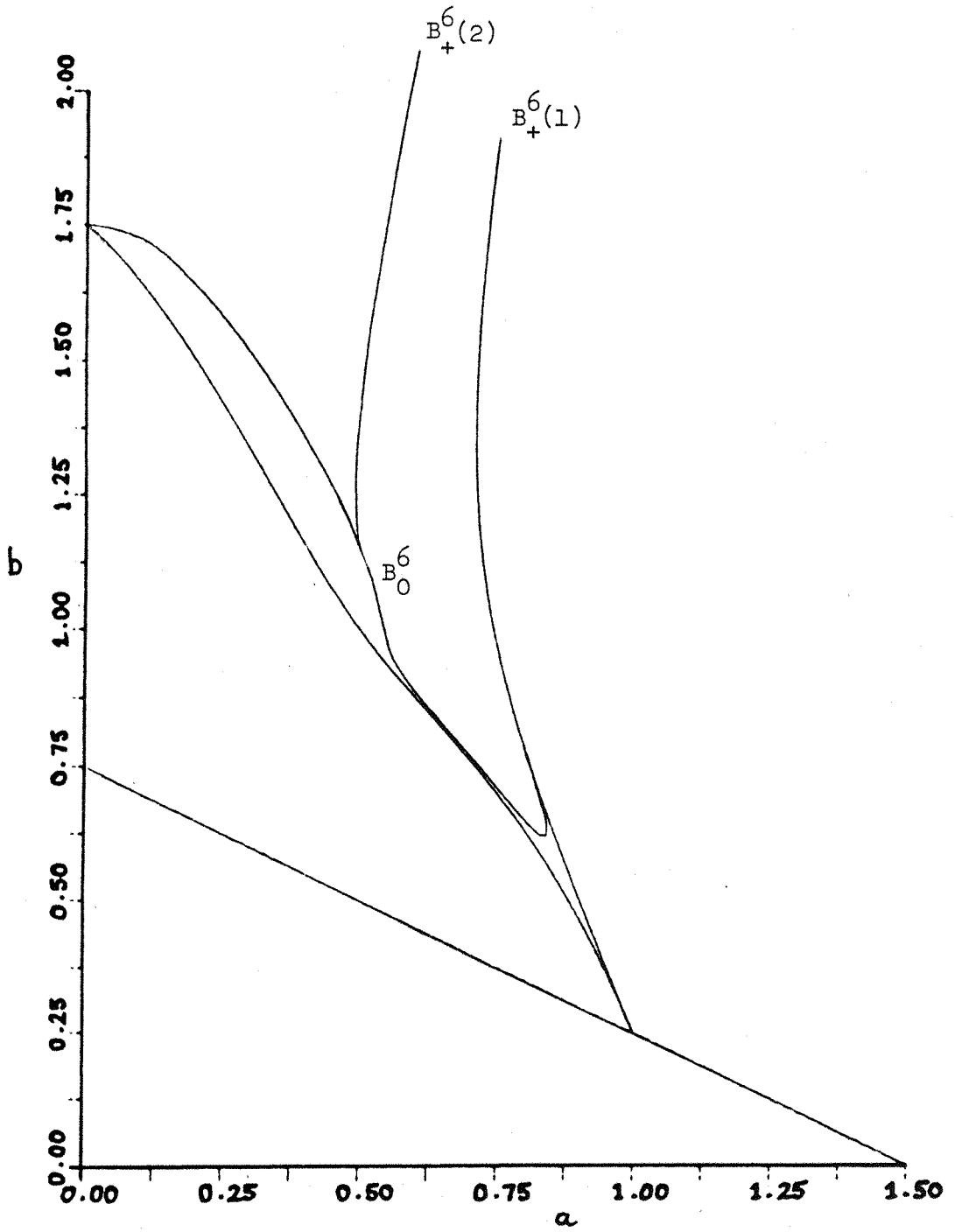

Figure 4.6. Period Six.

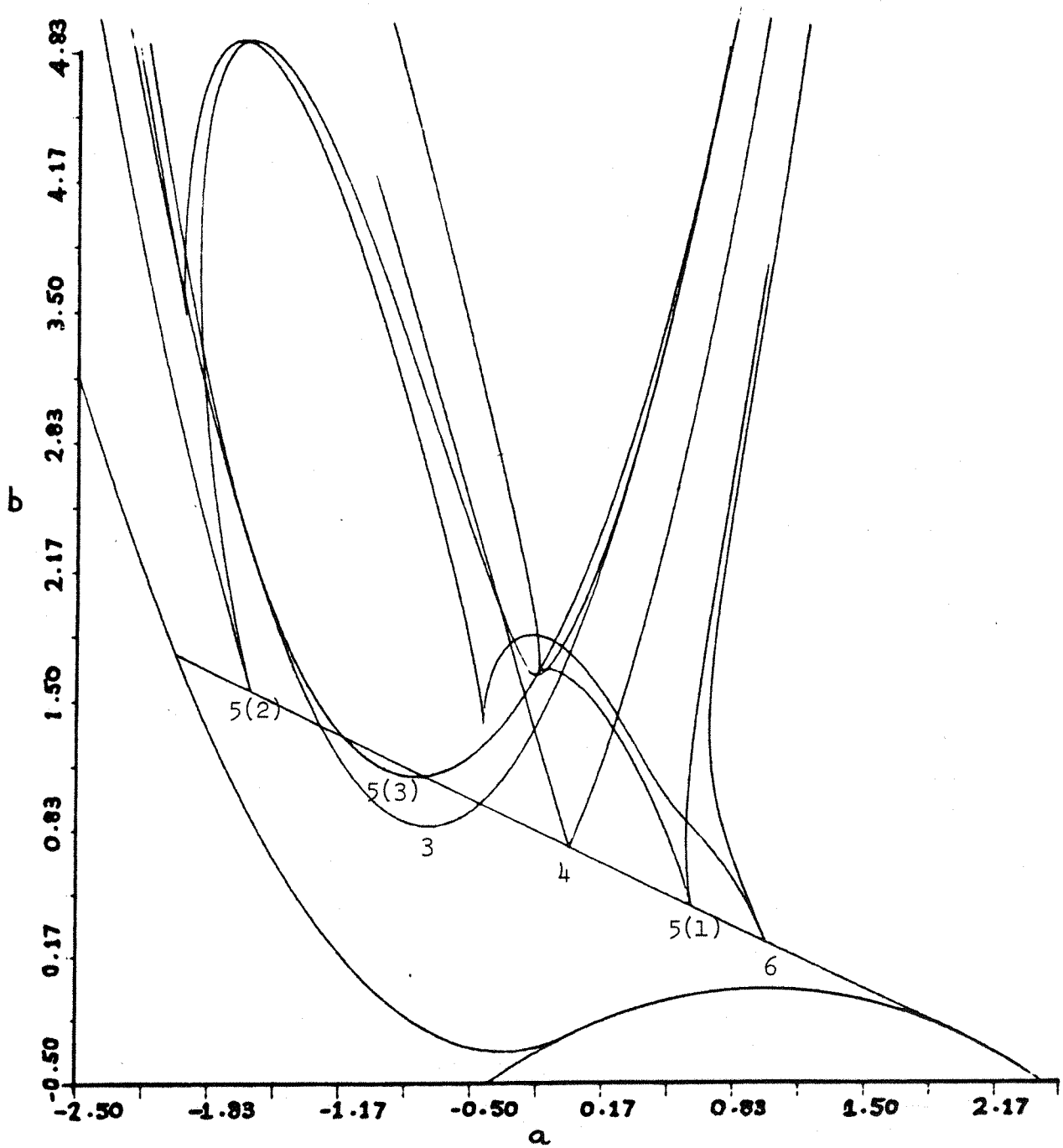

Figure 4.7. The Bifurcation Diagram.

from the subset of the parameter plane where they exist into the (Δ,σ)-plane of figure 2.10, and the preimages of the resonance tongues in figure 2.10 lie on the curves B_o^n in the (a,b)-plane where an n-point cycle has complex eigenvalues on the unit circle. As the parameters cross these curves the n-point cycle undergoes a Hopf bifurcation: an invariant circle bifurcates from each of the n points in the orbit, the circles being invariant under F^n and mapped cyclically around the orbit by F. The behaviour of the map on these circles is then subject to the same resonance considerations as apply to the original circle which bifurcates from the fixed point P, and the whole story is repeated, in an analogous way to the repeated period doubling bifurcations of maps of the interval, perhaps involving, in some sense, Feigenbaum's universal constants.

Clearly the manner in which these tongues piece together in the parameter space is enormously complicated and the regions where there are stable periodic orbits tend to be very long and narrow strips in the (a,b)-plane. A one-parameter path through the parameter plane will pass through many sequences of bifurcation points whose limit points produce complicated 'strange' attracting sets of which virtually nothing is known. We now present a series of phase portraits for such a path.

§4.2. Phase Portraits

The following figures (a)-(0) are computer drawn phase portraits for parameter values along the vertical line $a = 1/2$ in the (a,b)-plane. The portraits are actually for the map

$$g(X,Y) = (Y, aY + bX(1-X)) \qquad (4.2)$$

but this is equivalent to the Maynard Smith family

$$F(x,y) = (y, Ay + B - x^2)$$

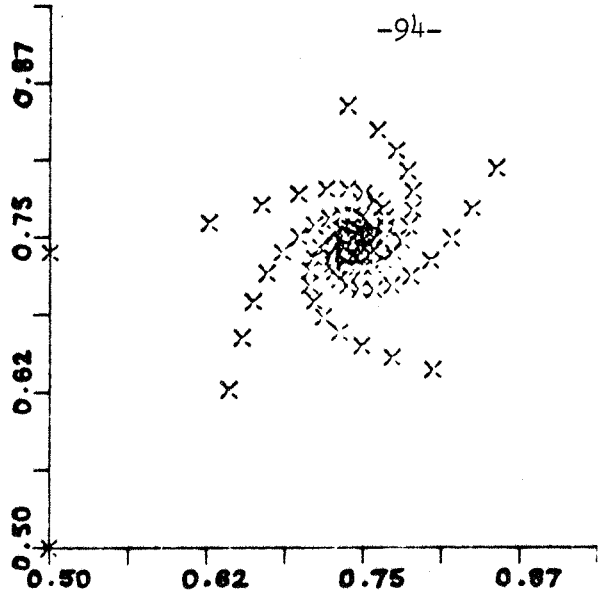

(a) b=1.95

The fixed point P of (3.1) with coordinates x = y = (a+b-1)/b is a sink, when a = 1/2, for 1/2 < b < 2, and at b = 1.95 the eigenvalues of dg(P) are complex so that orbits of points near P spiral into P as shown in (a)

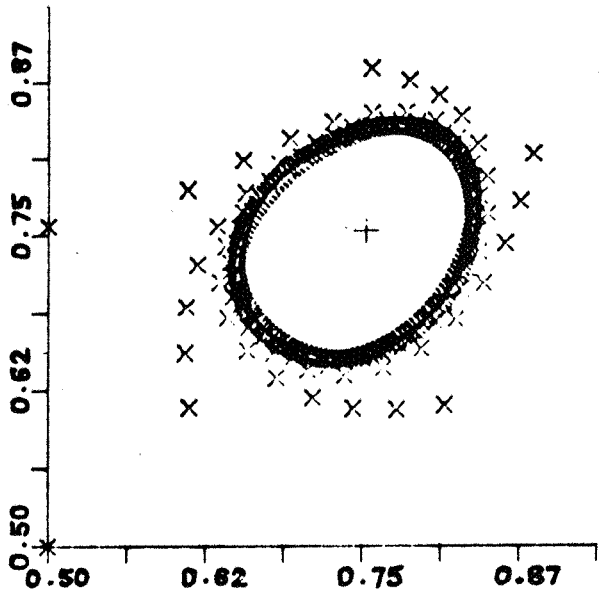

(b) b=2.03

At b = 2 P undergoes a supercritical Hopf bifurcation which creates the attracting invariant circle in figure (b). The + sign marks the position of the unstable fixed point.

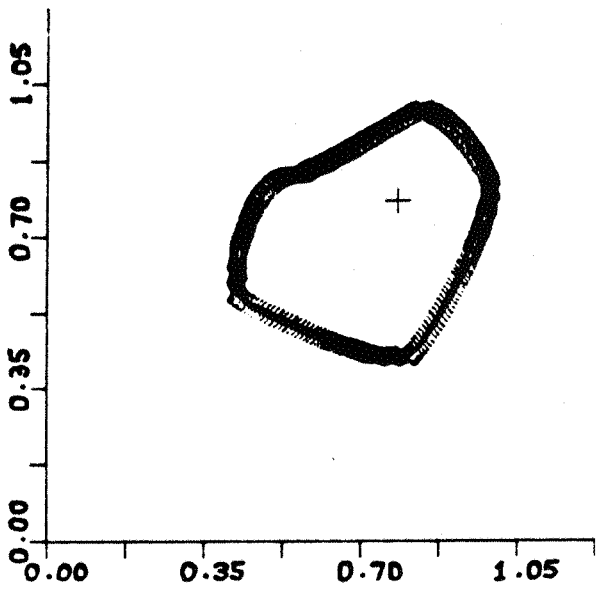

(c) b=2.3

As b is increased the circle grows and crosses the fold line x = 1/2, though the map does not fold the circle onto itself. The influence of the fold causes the circle to distort, producing kinks which gradually become more pronounced....

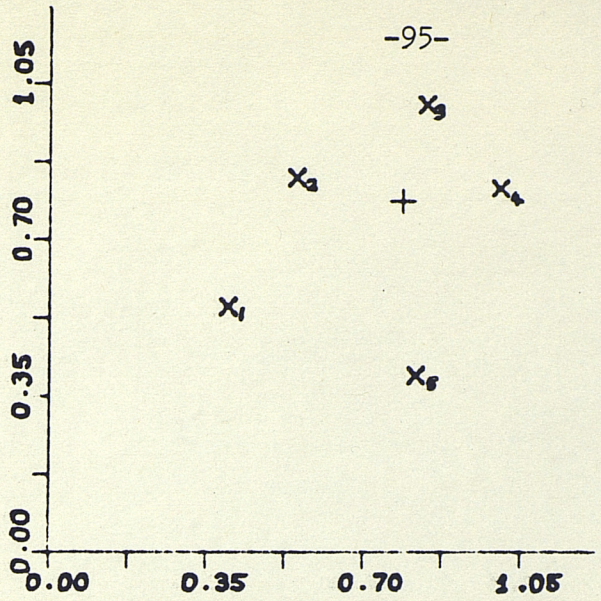

(d) b=2.36

... until we enter the five tongue (at b $\simeq$ 0.8 in Maynard Smith's map; see figure 4.4) related to resonance Hopf bifurcation at a = 0.618. The dynamics on the invariant circle have now "locked-on" to a pair of five point cycles, one of sinks, shown in (d), and one of saddles.

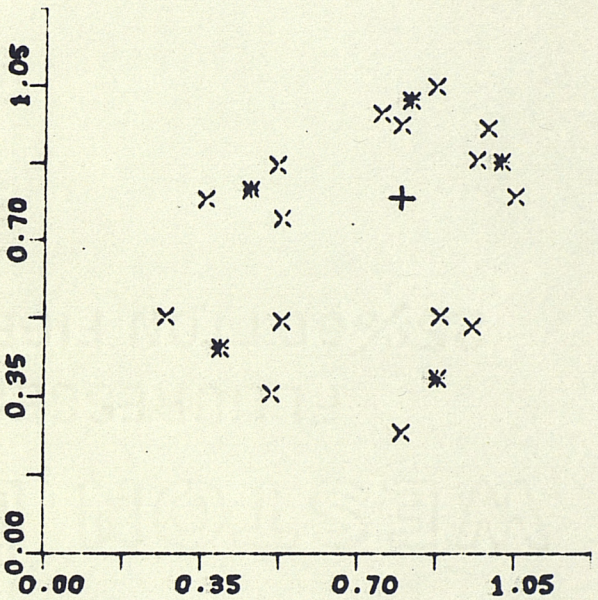

(e) b=2.46

In (e), when b = 2.46, a stable orbit of period 15 has appeared, but this does not bifurcate from the five point cycle, marked *, which is still stable. For g^5 this means that a stable 3 point cycle has appeared around each of the five fixed points, which is comparable to the behaviour of F for parameters near the minimum of the curve B_+^3 in figure 4.1.

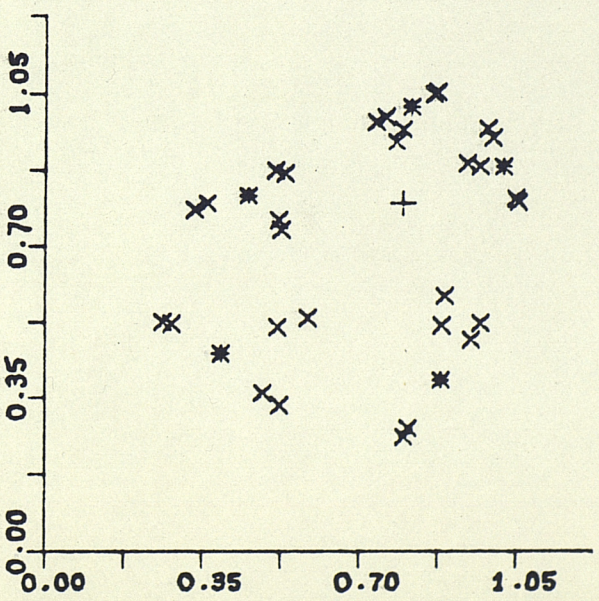

(f) b=2.47

The period of the larger cycle has doubled at b = 2.47 to give an orbit of period 30, plus the five point cycle. This period doubling continues...

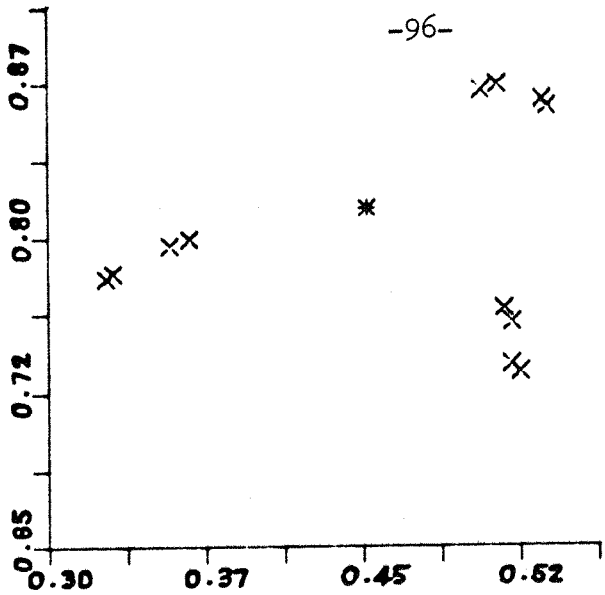

(g) b=2.472

... to give an orbit of period 60 at b = 2.472 (g) and period 120 at b = 2.473 (h). These two figures show only part of the phase space, containing a fixed point * (still stable) and orbits of period 12 and 24 respectively for g^5.

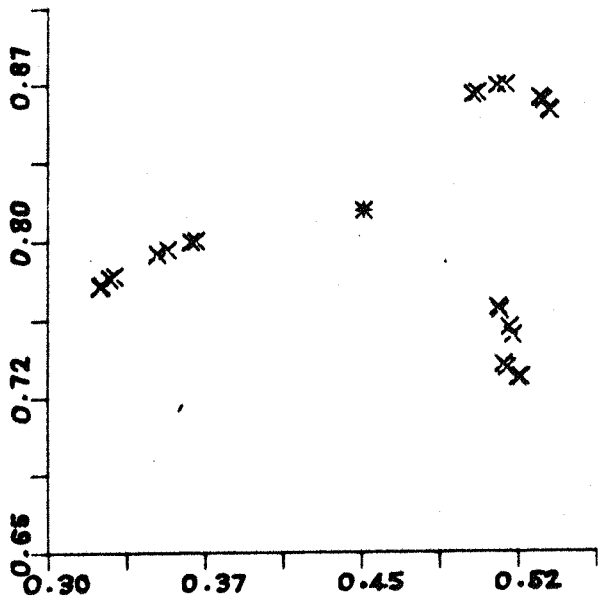

(h) b=2.473

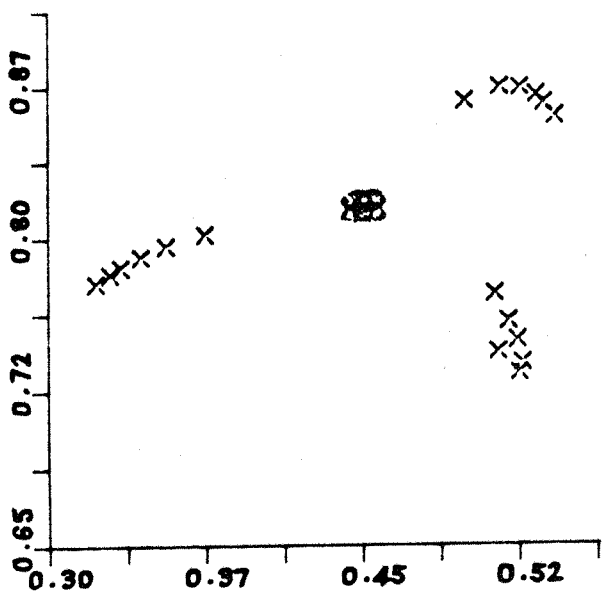

(i) b=2.474

At b = 2.474 g^5 has a stable orbit of period 18 (period 90 for g), but it is difficult to tell whether the five point cycle is still stable. Nearby points do approach it, but it may have bifurcated, throwing off an invariant circle.

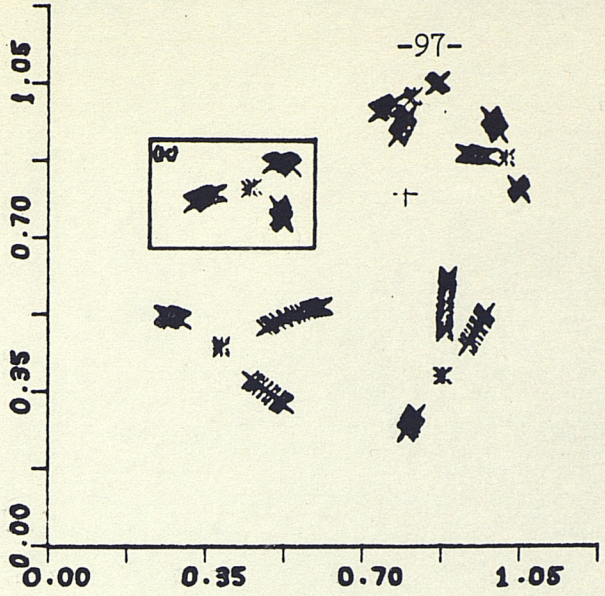

(j) b=2.475

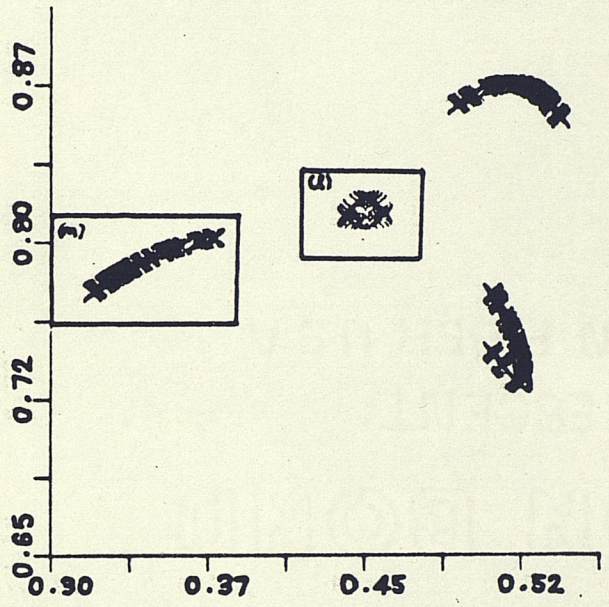

(K) b=2.475

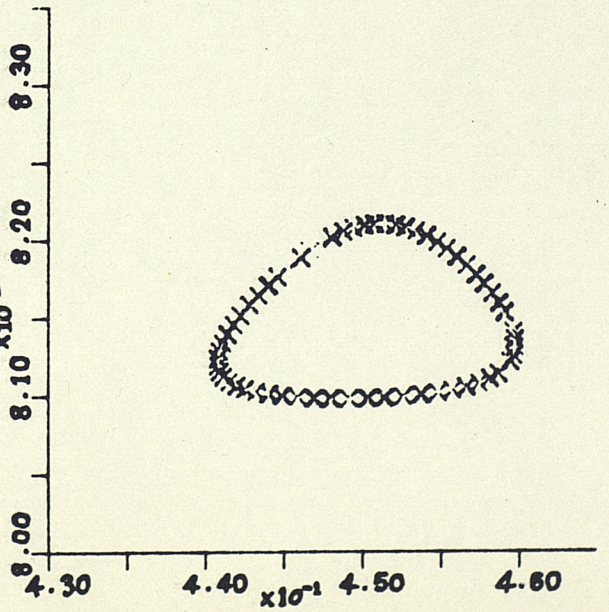

(l) b=2.475

In (j), b = 2.475, we return to the full phase portrait for g. The long periodic orbit has been superceded by a more complicated attracting set, each component of which has period 15 under g, (see the enlargements in (k) and (m)) while the orbit of period five has now definitely undergone a Hopf bifurcation, producing the invariant circle in (k) and (ℓ).

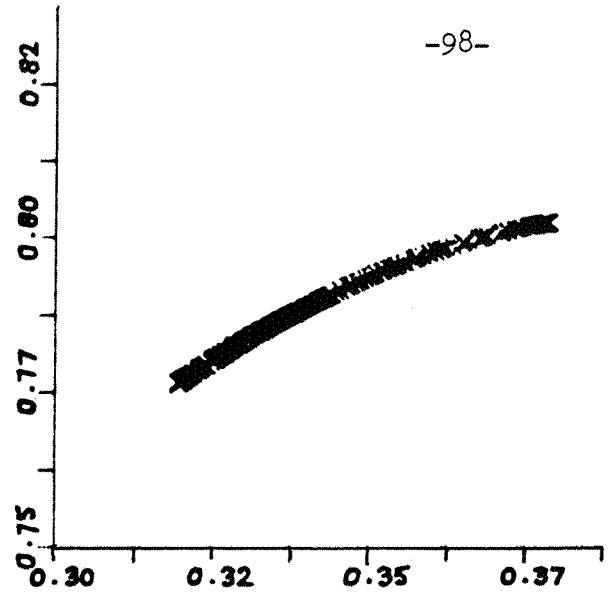

(m) b=2.475

The set shown in (m) has many of the characteristics of the 'twisted horseshoe' of Guckenheimer et al. [14]. An examination of the action of the map shows that under g^{15} a neighborhood of the set is stretched in the direction along the set, contracted tranverse to it and then folded back on itself. In fact several of the images of the set lie on the fold line $x = 1/2$ (see (j)) so the set is folded into itself more than once before being mapped back to its original position by g^{15}.

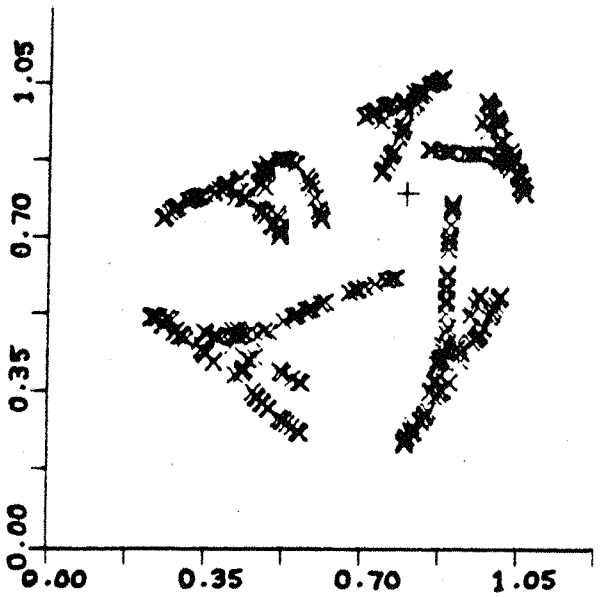

(n) b=2.5

At larger values of b the 15 components of the attractor join to form first five pieces (n), and then the single large set in (0). For slightly larger values of b the attractor vanishes, with apparently all orbits diverging.

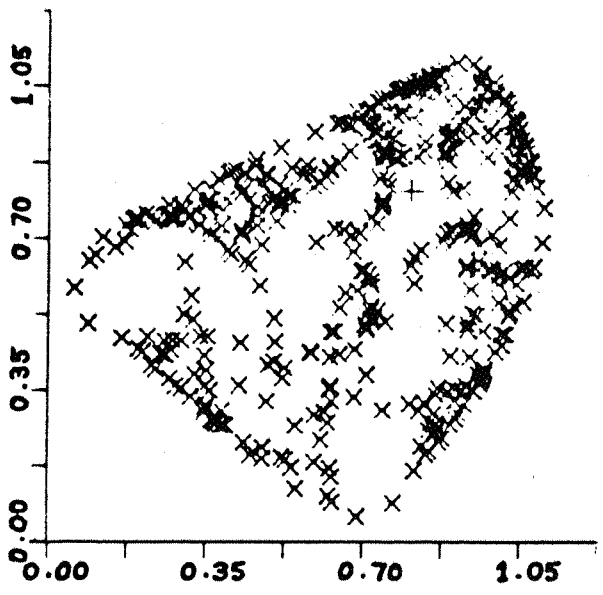

(o) b=2.6

via the parameter dependent coordinate change

$$x = bX - \frac{b}{2}, \quad y = bY - \frac{b}{2}$$
$$A = a, \quad B = \frac{ab}{2} + \frac{b^2}{4} - \frac{b}{2} \tag{4.3}$$

when $b \neq 0$. The parameter b given in these figures should be transformed by (4.3) to give the b in Maynard Smith's map. The only other difference is that the fold line $x = 0$ in Maynard Smith's map is translated by (4.3) to the line $X = 1/2$ in (4.2).

In each figure the point (0.5, 0.5), which lies at the intersection of the fold line in (3.14) and its preimage, was iterated, but, except in the first two figures, the first fifty points of the orbit are not shown. In figures (e)-(j) a point near the orbit of period five in figure (d) was also also iterated. Now not all points in the phase plane are attracted to the sets shown in (a)-(0). To conclude this chapter we describe the construction of the boundary of the set of points which do approach these attractors, and this will also suggest a mechanism which would cause the attractor to disappear as it does in this sequence of phase portraits when $b \geq 2.6$. Very roughly, points within the circle with centre (0.5,0.5) and with the line joining this point to the origin as radius will be attracted to the sets in the figures. Points outside this region diverge, with the coordinates of their iterates becoming increasingly large and negative.

Similar behaviour is observed in other one-parameter paths at $a = 1/4$, and $a = 3/4$. The overall picture as b increases is of a Hopf bifurcation, followed by a 'lock-on' to a periodic orbit as we enter a resonance tongue, the parameters perhaps passing through several of these tongues before the invariant circle becomes distorted and gives way either

directly to a nontrivial attractor, or to a sequence of period-doubling bifurcations leading to a complicated set. Initially these attractors have several components, which merge as the parameter is increased and then finally disappear at some value of b. In the path at $a = 3/4$ a large attractor formed in an annular region of the phase plane and then shrank, as b increased, eventually becoming a rather irregular circle which gave way to a seven point cycle. This cycle then began a period doubling sequence which was not completed before the attractor vanished. We now consider this abrupt disappearance of the attracting set.

Firstly, consider the map in one variable $h_b(x) = b-x^2$. Recall that h_b maps the interval $I = [x_-,-x_-]$ into itself for $b \in [-1/4,2]$, but suppose that b is slightly larger than 2; the graph of h_b for such a case is shown in figure 4.8. Clearly h_b maps an open subinterval J of I, with the critical point $0 \in J$, outside the previously invariant interval I. The first image of J under h_b lies above $-x_-$, then further images lie below x_-, with the left hand endpoint of $h^n(J)$ tending to $-\infty$ as $n \to \infty$.

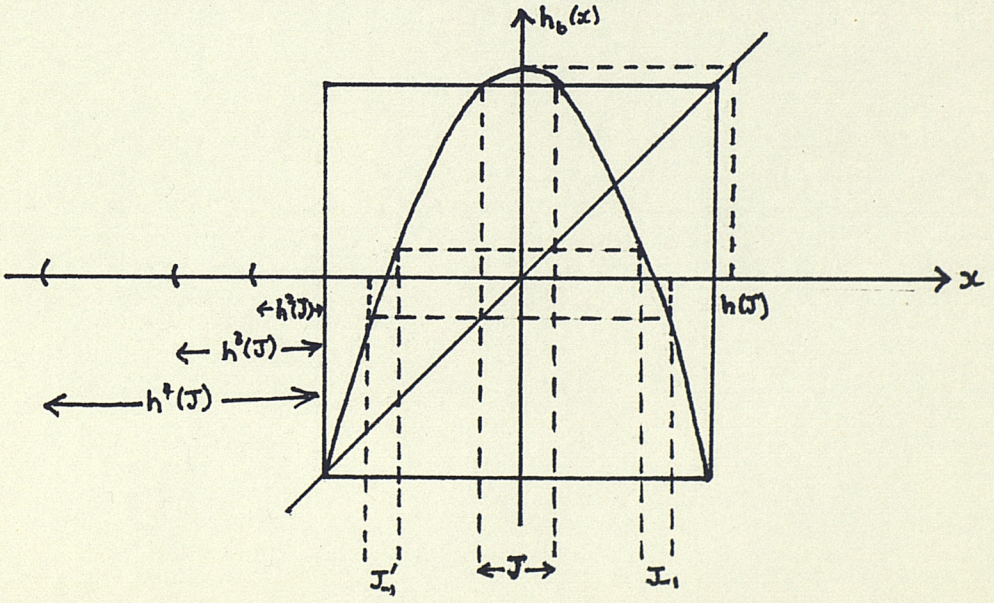

Figure 4.8.

Thus the subinterval J and all its preimages eventually escape from the interval I. Now J has two preimages under h, J_{-1} and J'_{-1}, each of which has two preimages in turn, so the set of points which remain in I under all iterates of h, $C = I \setminus \bigcup_{n=0}^{\infty} h_b^{-n}(J)$, is constructed in the same way as the standard Cantor set. Henry [41] proves that C contains no open intervals and therefore is a Cantor set.

For Maynard Smith's map with $a = 0$ the fold line $x = 0$ is mapped to the horizontal line $y = b$, and for $b > 2$ this line lies above the line $y = -x_-$ which forms part of the boundary of the square $S = I \times I$. In this case an open rectangle R is mapped out of the square and then around the boundary of S until it lies below the line $y = x_-$.

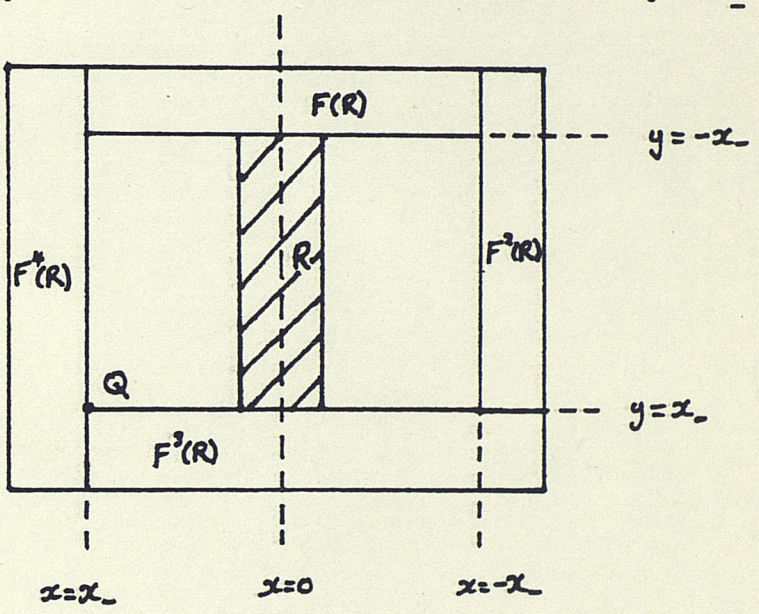

Figure 4.9.

Now the lines $y = x_-$ and $x = x_-$ are interchanged by $F_{(0,b)}$ and so after three applications of the map the image of R is switched backwards and forwards between the bottom of the square S and the left hand side of S. However the fixed point $Q = (x_-, x_-)$ is a source when $a = 0$ and so successive images of R are expanded away from the square. Again the set of points remaining in the square is a Cantor set.

For the case when $a \neq 0$ we must first construct an invariant set in place of the square S. This construction is given for several similar maps by Gumovski and Mira [15], who find numerically the boundaries of these invariant sets. We outline an argument for their existence in the Maynard Smith family, relying on some unproved assumptions.

Suppose that Q is a saddle and consider the local stable manifold $W^s_{loc}(Q)$. Our first assumption is that this curve cuts the fold line $x = 0$ at R, say. The image of QR is QS where $S = F(R)$ lies on the image ℓ_1 of the fold line ℓ. Now consider successive preimages of RS, as shown in figure 4.10. The first preimage is the curve R_{-1}, R'_{-1} where $F(R_{-1}) = F(R'_1) = R$. This lies symmetrically about the fold line and the map first folds it onto itself, with R'_{-1} mapping to R_{-1}, and then acts as an affine transformation taking R to S and R_{-1} to R.

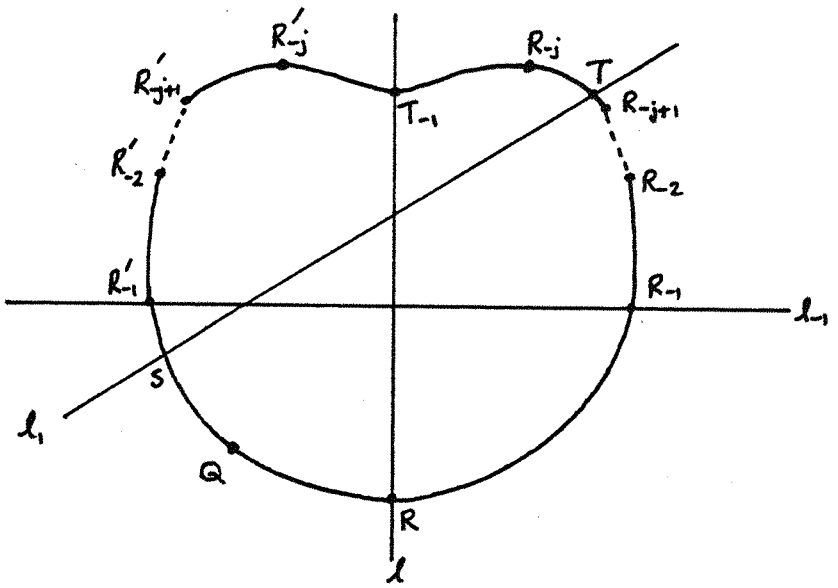

Figure 4.10.

Now suppose that some preimage of R, R_{-j} say, lies above ℓ_1 on the right hand side of ℓ, and so the invariant curve through Q now stretches from R_{-j} to R'_{-j}, its reflection in ℓ. The preimage of the point T where the curve cuts ℓ_1 lies on the fold line ℓ and the preimage of the curve segment $TR_{-(j-1)}$ is $R_{-j}R'_{-j}$, completing the invariant curve.

This construction is hardly rigorous. For any particular values of the parameters we may attempt to confirm whether the construction works, but general conditions which ensure the construction holds are very difficult to give. For examples in which this argument does work, as well as for some with rather different behaviour, we refer to Gumovski and Mira [15].

For the bifurcation which causes the attractor to disappear in this case, suppose that the parameters are changed until the last link in the curve, $R_{-j}R'_{-j}$, lies partly below ℓ_1 as in figure 4.11. Now points above ℓ_1 have no preimages, but points below this line have two preimages and so the construction of the curve continues in this case.

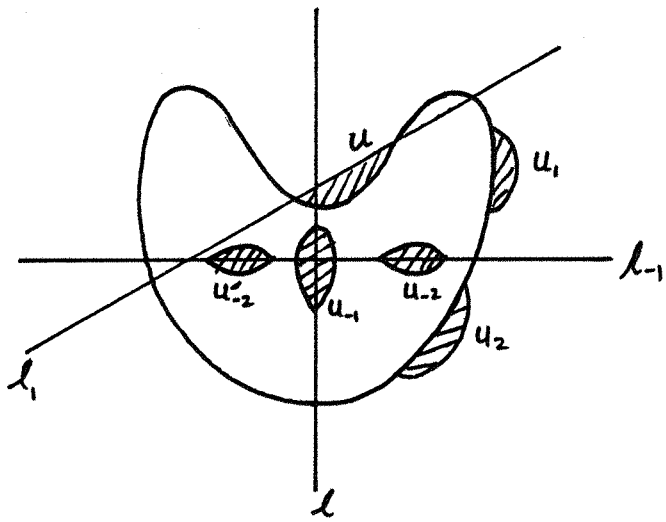

Figure 4.11.

If U is the open set whose frontier consists of that part of the curve below ℓ_1 and a part of ℓ_1 as shown in the figure, then U is mapped around the outside of the curve by successive iterates until it comes under the influence of the fixed point Q, and since the direction transverse to the curve P is always unstable further iterates are expanded away from the curve. Now U has a sequence of preimages inside the invariant curve which are mapped outside the previously invariant set.

The actual point of bifurcation occurs when the invariant curve has a point of tangency with ℓ_1 and is clearly difficult to detect. There is also the question of the set of points which do not escape from the interior of the curve. Although the construction of this set is similar to that of the Cantor sets in the case $a = 0$, some of the narrow regions corresponding to stable periodic orbits found numerically above, stretch across the parameter plane at values of b larger than those where this global bifurcation occurs. Therefore there are still open sets in the phase plane which remain inside the invariant curve after the global bifurcation.

Chapter Five

Maps Related to Maynard Smith's

The behaviour illustrated by the sequence of phase portraits in §4.2 is certainly not unique to the Maynard Smith family. Several sets of similar pictures have appeared in the literature. Beddington, Free and Lawton [4] discuss simulations of a discrete predator-prey model which is also one of the many examples considered by Gumovski and Mira [15], some of which have particularly striking phase portraits. Guckenheimer, Oster and Ipatchki [14] study a model of a population with two age-classes, arguing that for certain parameter values the model has a strange attractor based on a 'twisted horseshoe'. Curry and Yorke [8] investigate two families of maps of the plane. One is a non-invertible map whose phase portraits follow the pattern of those in §4.2, with a Hopf bifurcation creating an invariant circle which grows, distorts and then breaks up, leading to a complicated attractor which disappears at higher parameter values. The other is a family of homeomorphisms of the plane and for certain values of the parameter the phase portraits show an attractor with a structure similar to that in the map studied by Henon [16]:

$$(X,Y) \to (Y+1 - \alpha X^2, \beta X)$$

For $\alpha = 1.4$, $\beta = 0.3$ Henon produced computer plots of an orbit of this map approaching an attractor which appears locally to be the product of an interval with a Cantor set, although the possibility that it is simply a periodic orbit of a very large period cannot be discounted.

Now if α and β in the Henon map are non-zero we can change coordinates, setting $x = \frac{\alpha Y}{\beta}$, $y = \alpha X$, and rename the parameters $\alpha = b$, $\beta = a$, to obtain

$$G: \mathbb{R}^2 \to \mathbb{R}^2$$

$$(x,y) \to (y, ax+b-y^2) \qquad (5.1)$$

In §5.1 we examine the three-parameter family

$$H_t(x,y) = (1-t)G(x,y) + tF(x,y) \quad t \in [0,1]$$

which connects the Henon map G to Maynard Smith's map F, and we find that the map $H_{\frac{1}{2}}$ has symmetry properties related to those of Guckenheimer, Oster and Ipatchki's map.

To conclude, we return in §5.2 to the original biological problem and consider a more realistic version of Maynard Smith's model. However, even after correcting some of the biologically unjustified assumptions which led to Maynard Smith's map, we are still left with a model which contains the same basic complexities.

§5.1. The Henon-Maynard Smith Family

The family we shall consider is

$$H_t(x,y) = (y, aty + a(1-t)x + b - tx^2 - (1-t)y^2) \quad t \in [0,1] \qquad (5.2)$$

There are two fixed points, P and Q, with coordinates $x = y = \frac{1}{2}(a-1 \pm \sqrt{(a-1)^2+4b})$ independent of the third parameter t, and we can analyse the local stability of these fixed points as in Chapter Three. In fact we will examine the way in which the bifurcation diagram in the (a,b)-plane for P varies as t changes from 0 to 1. First though, we compare the geometrical action of the map with that of the Maynard Smith family shown in figure 3.1.

To visualize the action of the Henon map consider the graph T of the function $(x,y) \to z = ax+b-y^2$. T is a parabolic tunnel which lies parallel to the x-axis and the map takes a point P in the (x,y)-plane

to the point on T vertically above it, and then projects this point onto the (y,z)-plane (see figure 5.1). This is then identified with the original (x,y)-plane to recover the image of p under G.

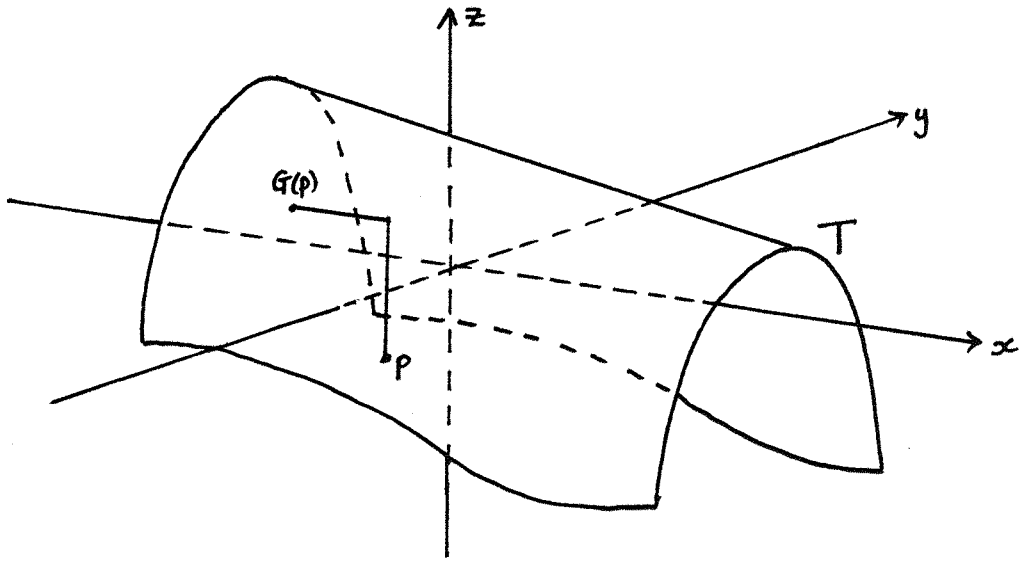

Figure 5.1.

As in Maynard Smith's family the parameter a governs the slope of T and b the height of its intersection with the z-axis. It is clear from figure 5.1 that G is one-to-one, except when $a = 0$, in which case the whole plane is mapped to the parabola $y = b-x^2$. The dynamics of the map on the parabola are then identical to those of the one-dimensional map $h_b(x) = b-x^2$ described by the results of §1.1.

If $t \in (0,1)$ then the second coordinate function in (5.2) $(x,y) \to z$, has a single critical point at $x = \frac{a(1-t)}{2t}$, $y = \frac{at}{2(1-t)}$ and the graph of the function is an elliptic dome D with a maximum at this point. See figure 5.2. As before the map H_t takes a point in the (x,y)-plane to the point above it on D and then projects onto the (y,z)-plane.

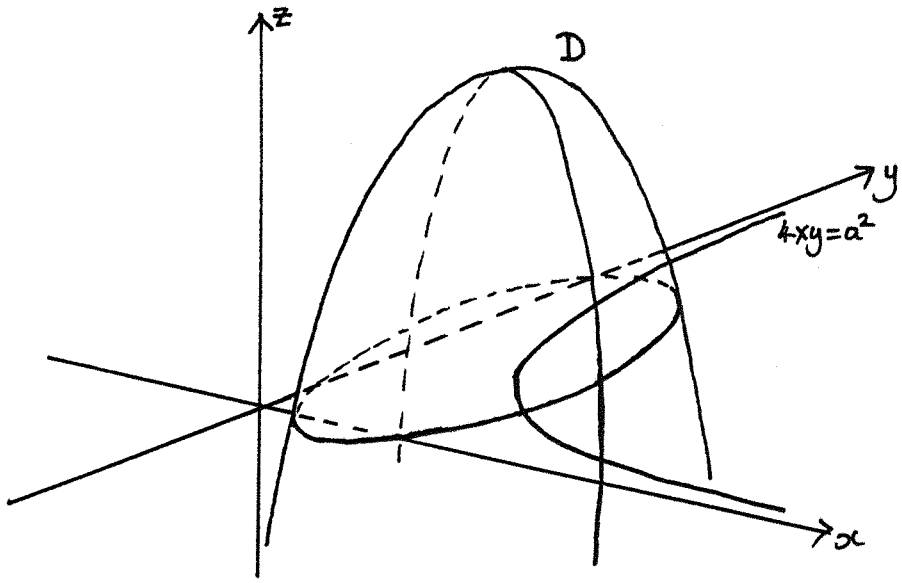

Figure 5.2.

Now as t varies from 0 to 1 the critical point traverses the hyperbola $4xy = a^2$ in the positive (negative) quadrant if $a > 0$ ($a < 0$). Thus the Henon and Maynard Smith maps are the limiting cases as the critical point moves off to infinity along the direction of the x- or y-axes respectively, leaving behind the fold line in F, or its counterpart in G, the line along the top of T in figure 5.1.

For each $t \in [0,1]$, H_t has two fixed points if the parameters a and b lie above the parabola P_1: $(a-1)^2+4b = 0$. For the other two curves which, for a fixed value of t, bound the region of the (a,b)-plane where the fixed point P is stable note that the Jacobian of H_t

$$dH_t(x,y) = \begin{pmatrix} 0 & 1 \\ a(1-t)-2tx & at-2(1-t)y \end{pmatrix}$$

has determinant $\Delta = 2tx-a(1-t)$ and trace $\sigma = at-2(1-t)y$. Hence at P, where $x = y = \frac{1}{2}(a-1+\sqrt{(a-1)^2+4b})$ the relevant boundaries are:

(i) $\Delta + \sigma + 1 = 0$ (corresponding to one eigenvalue of dH_t being -1)

$$-3a^2(2t-1)^2 + 2a(2t-1)(2t-3) + 4b(2t-1)^2+4t-3 = 0$$

provided $a-2at+t-1 \leq 0$ (≥ 0) if $t < \frac{1}{2}$ ($t > \frac{1}{2}$). No solution if $t = \frac{1}{2}$.

(ii) $\Delta = 1$ (complex eigenvalues of unit modulus when $|\sigma| < 2$)

$$a^2(2t-1)(1-t) + 2a(t^2+t-1) + 4bt^2-2t-1 = 0$$

provided $1+a+t-2at \geq 0$.

For fixed t (ii) defines a parabola H in the (a,b)-plane unless $t = 0, 1/3$, or 1, when it is a straight line. For $t \neq \frac{1}{2}$, (i) defines a parabola with a minimum. Figure 5.3 shows these boundaries in the (a,b)-plane for various values of t and the region where P is a sink is shaded.

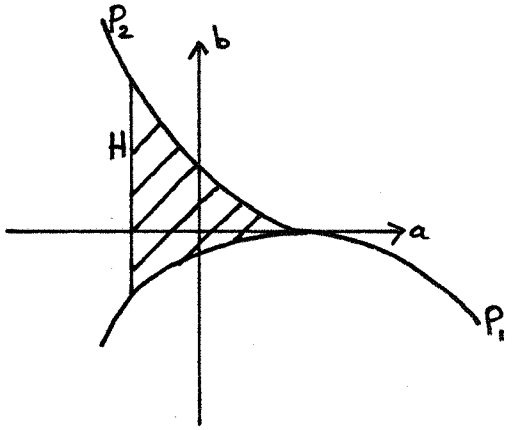

(a) $t = 0$. Henon map

$\Delta = 1, |\sigma| \leq 2$: $a=-1, -1 \leq b \leq 3$

$\Delta+\sigma+1=0$: $3(a-1)^2=4b$, $a \leq 1$

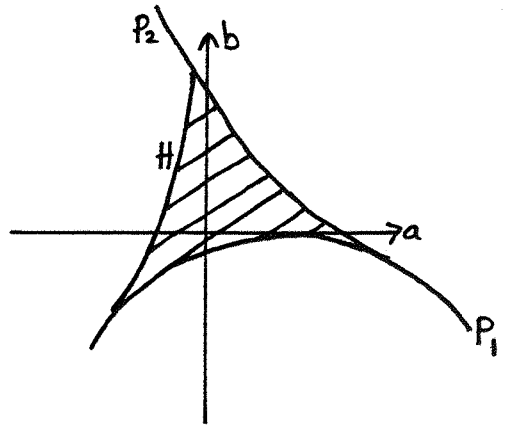

(b) $t = \frac{1}{4}$

$\Delta = 1$: $4b=(3a+4)(a+6)$, $a \geq -5/2$

$\Delta+\sigma+1=0$: $4b=(3a-4)(a-2)$, $a \leq 3/2$

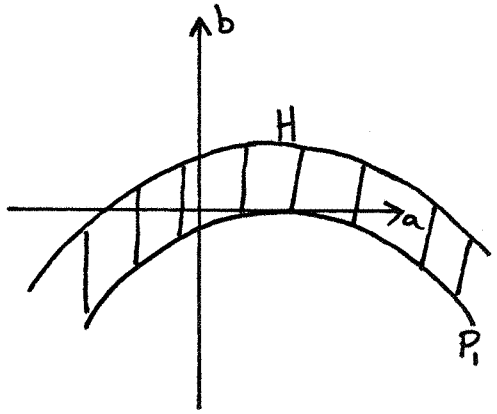

(d) $t = \frac{1}{2}$

$\Delta = 1$: $(a-1)^2+4b=9$

$\Delta+\sigma+1=0$: No solution

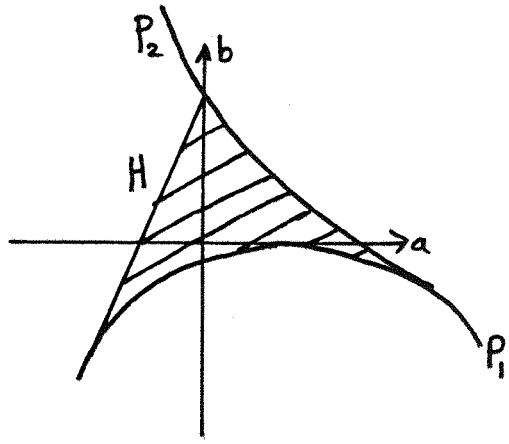

(c) $t = 1/3$

$\Delta = 1, |\sigma| \leq 2$: $4b=10a+15$, $-4 \leq a \leq 0$

$\Delta+\sigma+1=0$: $4b=(3a-5)(a-3)$, $a \leq 2$

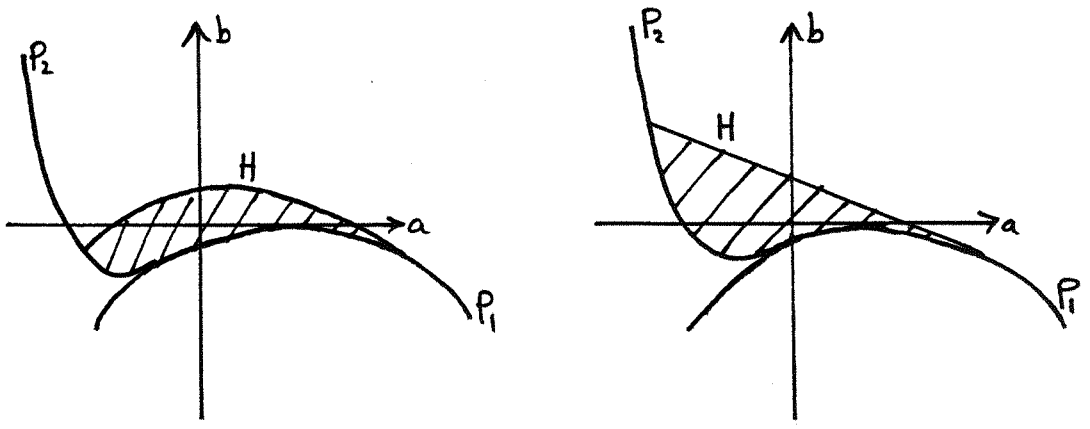

(e) $\underline{t = 3/4}$
$\Delta = 1$: $5(a-2)(a+4)+36b=0$, $a \leq 7/2$
$\Delta + \sigma + 1 = 0$: $4b=3a(a+2)$, $a \leq -\frac{1}{2}$

(f) $\underline{t = 1}$. Maynard Smith's map
$\Delta = 1, |\sigma| \leq 2$: $2a+4b=3$, $|a| \leq 2$
$\Delta+\sigma+1=0$: $4b=(3a-1)(a+1)$, $a \leq 0$.

Figure 5.3. Stability of P.

Clearly any family joining F and G must contain some degeneracy so that the Hopf line H can move from the left hand side of the parabola P_2 in figure 5.3(a) to the right hand side in (f). In the family H_t this degeneracy occurs at $t = \frac{1}{2}$ when the graph of the second coordinate function is a symmetric circular dome, and due to this symmetry the eigenvalues of $dH_t(P)$ at any point on the Hopf line are cube roots of unity.

The same phenomenon occurs in the map

$$f(x,y) = ((b_1x+b_2y)e^{-a(x+y)}, Sx)$$

studied by Guckenheimer, Oster and Ipatchki [14], when $b_1 = b_2$. The map models a population with two age-classes, x and y, whose growth is governed by a density dependent relationship of the form

$$\begin{pmatrix} x \\ y \end{pmatrix}_{t+1} = \begin{pmatrix} m_1 & m_2 \\ S & 0 \end{pmatrix} \begin{pmatrix} x \\ y \end{pmatrix}_t$$

Here $m_i(\cdot)$ are per capita growth rates for the two age-classes and are taken to be

$$m_i(x,y) = b_i e^{-a(x+y)}$$

and S is the fraction of the first age-class which survives to the second. For $b_1 = b_2 = b$ and $S = 1$ the map has a fixed point at $x = y = \frac{\ell n(2b)}{2a}$ and when $b = e^3/2$ the associated eigenvalues are cube roots of unity. For the one-parameter section at $a = 0.1$ Guckenheimer, Oster and Ipatchki report that at a value of b slightly less than $e^3/2$ two orbits of period three, one stable and one unstable, are created by a fold bifurcation. The unstable orbit coalesces with the fixed point at $b = e^3/2$ which then loses stability, and this is the behaviour we expect from §2.4 provided the relevant coefficients do not vanish. As b increases, the orbit of period three goes through a period doubling sequence which leads to a chaotic regime apparently based on a 'twisted horseshoe'. (We refer to [14] for the details.) At higher values of b this regime collapses to a stable four point cycle which undergoes a period doubling sequence leading to a further chaotic regime. This behaviour repeats as b increases with a period doubling sequence based on an n-point cycle giving way to a chaotic regime which collapses onto an (n+1)-point cycle, and the range of parameter values giving stable periodic orbits becomes progressively narrower as the length of the orbits increases.

This collapsing of a non-trivial attractor onto a stable periodic orbitwas observed in Maynard Smith's map when $a = 0.75$, $b \simeq 2.07$, where a stable seven point cycle was created, and the behaviour described above suggests that the cusped regions associated with weakly resonant Hopf bifurcations in Maynard Smith's map have, in $H_{\frac{1}{2}}$, become bands stretching across the (a,b)-plane above the Hopf line in figure 5.3(c). No attempt

has been made to verify this, in fact the computations required to show that the Hopf bifurcation in the family H_t is supercritical have not been carried out. We do know though that no invariant circles bifurcate from P as the parameters cross the Hopf line in the Henon map. This is because the derivative

$$dG(x,y) = \begin{pmatrix} 0 & 1 \\ a & -2y \end{pmatrix}$$

has determinant $-a$ at any point $(x,y) \in \mathbb{R}^2$. Hence G multiplies the area of any subset of the plane by a factor of a and since the area inside an invariant circle must remain constant the only possible parameter values for which G could have a closed invariant curve are $a = \pm 1$.

It is easy to check that the conditions (a)-(d) of the Hopf bifurcation Theorem 2.5 are satisfied by the Henon map for a suitable one-parameter path and since no circle bifurcates from the fixed point the stability criterion must be violated: $a(0) = 0$. In fact the results of Iooss [19] show that many more coefficients in the normal form for the map must vanish. For a one-parameter family F_μ whose eigenvalues cross the unit circle at $\lambda, \bar{\lambda}$ with $\lambda^n \neq 1$ for $n = 1,2,\ldots,N$, we can change coordinates by Lemma 2.6 so that

$$F_\mu(z) = \lambda(\mu)z + \sum_{m=1}^{\frac{1}{2}(N-2)} a_{2m+1}(\mu) z^{m+1} \bar{z}^{m} + O(|z|^N)$$

and in polar coordinates the map in the radial coordinate has the form

$$R = A(\mu)r + \sum \alpha_{2m+1}(\mu) r^{2m+1} + O(r^N).$$

Iooss proves that if any of the $\alpha_{2m+1}(0)$ are non-zero then invariant circles do bifurcate from the fixed point. Thus in the Henon map all these coefficients must vanish.

§5.2. A More Realistic Model.

Returning to the original problem notice there are some biologically unsatisfactory aspects of Maynard Smith's map (0.7). One minor point is that there should be a fixed point corresponding to zero population for all relevant values of the parameters. This is not the case because of the coordinate changes made in the introduction. However, these changes were made intentionally so that the family contained a fold bifurcation rather than a transcritical one, making the analysis a little easier--we only have fixed points in a half-plane in the parameter space rather than the whole plane--and the model is easily changed, by a linear coordinate change, to one where the origin is always a fixed point without altering any of the complexities associated with the Hopf bifurcation.

More important is the fact that many of the orbits of (1.7) contain points which correspond to negative populations, which is clearly nonsense as far as the biology is concerned. This can be avoided, as in Griffiths and Rand [11], by restricting attention only to those orbits which correspond to non-negative populations, but it is easy to see how to change the model to correct this deficiency.

The basic idea behind Maynard Smith's model is very simple. The number of adults at time $n+1$ is supposed to be a proportion of those at time n plus the new adults which hatch from eggs laid at time $n-\tau$. If we assume that x adults will produce $f(x)$ eggs which hatch into adults τ time units later, where $f(x)$ is some suitably chosen function , then the model is

$$x_{n+1} = ax_n + f(x_{n-\tau}), \qquad a \in (0,1)$$

Comparing this with (1.1) we see that in the original model $f(x)$ took negative values for $x > b/c$, leading to the negative populations

referred to above. To correct this we simply choose a more plausible function $f(x)$ and then investigate the model in the case $\tau = 1$ as before.

We will assume that $f(x) > 0$ when $x > 0$ and that $f(0) = 0$. We will also think of a typical function f as having a single positive maximum and $\lim_{x\to\infty} f(x) = 0$ as shown in figure 5.4, but these properties will not be strictly necessary for the whole of the analysis which follows.

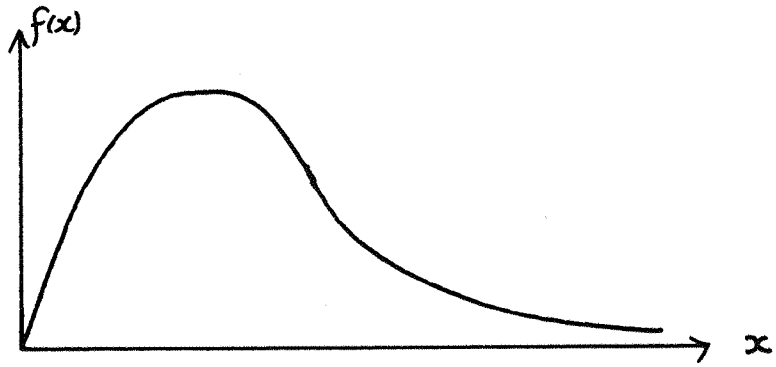

Figure 5.4.

The model for $\tau = 1$ gives the map

$$\Phi: \mathbb{R}^2 \to \mathbb{R}^2$$

$$(x,y) \to (y, ay+f(x))$$

whose fixed points lie on the diagonal $x = y$ and satisfy $f(x) = (1-a)x$. The stability of a fixed point $P = (p,p)$ of Φ is governed by the eigenvalues λ of

$$D\Phi(P) = \begin{pmatrix} 0 & 1 \\ f'(p) & a \end{pmatrix}$$

which are roots of

$$\lambda^2 - a\lambda - f'(p) = 0$$

It follows from Lemma 3.2 that the stability of p varies with a and $f'(p)$ as indicated in Figure 5.5.

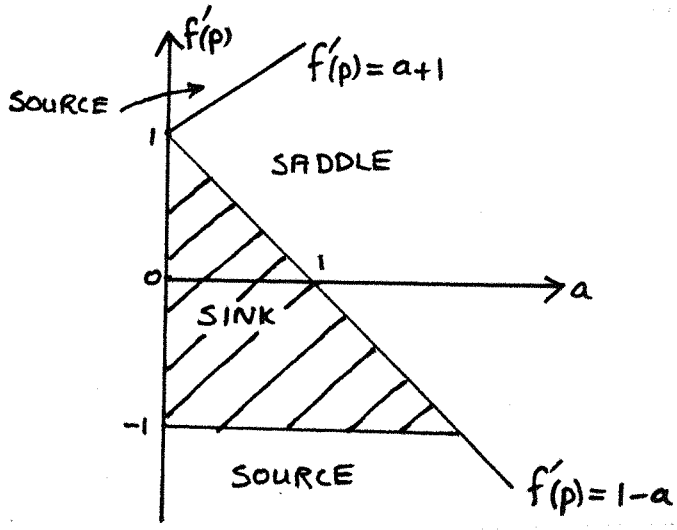

Figure 5.5. Stability of p.

Since $f(0) = 0$ the origin is always a fixed point of Φ and for $x > 0$ we may define $B(x) = \frac{f(x)}{x}$ so that the remaining fixed points are given by $B(x) = 1-a$. There are many possibilities for the shape of the graph of $B(x)$ and hence for the number of fixed points of Φ. For example we could choose $f(x) = x\exp(1-x)$ so that Φ has just one non-zero fixed point, (see Figure 5.6(a)), or take $f(x) = x^2\exp(1-x)$ to obtain two non-zero fixed points (Figure 5.6(b)).

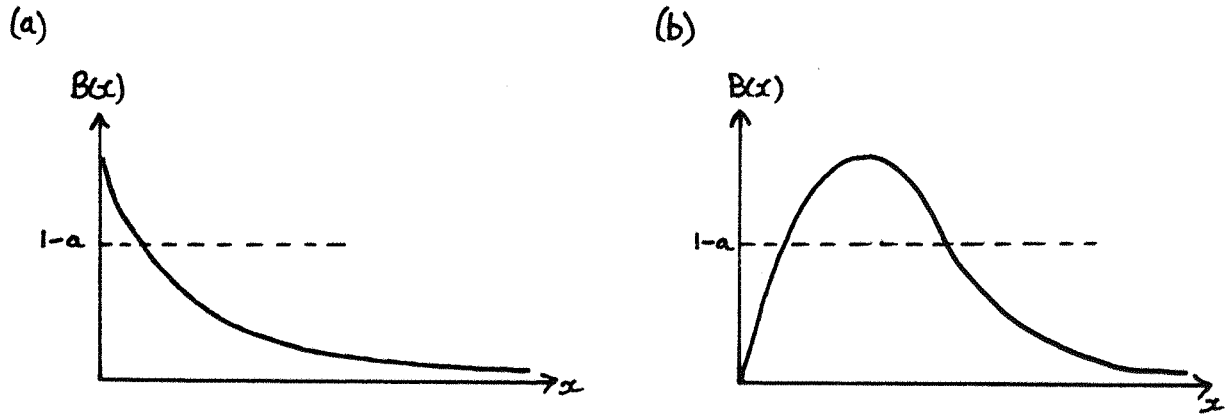

Figure 5.6. (a) $f(x) = x\exp(1-x)$
(b) $f(x) = x^2\exp(1-x)$

We will assume that Φ has at least one non-zero fixed point P and that $B'(p) < 0$. In terms of $B'(p)$ the eigenvalues of $D\Phi(P)$ are given by

$$\lambda^2 - a\lambda - (pB'(p) + 1-a) = 0$$

and P is either a sink or a source according to whether $pB'(p)$ is greater than or less than a-2.

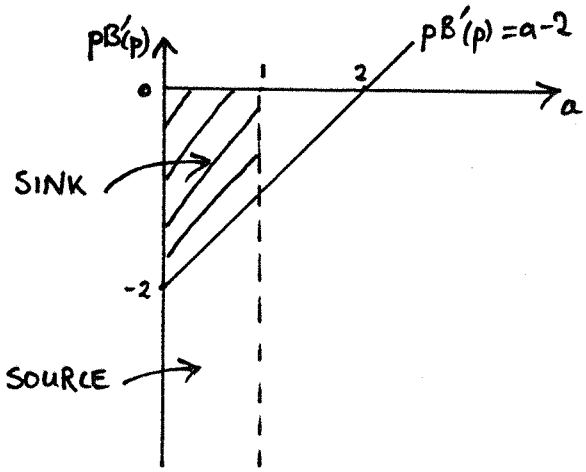

Figure 5.7. Stability of p.

Now suppose that $a \in (0,1)$ is fixed and we vary the function $B(x)$, and hence $f(x)$, so that the gradient $B'(p)$ becomes increasingly large and negative. If we do so in such a way that the value of $pB'(p)$ crosses the line $pB'(p) = a-2$ in figure 5, the fixed point P changes from a sink to a source and we expect a Hopf bifurcation to occur. More precisely we suppose that

$$B: \mathbb{R} \times \mathbb{R} \to \mathbb{R}$$

$$(\mu,x) \to B_\mu(x)$$

is a one-parameter family of functions B_μ, with $B_\mu(x) > 0$ when $x > 0$, and that $pB'(p)$ is a strictly decreasing function of μ with $pB'_{\mu_*}(p) = a-2$ for some value $\mu = \mu_*(a)$. We then have the following results for the family

$$\Phi(x,y) = (y, ay + xB_\mu(x)) \tag{5.3}$$

Proposition 5.1. The one parameter family Φ_μ has a supercritical Hopf bifurcation at $\mu = \mu_*(a)$ for each $a \in (0,1)$ provided

$$\frac{\alpha^2(3-a)}{2(2-a)} + \frac{3\beta}{4} > 0$$

where $\alpha = B'_{\mu_*}(p) + \frac{pB''_{\mu_*}(p)}{2!}$, $\beta = \frac{B''_{\mu_*}(p)}{2!} + \frac{pB'''_{\mu_*}(p)}{3!}$

Proof. We first check that conditions (a)-(d) of Theorem 2.5 are satisfied. Translating P to the origin the map becomes

$$\Phi_\mu(x,y) = (y, a(y+p) + (x+p)B_\mu(x+p))$$

and expanding $B_\mu(x+p)$ gives

$$B_\mu(x+p) = B_\mu(p) + xB'_\mu(p) + \frac{x^2}{2!}B''_\mu(p) + \frac{x^3}{3!}B'''_\mu(p) + O(x^4)$$

so neglecting terms of order greater than three, and since $B_\mu(p) = 1-a$,

$$\Phi_\mu(x,y) = (y, ay+(1-a+pB'_\mu(p))x + \alpha x^2 + \beta x^3)$$

where $\alpha = B'_\mu(p) + p\,\frac{B''_\mu(p)}{2!}$, $\beta = \frac{B''_\mu(p)}{2'} + p\,\frac{B'''_\mu(p)}{3'}$.

The eigenvalues of $d\Phi_\mu(0)$ are

$$\lambda(\mu) = \frac{1}{2}\left(a \pm \sqrt{a^2-4a+4+4\,B'_\mu(p)}\right)$$

so changing parameters, putting $\nu = a-2-B'_\mu(p)$, we have

$$\lambda(\nu) = \frac{1}{2}(a+i\sqrt{4(1+\nu)-a^2})$$

and $|\lambda(\nu)| = \sqrt{1+\nu}$. Since $B'_\mu(p)$ is assumed to be a strictly decreasing function of μ we have $\frac{d}{d\nu}|\lambda(\nu)|\Big|_{\nu=0} > 0$. Thus conditions (a),(b) and (c) of Theorem 2.5 are satisfied. For (d), note that $\lambda(0) = \frac{1}{2}(a+i\sqrt{4-a^2})$ so the parameter values leading to strong resonances are $a = -2,-1,0$, and 2, none of which lie in the open interval $0 < a < 1$ of interest here. Therefore Φ_ν has a Hopf bifurcation along the line $pB'(p) = a-2$ of Figure 4.5(b) which is supercritical if the coefficient a(0) defined by (2.1) is positive. To find a(0) note that (2.1) involves only terms of order less than four in the normal form for the map so we can work with

$$\Phi_o(x,y) = (y, ay-x+\alpha x^2+\beta x^3).$$

Defining new coordinates X, Y by

$$\begin{pmatrix} x \\ y \end{pmatrix} = \begin{pmatrix} 1 & 1 \\ \frac{a+R}{2} & \frac{a-R}{2} \end{pmatrix}\begin{pmatrix} X \\ Y \end{pmatrix}$$

where $R = \sqrt{4-a^2}$ we have

$$\Phi_o(X,Y) = \left(\frac{a}{2}X - \frac{R}{2}Y + \frac{\alpha}{R}(X+Y)^2 + \frac{\beta}{R}(X+Y)^3,\ \frac{R}{2}X + \frac{a}{2}Y - \frac{\alpha}{R}(X+Y)^2 - \frac{\beta}{R}(X+Y)^3\right)$$

writing Φ_o in complex notation,

$$\Phi_o(z) = \lambda z + \sum_{\ell=2,3} \sum_{p+q=\ell} \xi_{pq} z^p \bar{z}^q$$

the quadratic coefficients are given by the formulae in the proof of Proposition 3.5 and the cubic coefficients are

$$\xi_{30} = \tfrac{1}{8}[(\gamma_{30} + \tilde{\gamma}_{21} - \gamma_{12} - \tilde{\gamma}_{03}) + i(\tilde{\gamma}_{30} - \gamma_{21} - \tilde{\gamma}_{12} + \gamma_{03})]$$

$$\xi_{21} = \tfrac{1}{8}[(3\gamma_{30} + \tilde{\gamma}_{21} + \gamma_{12} + 3\tilde{\gamma}_{03}) + i(3\tilde{\gamma}_{30} - \gamma_{21} + \tilde{\gamma}_{12} - 3\gamma_{03})]$$

$$\xi_{12} = \tfrac{1}{8}[(3\gamma_{30} - \tilde{\gamma}_{21} + \gamma_{12} - 3\tilde{\gamma}_{03}) + i(2\tilde{\gamma}_{30} + \gamma_{21} + \tilde{\gamma}_{12} + 3\gamma_{03})]$$

$$\xi_{03} = \tfrac{1}{8}[(\gamma_{30} - \tilde{\gamma}_{21} - \tilde{\gamma}_{12} + \tilde{\gamma}_{03}) + i(\tilde{\gamma}_{30} + \gamma_{21} - \tilde{\gamma}_{12} - \gamma_{03})].$$

Therefore

$$\Phi(z) = \tfrac{1}{3}(a+iR)z - \frac{\alpha}{2R}(1+i)z^2 + \frac{\alpha}{R}(1-i)z\bar{z} + \frac{\alpha}{2R}(1\pm i)\bar{z}^2$$

$$- \frac{\beta}{2R} z^3 - \frac{3\beta}{2R} iz^2\bar{z} + \frac{3\beta}{2R} z\bar{z}^2 + \frac{\beta i}{2R} \bar{z}^3$$

and using the formula (2.1) we find

$$a(0) = \frac{\alpha^2(3-a)}{2(2-a)} + \frac{3\beta}{4}$$

Thus the family (5.3) has a Hopf bifurcation at $\mu = \mu_*(a)$ for each $a \in (0,1)$ and the bifurcation is supercritical if $a(0) > 0$. Also, since the argument of the eigenvalue $\lambda(\mu_*(a))$ is not constant for $a \in (0,1)$

we can expect to find a resonance tongue based at each 'rational' point on the Hopf bifurcation line exactly as in Maynard Smith's family.

As a specific example consider the family (5.3) with the functions

$$B_b(x) = \exp[b(1-x)] \tag{5.4}$$

parameterized by $b > 0$. Here Φ has a single non-zero fixed point $P = (p,p)$ with

$$p = 1 - \frac{1}{b}\ell n(1-a)$$

and P has complex eigenvalues of modulus one along the Hopf line

$$b = \frac{a-2}{a-1} + \ell n(1-a), \quad a \in (0,1) \tag{5.5}$$

sketched below.

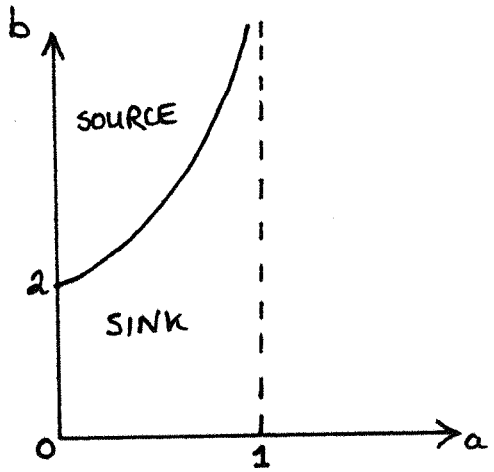

Figure 5.8. Stability of P.

For this example we have

$$B_b'(p) = -b(1-a), \quad B_b''(p) = b^2(1-a), \quad B_b'''(p) = -b^3(1-a)$$

and so

$$a(0) = \frac{b^2(2-5a+5a^2-a^3)}{8(2-a)}$$

with b given by (5.5). This is easily checked to be strictly positive for $a \in (0,1)$ and we have proved the following result.

Proposition 5.2. For each $a \in (0,1)$ the family

$$\Phi_b(x,y) = (y, ay+xexpb(1-x))$$

has a supercritical Hopf bifurcation at the fixed point with coordinates $x = y = 1 - \frac{1}{b}\,\ell n(1-a)$ when $b = \frac{a-2}{a-1} + \ell n(1-a)$.

APPENDIX

Numerical Results

TABLE 1

Three-Point Cycles with one Eigenvalue equal to One

a	b	Second Eigenvalue	a	b	Second Eigenvalue
1.25	7.6094	1.27	-0.7	0.8575	-0.15
1.2	7.2700	0.97	-0.8	0.8700	-0.07
1.1	6.6175	0.44	-0.9	0.9176	-0.02
1.0	6.0000	0.00	-1.0	1.0000	0.00
0.9	5.4175	-0.36	-1.1	1.1175	-0.02
0.8	4.8700	-0.65	-1.2	1.2700	-0.09
0.7	4.3575	-0.87	-1.3	1.4575	-0.21
0.6	3.8800	-1.02	-1.4	1.6800	-0.38
0.5	3.4375	-1.13	-1.5	1.9375	-0.63
0.4	3.0300	-1.18	-1.6	2.2300	-0.94
0.3	2.6575	-1.18	-1.7	2.5575	-1.32
0.2	2.3200	-1.15	-1.8	2.9200	-1.79
0.1	2.0175	-1.09	-1.9	3.3175	-2.35
0.0	1.7500	-1.00	-2.0	3.7500	-3.00
-0.1	1.5175	-0.89	-2.1	4.2175	-3.75
-0.2	1.3200	-0.77	-2.2	4.7200	-4.61
-0.3	1.1575	-0.64	-2.3	5.2575	-5.58
-0.4	1.0300	-0.50	-2.4	5.8300	-6.66
-0.5	0.9375	-0.38	-2.5	6.4375	-7.88
-0.6	0.8800	-0.26			

TABLE 2

Three-Point Cycles with one Eigenvalue equal to Minus One

a	b	Second Eigenvalue	a	b	Second Eigenvalue
1.0	6.0012	1.93	0.0	1.7500	1.00
0.9	5.4181	1.60	-0.1	1.5179	1.11
0.8	4.8702	1.33	-0.2	1.3231	1.25
0.7	4.3575	1.12	-0.3	1.1735	1.44
0.6	3.8800	0.98	-0.4	1.1216	1.74
0.5	3.4376	0.88	-0.5	1.3500	2.27
0.4	3.0302	0.83	-0.6	1.6705	2.81
0.3	2.6577	0.83	-0.7	1.9733	3.33
0.2	2.3202	0.85	-0.8	2.2569	3.81
0.1	2.0176	0.91	-0.9	2.5219	4.26

TABLE 2 (Cont.)

a	b	Second Eigenvalue	a	b	Second Eigenvalue
-1.0	2.7675	4.66	-1.6509	2.6	2.38
-1.1	2.9910	4.99	-1.6394	2.5	2.17
-1.2	3.1880	5.24	-1.6258	2.4	1.94
-1.3	3.3518	5.37	-1.6050	2.2605	1.44
-1.4	3.4710	5.36			
-1.5	3.5238	5.15			
-1.6217	3.4	4.39	-1.615	2.2770	1.05
-1.6472	3.3	4.05	-1.7	2.5742	0.24
-1.6614	3.2	3.76	-1.8	2.9600	-0.51
-1.6690	3.1	3.49	-1.9	3.3787	-1.29
-1.6718	3.0	3.25	-2.0	3.8310	-2.14
-1.6709	2.9	3.02	-2.1	4.3170	-3.08
-1.6669	2.8	2.80	-2.2	4.8372	-4.11
-1.6601	2.7	2.59	-2.25	5.1102	-4.67

TABLE 3

Three Point Cycles with Complex Eigenvalues of Modulus One

a	b	Argument	a	b	Argument
1.2055	7.3069	1	-0.4	1.0804	81
1.2	7.2700	10	-0.5	1.0000	79
1.1	6.6176	43	-0.6	0.9549	78
1.0	6.0003	59	-0.7	0.9433	77
0.9	5.4182	70	-0.8	0.9634	77
0.8	4.8713	78	-0.9	1.0142	78
0.7	4.3596	84	-1.0	1.0955	79
0.6	3.8831	89	-1.1	1.2080	81
0.5	3.4420	92	-1.2	1.3583	84
0.4	3.0361	93	-1.3	1.5330	88
0.3	2.6658	94	-1.4	1.7483	93
0.2	2.3309	93	-1.5	2.0000	101
0.1	2.0317	92	-1.6	2.2883	111
0.0	1.7685	90	-1.7	2.6131	124
-0.1	1.5415	88	-1.8	2.9741	145
-0.2	1.3510	85	-1.8636	3.2225	179
-0.3	1.1973	83			

TABLE 4

Four Point Cycles with one Eigenvalue equal to one

a	b	Second Eigenvalue	a	b	Second Eigenvalue
0.0	0.75	0.00	-0.1	1.0878	-0.44
0.1	1.0024	-0.57	-0.2	1.4336	-1.94
0.2	1.2939	-2.46	-0.3	1.7849	-3.50
0.3	1.6243	-4.68	-0.4	2.1394	-5.11
0.4	1.9938	-7.24	-0.5	2.4948	-6.78
0.5	2.4022	-10.15	-0.6	2.8490	-8.47
0.6	2.8495	-13.41	-0.7	3.1997	-10.19
0.7	2.3357	-17.02	-0.8	3.5446	-11.90
0.8	3.8609	-20.98	-0.9	3.8812	-13.59
0.9	4.24	-25.29	-1.0	4.2069	-15.21
1.0	5.0277	-29.95			

TABLE 5

Four Point Cycles with one Eigenvalue equal to Minus One

a	b	Second Eigenvalue	a	b	Second Eigenvalue
1.0	5.1124	-30.15	-1.0	4.3714	-16.73
0.9	4.5205	-25.63	-0.9	4.0508	-15.13
0.8	3.9699	-21.46	-0.8	3.7211	-13.46
0.7	3.4612	-17.64	-0.7	3.3857	-11.76
0.6	2.9957	-14.19	-0.6	3.0481	-10.05
0.5	2.5747	-11.10	-0.5	2.7118	-8.37
0.4	2.2006	-8.38	-0.4	2.3810	-6.73
0.3	1.8763	-6.02	-0.3	2.0611	-5.16
0.2	1.6060	-4.03	-0.2	1.7591	-3.67
0.1	1.3949	-2.37	-0.1	1.4843	-2.29
0.0	1.2500	-1.00	0.0	1.2500	-1.00
-0.1	1.1892	0.26	0.1	1.0812	0.36
-0.12	1.1944	0.56	0.12	1.0665	0.80

TABLE 6

Five Point Cycles with one Eigenvalue equal to one (II)

a	b	Second Eigenvalue
1.0	3.7833	-25.81
0.9	3.1346	-17.91
0.8	2.5013	-11.62
0.7	1.8556	-6.63
0.6	0.9980	-1.91
0.5931	0.8	-0.96
0.5941	0.7	-0.47
0.5990	0.6	0.06
0.6023	0.55	0.34
0.6180	0.4410	1.00
0.6028	0.5	0.63
0.5882	0.55	0.34
0.5	0.8008	-0.84
0.4	1.0333	-1.50
0.3	1.2299	-1.75
0.2	1.3951	-1.72
0.1	1.5281	-1.46
0.0	1.6244	-1.00
-0.1	1.6723	-0.31
-0.15	1.6661	0.17
-0.1623	1.6563	0.40

a	b	Second Eigenvalue
-0.1623	1.6563	0.42
-0.1559	1.7	0.68
-0.1618	1.8	1.13
-0.1923	2.0	2.22
-0.2312	2.2	3.61
-0.2740	2.4	5.29
-0.3188	2.6	7.25
-0.3650	2.8	9.49
-0.4120	3.0	12
-0.4598	3.2	15
-0.5080	3.4	18
-0.5568	3.6	21
-0.6060	3.8	25
-0.6557	4.0	29
-0.7058	4.2	33
-0.7565	4.4	37
-0.8078	4.6	42
-0.8597	4.8	47
-0.9123	5.0	52

TABLE 7

Five Point Cycles with Complex Eigenvalues of Modulus One (I)

a	b	Argument
-0.1591	1.7727	1
-0.1573	1.75	19
-0.15	1.6698	50
-0.1	1.6751	68
-0.0	1.6284	90
0.1	1.5044	106
0.2	1.4054	116

a	b	Argument
0.3	1.2484	122
0.4	1.0724	120
0.5	0.9121	114
0.55	0.9015	117
0.57	0.9547	126
0.59	1.0723	150
0.5975	1.1286	177

TABLE 8

Five Point cycles with one Eigenvalue equal to Minus One (I)

a	b	Second Eigenvalue
1.0	3.7953	-25.09
0.9	3.1497	-17.05
0.8	2.5223	-10.63
0.7	1.8918	-5.56
0.6	1.1548	-1.14
0.5932	0.81	0.98
0.593	0.8022	1.06
0.59	0.7866	1.26
0.55	0.7775	1.59
0.50	0.8103	1.28
0.482	0.8458	1.01
0.481	0.8483	0.99
0.45	0.9290	0.59
0.40	1.0443	0.26
0.35	1.2372	0.07
0.3	1.3985	0.18
0.1	1.5291	0.51
0.0	1.6244	1.00

TABLE 9

Five Point cycles with one Eigenvalue equal to One (III)

a	b	Second Eigenvalue
1.0	5.8887	38.58
0.9	5.3511	29.98
0.8	4.8463	22.89
0.7	4.3745	17.10
0.6	3.9355	12.40
0.5	3.5293	8.63
0.4	3.1558	5.64
0.3	2.8149	3.29
0.2	2.5064	1.47
0.1	2.2300	0.07
0.0	1.9854	-1.00
-0.1	1.7723	-1.81
-0.2	1.5901	-2.42
-0.3	1.4383	-2.88
-0.4	1.3165	-3.24
-0.5	1.2240	-3.52
-0.6	1.1605	-3.76
-0.7	1.1255	-3.96
-0.8	1.1190	-4.14
-0.9	1.1412	-4.30
-1.0	1.1927	-4.43
-1.1	1.2746	-4.51
-1.2	1.3886	-4.51
-1.3	1.5370	-4.38
-1.4	1.7234	-4.04
-1.5	1.9523	-3.37
-1.6	2.2304	-2.19
-1.7	2.5673	-0.28
-1.8	2.9768	2.04
-1.9	3.4599	0.19
-2.0	3.9952	-4.50
-2.1	4.5755	-12.75
-2.2	5.1988	-23.39

TABLE 10

Five Point Cycles with one Eigenvalue equal to One (II)

a	b	Second Eigenvalue
1.0	6.0242	-24.51
0.9	5.4310	-21.39
0.8	4.8758	-18.33
0.7	4.3587	-15.38
0.6	3.8801	-12.60
0.5	3.4402	-10.04
0.4	3.0398	-7.71
0.3	2.6797	-5.63
0.2	2.3612	-3.82
0.1	2.0867	-2.28
0.0	1.8606	-1.00
-0.1	1.6934	-0.01
-0.2	1.6528	0.35
-0.3	1.8405	0.17
-0.4	2.0977	-0.16
-0.5	2.3832	-0.67
-0.6	2.6809	-1.35
-0.7	2.9812	-2.15
-0.8	3.2779	-3.02
-0.9	3.5659	-3.91
-1.0	3.8407	-4.76
-1.1	4.0980	-5.53
-1.2	4.3329	-6.16
-1.3	4.5397	-6.62
-1.4	4.7107	-6.89
-1.5	4.8356	-6.94
-1.6	4.8978	-6.77
-1.7	4.8663	-6.40
-1.8	4.6616	-5.79

a	b	Second Eigenvalue
-1.85	4.3984	-5.30
-1.87	4.1914	-4.97
-1.883	3.7250	-4.20
-1.88	3.5546	-3.90
-1.85	3.0191	-2.80
-1.80	2.5445	-1.64
-1.75	2.2008	0.73
-1.70	1.9224	0.04
-1.6749	1.8	0.37
-1.6527	1.7	0.64
-1.6286	1.6	0.90
-1.6180	1.5590	1.00
-1.6492	1.67	0.75
-1.66	1.7081	0.66
-1.67	1.7434	0.58
-1.68	1.7788	0.50
-1.69	1.8144	0.42
-1.7	1.8502	0.34
-1.8	2.2189	-0.52
-1.9	2.6121	-1.53
-2.0	3.0328	-2.74
-2.1	3.4823	-4.23
-2.2	3.9616	-6.07
-2.3	4.4712	-8.35
-2.4	5.0116	-11.17
-2.5	5.5829	-14.66

TABLE II

Six Point Cycles with one Eigenvalue Equal to one

a	b	Second Eigenvalue
1.5	7.2923	146
1.4	6.4902	129
1.3	5.7242	110
1.2	4.9927	92
1.1	4.2934	73
1.0	3.6216	56
0.9	2.9672	40
0.8	2.3004	25
0.71	1.3138	7.44
0.8	0.7814	0.96
0.9	0.5031	-0.22
1.0	0.25	1.00
0.9	0.4657	-0.23
0.8	0.6311	-0.26
0.7	0.7635	-0.09
0.6	0.8775	-0.35
0.5	0.9993	-1.32
0.4	1.1569	-2.31
0.3	1.3331	-3.25
0.2	1.4993	-4.32
0.1	1.6407	-5.36
0.0	1.7500	-6.11
-0.1	1.8212	-6.35
-0.2	1.8453	-5.87
-0.3	1.8037	-4.48
-0.4	1.6338	-1.80
-0.436	1.4121	0.01

a	b	Second Eigenvalue
-0.4358	1.389	-0.31
-0.5	1.7711	-6.76
-0.6	2.2091	-12.95
-0.7	2.6005	-18.10
-0.8	2.9643	-22.44
-0.9	3.3051	-25.97
-1.0	3.6234	-28.66
-1.1	3.9176	-30.46
-1.2	4.1851	-31.33
-1.3	4.4216	-31.20
-1.4	4.6216	-30.02
-1.5	4.7768	-27.71
-1.6	4.8753	-24.17
-1.7	4.8969	-19.27
-1.8	4.8026	-12.89
-1.9	4.4833	-5.07
-1.95	4.0789	-1.27
-1.96	3.9111	-0.92
-1.9645	3.7553	-1.22
-1.96	3.5479	-2.81
-1.9546	3.4905	-4.02
-1.9546	3.4905	-4.29
-2.0	3.7500	-7.00
-2.1	4.3051	-10.26
-2.2	4.8882	-13.21
-2.3	5.5066	-15.86
-2.4	6.1620	-18.00
-2.5	6.8550	-19.27

TABLE 12

Six Point Cycles with one Eigenvalue equal to One (II)

a	b	Second Eigenvalue
-2.5	5.8111	3.96
-2.4	5.2893	0.81
-2.3	4.7982	-1.25
-2.2	4.3385	-2.53
-2.1	3.9116	-3.29
-2.0	3.5221	-3.81
-1.9	3.1834	-4.25
-1.8	2.8803	-2.98
-1.7	2.5700	-0.65
-1.638	2.3644	0.46
-1.638	2.3644	0.38
-1.7	2.6218	-1.82
-1.8	3.1365	-6.24
-1.9	3.8322	-14
-2.0	5.4199	-41
-1.9	6.4861	-55
-1.8	6.6670	-49
-1.7	6.6764	-39
-1.6	6.5894	-27
-1.5	6.4372	-15
-1.4	6.2370	-4.40
-1.3	5.9999	5.24
-1.2	5.7338	13
-1.1	5.4446	20
-1.0	5.1371	24

a	b	Second Eigenvalue
-0.9	4.8153	27
-0.8	4.4827	29
-0.7	4.1424	29
-0.6	3.7971	28
-0.5	3.4496	25
-0.4	3.1025	22
-0.3	2.7581	19
-0.2	2.4183	14
-0.1	2.0860	9.76
0.0	1.7500	-1.00
0.1	1.7233	7.35
0.2	1.6369	1.64
0.3	1.5126	5.61
0.4	1.3548	3.03
0.5	1.1456	-1.91
0.501	1.1424	-2.24
0.501	1.1426	-2.98
0.5	1.1470	-3.42
0.491	1.2727	-8
0.5	1.4225	-13
0.6	2.0789	-36
0.7	2.6393	-62
0.8	3.2089	-93
0.9	3.8034	-130
1.0	4.4287	-175

TABLE 13

Six Point Cycles with Complex Eigenvalues of Modulus One

a	b	Argument	a	b	Argument
0.80	0.7814	12	0.65	0.8281	70
0.84	0.6206	70	0.60	0.8877	80
0.80	0.6511	72	0.55	0.9719	106
0.75	0.7108	69	0.50	1.1501	70
0.70	0.7702	67	0.46	1.2407	16

TABLE 14

SIX POINT CYCLES with one Eigenvalue equal to One (III)

a	b	Second Eigenvalue
-2.5	7.4099	321
-2.4	6.6424	221
-2.3	5.9154	146
-2.2	5.2291	90
-2.1	4.5835	51
-2.0	3.9788	26
-1.945	3.6630	16
-1.951	3.6970	18
-2.0	4.0022	-2
-2.1	4.7801	-51
-2.2	6.1512	-188
-2.1	8.0293	-502
-2.0	8.2247	-547
-1.9	8.2383	-555
-1.8	8.1463	-542
-1.7	7.9817	-514
-1.6	7.7631	-478
-1.5	7.5022	-436
-1.4	7.2075	-392
-1.3	6.8852	-347
-1.2	6.5402	-303
-1.1	6.1766	-260
-1.0	5.7978	-220
-0.9	5.4068	-184
-0.8	5.0062	-150
-0.7	4.5984	-121
-0.6	4.1857	-95
-0.5	3.7702	-72
-0.4	3.3541	-53
-0.3	2.9398	-37
-0.2	2.5302	-24
-0.1	2.1297	-12
0.0	1.7500	1.00
0.1	1.8876	-12
0.2	2.1067	-21
0.3	2.3851	-33
0.4	2.7151	-47
0.5	3.0928	-64
0.6	3.5155	-84
0.7	3.9817	-109
0.8	4.4900	-138
0.9	5.0396	-172
1.0	5.6300	-211

References

[1] D.J. Allwright. Hypergraphic Functions and Bifurcations in Recurrence Relations. Siam J. Appl. Math. 34, 687-691, 1978.

[2] V.I. Arnol'd. Lectures on Bifurcations in Versal Families. Russian Math. Surveys. 27, 54-123, 1972.

[3] V.I. Arnol'd. Loss of Stability of Self-Oscillations Close to Resonance and Versal Deformations of Equivariant Vector Fields. Funct. Anal. Appl. 11, 85-92, 1977.

[4] J.R. Beddington, C.A. Free and J.H. Lawton. Dynamic Complexity in Predator-Prey Models Framed in Difference Equations. Nature. 255, 58-60, 1975.

[5] P. Brunovsky. One-Parameter Families of Diffeomorphisms. Springer Lecture Notes in Maths. 206, 29-32, 197.

[6] M. Campanino and H. Epstein. On the Existence of Feigenbaum's Fixed Point. Comm. Math. Phys. 79, 261-302, 1981.

[7] P. Collet, J-P. Eckmann and O.E. Lanford III. Universal Properties of Maps on an Interval. Comm. Math. Phys. 76, 211-254, 1980.

[8] J.H. Curry and J.A. Yorke. A Transition from Hopf Bifurcation to Chaos: Computer Experiments with Maps on $\mathbb{R}^2$. Springer Lecture Notes in Math. 668, 48-66, 1977.

[9] J. Dieudonné. Foundations of Modern Analysis. Academic Press, 1960.

[10] M.J. Feigenbaum. Quantitative Universality for a Class of Non-Linear Transformations. J. Stat. Phys. 19, 25-52, 1978.

[11] H.B. Griffiths and D.A. Rand. An Essay on Elites and Mathematical Modelling. Preprint, Southampton 1977.

[12] J. Guckenheimer. On the Bifurcation of Maps of the Interval. Invent. Math. 39, 165-178, 1977.

[13] J. Guckenheimer. Sensitive Dependence on Initial Conditions for One-Dimensional Maps. Comm. Math. Phys. 70, 133-160, 1979.

[14] J. Guckenheimer, G. Oster and A. Ipatchki. The Dynamics of Density Dependent Population Models. J. Math. Biol. 4, 101-147, 1977.

[15] I. Gumovski and C. Mira. Recurrences and Discrete Dynamical Systems. Springer Lectures Notes in Maths. 809, 1980.

[16] M. Henon. A Two-Dimensional Mapping with a Strange Attractor. Comm. Math. Phys. 50, 69-78, 1976.

[17] M.R. Herman. Measure de Lebesgue et Nombre de Rotation. Springer Lecture Notes in Math. 597, 271-293, 1977.

[18] M.R. Herman. Sur la conjugaison Differentiable des Diffeomorphisms du Circles des Rotations. Pub. IHES. 49, 5-234, 1979.

[19] G. Iooss. Bifurcation of Maps and Applications. North Holland Pub. Co., 1979.

[20] L. Jonker. Periodic Orbits and Kneading Invariants. Proc. Lond. Math. Soc. 39, 428-450, 1979.

[21] L. Jonker and D.A. Rand. Bifurcations in One Dimension
I. The Non-Wandering Set. Invent. Math. 62, 347-365, 1981.
II. A Versal Model for Bifurcations. Invent. Math. 63, 1-15, 1981.

[22] E.I. Jury. A Simplified Stability Criterion for Linear Discrete Systems. Proc. IRE 50, 1493-1500, 1962.

[23] O.E. Lanford III. Bifurcation of Periodic Orbits into Invariant Tori. The Work of Ruelle and Takens. Springer Lecture Notes in Maths. 322, 159-192, 1973.

[24] F. Lemaire-Body. Bifurcation de Hopf pour les Applications dans un cas Resonnant. C.R. Acad. Sc. Paris, t. 287, A, 727-730, 1978.

[25] T-Y. Li and J.A. Yorke. Period Three Implies Chaos. Am. Math. Monthly, 82, 985=992, 1975.

[26] M. Marden. The Geometry of the Zeros of a Polynomial in a Complex Variable, A.M.S. Surveys, No. 3, 1949.

[27] F. Marroto. Snap-Back Repellers Imply Chaos in $\mathbb{R}^n$. J. Math. Anal. Appl. 63, 199-223, 1978.

[28] R.M. May. Biological Populations Obeying Difference Equations: Stable Points, Periodic Orbits and Chaos. J. Theor. Biol., 51, 511-524, 1975.

[29] J. Maynard Smith. Mathematical Ideas in Biology, CUP, 1968.

[30] J. Milnor. The Theory of Kneading and a Piecewise Linear Model for Kneading. Handwritten Notes.
J. Milnor and W. Thurston. On Iterated Maps of the Interval I. Princeton Preprint, 1977.

[31] Z. Nitecki. Differentiable Dynamics, MIT Press, 1971.

[32] D. Ruelle and F. Takens. On the Nature of Turbulence, Comm. Math. Phys. 20, 167-192, 1971.

[33] R.J. Sacker. On Invariant Surfaces and Bifurcation of Periodic Solutions of Ordinary Differential Equations, New York Univ. 1964.

[34] D. Singer. Stable Oribts and Bifurcation of Maps of the Interval. SIAM J. Appl. Math. 35, 260-267, 1978.

[35] S. Smale. Differentiable Dynamical Systems, Bull. Am. Math. Soc. 73, 774-817, 1967.

[36] P. Stefan. A Theorem of Sarkovskii on the Existence of Periodic Orbits of Continuous Endomorphisms of the Red Line, Comm. Math. Phys. 54, 237-248, 1977.

[37] S. van Strien. On the Bifurcations Creating Horseshoes, Univ. Utrecht. Preprint, 1980.

[38] F. Takens. Forced Oscillations and Bifurcations, Applications of Global Analysis I, Communications of the Mathematical Institute Rijksuniversiteit Utrecht, 1-59, 1974.

[39] Y-H. Wan. Computation of the Stability Condition for the Hopf Bifurcation of Diffeomorphisms on $\mathbb{R}^2$, SIAM J. Appl. Math. 34, 167-175, 1978.

[40] Y-H. Wan. Bifurcation into Invariant Tori at Points of Resonance, Arch. Rat. Mech. Anal. 68, 343-357, 1978

[41] B.R. Henry. Escape from the Unit Interval under the Transformation $x \to \lambda x(1-x)$, Proc. Am. Math. Soc. 41, 146-150, 1973.